cH

Study of Electrical Analogue for Electrodialysis

United States Department of the Interior

Office of Saline Water • Research and Development Progress Report No. 238

Research and Development Progress Report No. 238 • February 1967

Study of Electrical Analogue for Electrodialysis

By C. Berger, G. A. Guter, G. Belfort, Astropower Laboratory, Douglas Aircraft Company, Inc., Newport Beach, California, for Office of Saline Water; J. A. Hunter, Acting Director; K. C. Channabasappa, Chief, Membrane Division, M. E. Mattson, Project Engineer

UNITED STATES DEPARTMENT OF THE INTERIOR • Stewart L. Udall, Secretary
Frank C. Di Luzio, Assistant Secretary for Water Pollution Control

Created in 1849, the Department of the Interior--America's Department of Natural Resources--is concerned with the management, conservation, and development of the Nation's water, wildlife, mineral, forest, and park and recreational resources. It also has major responsibilities for Indian and Territorial affairs.

As the Nation's principal conservation agency, the Department of the Interior works to assure that nonrenewable resources are developed and used wisely, that park and recreational resources are conserved for the future, and that renewable resources make their full contribution to the progress, prosperity, and security of the United States--now and in the future.

FOREWORD

This is the two hundred and thirty eighth of a series of reports designed to present accounts of progress in saline water conversion with the expectation that the exchange of such data will contribute to the long-range development of economical processes applicable to large-scale, low-cost demineralization of sea or other saline water.

Except for minor editing, the data herein are as contained in the reports submitted by the Astropower Laboratory, Douglas Aircraft Company, Inc. under Contract No. 14-01-0001-676. The data and conclusions given in this report are essentially those of the contractor and are not necessarily endorsed by the Department of the Interior.

ABSTRACT

The highlight accomplishments of the program are as follows:

1. This study is a first attempt to perform an analysis of electrodialysis by considering the process as an electrical network composed of resistive elements representative of various electrochemical subprocesses. The total effect of all subprocesses is unified into the single mathematical equation for the network. This study represents a step of major magnitude in understanding the electrodialysis process because of the novel engineering equations developed that can be used to quantitatively analyze the electrical resistance of the stages in an electrodialysis plant. The treatment gives a breakdown of the various factors that contribute to electrical resistance and pinpoints those factors that must be improved to make technological improvements in the process.

2. Application of the analysis to the Webster, S. D. and Buckeye, Arizona, plants enables the resistance of the separate stages to be calculated. The average calculated values for the six stages of these plants agree to within 94% of the average measured values.

3. The major resistive factors found in the operation of the above plants are electrolyte resistance, ohmic polarization (due primarily to scale) and membrane potentials. Recommendations are made to reduce the latter two factors.

4. The minor resistive elements were found to be membrane resistance, electrode polarization, and parasitic duct losses. The membrane resistance in the first stage at Webster, S. D., represents about two percent of the total stack resistance. It is recommended that polarization effects be reduced even at the expense of increasing these minor resistive contributions, if necessary.

5. The electrical characteristics of the Webster and Buckeye plants were calculated based on assumed technological advances which can be made in operating techniques, improved hydrodynamics and use of exotic membranes. It was found that reductions in electrical resistance of from 15 to 45 percent are possible using these advances.

6. The resistive elements of a hypothetical sea water plant were also calculated by the method developed in this study. The results indicate that membrane resistance becomes an important factor. In the future, development of membranes for sea water use, low membrane resistance as well as reduction in ohmic polarization is a justifiable goal.

TABLE OF CONTENTS

APPENDIX C — Hydrodynamic Flow

APPENDIX D — Nomenclature

LIST OF ILLUSTRATIONS

LIST OF TABLES

1.0 INTRODUCTION

This is the final report of work under Contract 14-01-0001-676. An analytical engineering study of the electrodialysis process was performed and appropriate mathematical expressions were derived and applied to the calculation of the resistance of electrodialysis plants operating under a given set of conditions. The computed values are close to the actual plant operating values and indicate for the first time a quantitative breakdown and relative importance of the various factors which contribute to the electrical resistance.

Previous to this study no unified treatment of the electrodialysis process had been made. There did exist a large number of theoretical and laboratory studies on various subprocesses of electrodialysis. Engineering studies had also been made designed to give total operating costs of electrodialysis plants and costs of product water. In the latter studies, stack resistance assumed a minor role and did not require an analytical treatment. This study differs from former studies in that it is centered on the many electrochemical processes that constitute electrodialysis and contribute to stack operating characteristics. This study constitutes a preliminary attempt to analyze the operation of an electrodialysis plant by reducing all associated factors to an electrical resistance and unifies these factors by placing them in a network of resistive elements representative of the electrodialysis process.

The major objective of this study is to develop mathematical equations of an electrical network that is analogous to the electrodialysis process and that can be applied to both projected and present electrodialysis plants. The generalized equations contain parameters of operating plants and will facilitate computing the processing costs for a given water supply and set of operating parameters. The equations describe the resistive elements equivalent to discrete phenomena or subprocesses such as concentration polarization, ohmic polarization, bulk stream resistance, membrane resistance, electrical losses through ducts, water transfer processes, and membrane potentials.

This approach has provided a step of major magnitude in the understanding of electrodialysis plant operation. This study has resulted in an analytical tool, applicable not only to the analysis of the operation of large plants but the results pinpoint those technological advances in the processes which are required to lower plant operating costs and expand the utility of the process.

In this report each of the various resistive elements is discussed separately, and a resistance analogue expression is derived for each. The area resistance equivalent for each factor is calculated. The area resistances are then combined to give a total area resistance of a single cell pair. This procedure is applied to the electrodialysis plants at Webster, South Dakota; Buckeye, Arizona; a sea water plant; and a plant using assumed advanced technology. Recommendations concerning specific aspects of the electrodialysis process are given as a result of the calculations for the various plants.

2.0 PROGRAM OBJECTIVES AND SUMMARY

2.1 Program Objectives

The objectives of this study are as follows:

1. Formulate a general mathematical equation for electrodialysis by developing a unified electrical analogy concept in which critical component and subcomponent factors are represented in terms of an electrical resistance network.
2. Develop specific guidelines for future research and development work in improving electrodialysis technology by applying the equation to specific situations and determining how the variations in operating parameters and other variables influence performance and operating costs.

2.2 Summary of Specific Accomplishments

1. Engineering equations were derived that can be used to calculate the electrodialysis stack resistance and electrical operating costs if various operating parameters are known such as, water compositions, temperature, types of membranes, stack design, limiting current, operating current, flow rates, etc.

2. The use of the derived equations gives a breakdown of and allows a magnitude comparison of separate resistive components of the total process. This breakdown lists electrolyte resistance, resistance due to scale formation and membrane polarization among the major resistive elements and places membrane resistance and membrane concentration polarization among the relatively unimportant factors. Electrolyte resistance represents one-third of the total cell pair resistance for brackish water and two-thirds is due to a number of various polarization effects.

3. This study resulted in a number of recommendations for directing technical efforts to improve the electrodialysis process. These recommendations are listed below in Section 2.3.

4. Most of the resistive elements were calculated by integrating complex equations on a digital computer. Consequently, highly refined values were obtained and effects of changes in stack design can be readily evaluated.

5. An empirical correlation was made between ohmic polarization, operating time and current density. Equations were derived and

applied to operating plants. Estimates of ohmic polarization, which may involve phenomena such as scaling, fouling, and internal membrane changes, are quite high and suggest ohmic polarization as one of the most important and least understood of the membrane phenomena investigated.

2.3 Summary of Program Results

The objectives of this program were achieved by a four-phase study. During Phase I, Subcomponent Analysis, mathematical expressions were developed based on electrical analogies for each of the subcomponent factors influencing the operation of an electrodialysis system. The factors considered were concentration polarization, ohmic polarization, membrane selectivity, membrane resistance, parasitic electrical losses, electrode polarization, water transfer processes, concentrate and dialysate resistance, membrane polarization, and electrode polarization. The effects of hydrodynamic factors and temperature were included. The derivation of electrical resistive equations for each of the above factors is given in Section 3.0, Electrical Analogue Studies. Membrane, concentrate and dialysate resistances were combined into a single expression, designated as composite cell pair resistance. This expression, as well as that developed for membrane concentration polarization, parasitic duct losses, membrane selectivity, water transfer, membrane polarization, and electrode polarization, were translated into computer language to facilitate computations and to perform double integrations over the cross-sectional area of a membrane stack. A tool for studying design effects on these various resistive elements was thus introduced and successfully employed.

During Phase II, Integration of Subcomponent Mathematical Elements into a General Analytical Expression, the interrelationships between the resistive elements was studied and their combination into a general expression for a resistance network was accomplished. An expression for total stack resistance was then written in terms of the separate resistive elements and their combination into a resistance network. A simplified version of the resistance network for a single cell pair is given in Figure 1. The total current through an electrodialysis stack is the sum of i_1, i_2, and i_7. The currents i_8 and i_9 represent processes that do not actually conduct a current,

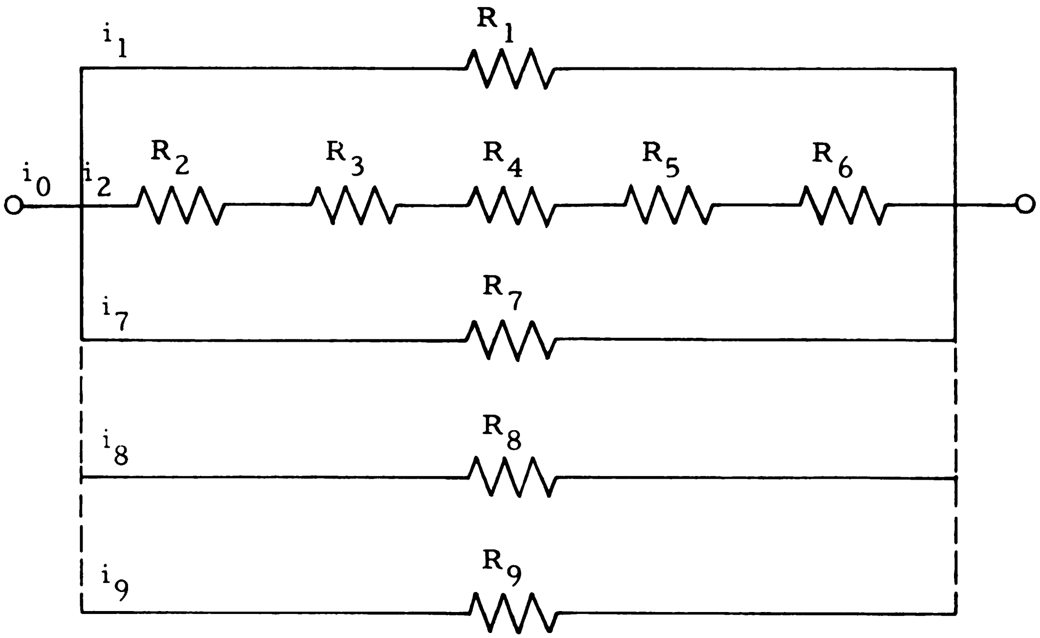

R_1 = parasitic duct resistance

R_2 - R_6 = cell pair resistances (composite cell pair, concentration polarization, ohmic polarization, membrane polarization, and electrode polarization)

R_7 = Co-ion transport through membranes

R_8 = water transfer loss (pseudo current loss)

R_9 = back diffusion of salt through membranes

C2221

Figure 1. Simplified Schematic of Cell Pair Resistive Network

however, their effect is to lower the efficiency of the desalting current, i_2; consequently, they are placed in parallel in the network. The cell pair resistance is then easily obtained from the algebraic expression for the total resistance of the network consisting of R_1 through R_7. Resistances R_2 through R_6 can be broken down to further series or parallel networks.

A power index, P_i, for a given stack design was then defined as

$$P_i = \frac{i R_p \Delta C}{\eta} \qquad (1)$$

where i is the stack current, R_p the stack resistance, and η is the current efficiency and ΔC is the change in dialysate concentration. The latter consists of the resistive elements R_7 and R_8 in Figure 1. This index is proportional to the power cost required for electrodialysis processing. A comparison of power indexes is possible for stacks of various designs, when product water rate, feed water concentration, and amount of total dissolved solids removed are held constant.

Under Phase III, Applications of Generalized Mathematical Solution to Specific Situations, the expression for the derived resistance network was applied to specific plant situations at Webster, South Dakota; Buckeye, Arizona; a hypothetical sea water plant; and a projected plant based on assumed advances in electrodialysis technology. A description of the calculation and combination of the resistive elements is given in detail in Section 3.3 of this report. A tabulation of results and comparison with the actual values are given in Tables I, II, III, and IV. The separate resistive component values are listed as well as their combined values. The calculations using assumed advanced technology is based on the Webster, South Dakota plant design. A comparison can thus be made of the present plant and what might be expected if certain advances are made in membrane performance, scale elimination, reduction of concentration polarization and membrane potentials.

Under Phase IV, recommendations on specific guidelines for future research and development work in improving electrodialysis technology were made. These recommendations are based on the analysis of the Webster and Buckeye plants, projected plants, and a hypothetical sea water plant. Recommendations are given below.

TABLE I

CELL PAIR RESISTANCE* OF WEBSTER PLANT

Stage	Composite Cell Pair	Concentration Polarization	Ohmic** Polarization	Duct Leakage	Selectivity	Membrane Polarization	Electrode Polarization	Cell Pair Resistance		Power Index
								Observed	Calculated	
I	102.25	7.16	109.59	225,363	4,496	56.3	0.234	303.9	259.3	6.90
II	136.42	10.06	106.17	247,869	5,674	94.6	0.309	369.4	327.1	4.07
III	185.16	13.20	84.21	273,688	7,230	173.1	0.610	459.0	428.8	1.75
IV	249.79	19.11	93.98	284,472	9,166	260.1	0.6179	567.3	581.4	1.34

* All resistance values in ohm cm^2 per cell pair.

**Rise in ohm cm^2 per cell pair for a 20 hour period.

TABLE II

CELL PAIR RESISTANCE* OF BUCKEYE PLANT

Stage	Composite Cell Pair	Concentration Polarization	Ohmic** Polarization	Duct Leakage	Selectivity	Membrane Polarization	Electrode Polarization	Cell Pair Resistance Observed	Cell Pair Resistance Calculated	Power Index
I	68.68	3.07	44	9,097	8,486	7.39	0.114	118.0	118.0	32.98
II	107.67	5.35	42	9,895	19,319	43.08	0.216	193.2	192.6	8.85

---

* All resistance values in ohm cm^2 per cell pair

**Rise in ohm cm^2 per cell pair for a 20 hour period.

TABLE III

CELL PAIR RESISTANCE* OF PROJECTED PLANTS

Stage	Composite Cell Pair	Concentration Polarization	Ohmic** Polarization	Duct Leakage	Selectivity	Membrane Polarization	Electrode Polarization	Cell Pair Resistance Calculated	Cell Pair Resistance % of Operating Stack***	Power Index
Webster, South Dakota										
I	100.02	3.83	10.9	—	—	17.93	—	132.7	51	3.42
II	134.20	5.38	10.6	—	—	44.04	—	194.2	59	2.40
III	182.79	7.07	8.4	—	—	108.13	—	306.4	71	1.24
IV	239.45	10.23	9.2	—	—	172.61	—	431.5	74	0.99
Buckeye, Arizona										
I	62.88	1.91	4.4	—	—	8.33	—	77.5	66	21.45
II	101.78	3.33	4.2	—	—	41.01	—	150.3	78	6.87

*All resistance values in ohm cm^2 per cell pair.

**Rise in ohm cm^2 per cell pair for a 20 hour period.

***Calculated value divided by calculated values from Tables I and II multiplied by 100.

TABLE IV

CELL PAIR RESISTANCE* OF SEA WATER PLANTS

Stage	Composite Cell Pair	Concentration Polarization	Ohmic** Polarization	Duct Leakage	Selectivity	Membrane Polarization	Electrode Polarization	Cell Pair Resistance Calculated	Power Index
I	18.32	0.344	30	54,772	7,121	3.10	—	51.4	80.46
II	21.85	0.525	30	86,327	9,736	8.71	—	60.7	10.31
III	29.60	0.962	30	105,301	12,460	49.75	—	109.3	2.80
IV	47.40	1.850	30	100,422	16,491	189.90	—	264.9	1.35
V	89.87	4.075	30	60,339	17,407	630.00	—	723.1	0.74

---

*All resistance values in ohm cm^2 per cell pair.

**Rise in ohm cm^2 per cell pair for a 20 hour period.

2.4 Recommendations

As a result of this study a number of recommendations concerning the electrodialysis process can be made.

1. The elimination or substantial reduction of ohmic polarization would significantly improve the economy of the process. This factor is the least understood of all those subprocesses encountered in this study. Although ohmic polarization is complex in nature, there appears to be no theoretical reason for not expecting improvement in this area. Ohmic polarization is considered to be due to build up of hard and soft scale, flocs, and opposing potentials that can build up within the membranes.

Improving the hydrodynamic flow at the membrane surface would reduce the diffusion layer concentration gradient and prevent formation of the hydroxide ion responsible for precipitation of hydroxides in the concentrate streams. There appears to be a relationship between spacer design and scale formation as indicated by an examination of used membranes which show scale formation occuring at specific locations relative to the spacer mesh. This relationship between local hydrodynamic flow and scale formation should be investigated.

Another approach for reducing ohmic polarization is to develop selective anion membranes to lower or limit the conduction of scale and floc forming ions into the concentrate stream. Work on cation membranes selective for calcium and magnesium has been considered in the past and appears feasible. It is reasonable to extend this approach to anion membranes as well.

The extremes to which membrane development for reduction of ohmic polarization can be carried is indicated by the relative effects of membrane resistance and ohmic polarization. Table I and Table IV give composite cell pair resistance for the four stages at Webster, S. D. The calculations were based on the assumption that membrane resistance for the projected plant (Table IV) was 50 percent of the membranes now in use (Table I). However, the composite cell pair resistance for Stage I differs only by two percent because most of the resistance is offered by the electrolyte streams. In the development of the selective membranes, it may be necessary to sacrifice good membrane conductivity for specific selectivity provided advantages of reducing polarization effects can be gained.

2. Methods of reducing membrane potentials must be considered to gain significant reduction in electrical power costs. Membrane potentials arise due to concentration differences across the membrane coupled with selective transport properties and are augmented by concentration gradients in the diffusion layers adjacent to the membrane. Elimination of the latter concentration gradients was assumed in calculating membrane potentials for the projected plants as given in Table IV. The latter values can be considered the lower limits obtainable with ideal flow conditions resulting in the elimination of the diffusion layer. A better understanding of the influence of spacer design on local hydrodynamic flow is required as an initial step to more effective spacer design. Concentration gradients can also be discharged by introducing pulsing and current reversal techniques as has already been suggested by other investigators. Studies, however, must be made to determine the magnitude of the advantages gained because current reversal will drastically reduce current efficiency.

3. Analytical studies to optimize plant design should be made. The breakdown of total stack resistance and capability to calculate separate resistive elements can readily be adopted to optimization of plant design and operating procedures. As was discussed above, the development of scale resistant membranes may require sacrificing good membrane conductivity. Once the characteristics of membranes are established, optimization of membrane choice can be made. Another obvious optimization is membrane potential. The method of feeding a multistage plant will influence both membrane potential and electrolyte resistance in an opposite manner. The two stages at the Buckeye plant use series feed for each of the inlet streams giving a greater membrane potential in the last stage than in the first due to larger concentration differences across the membrane. If series feed were used for the dialysate stream and parallel feed for the concentrate, as is done at Webster, lower concentration gradients would exist across the membranes resulting in lower membrane potentials.

Alterations in method of feed will also change electrolyte stream resistance and scaling tendencies. The latter is due to changes in calcium and magnesium ion concentration in the concentrate stream which will occur when different feed patterns are introduced. Because many of the resistive elements have common factors, design alterations optimum for one may not necessarily guarantee optimization for the other factors, or their net result. Optimization of design is possible, however, when all resistive factors are considered simultaneously as can be done by the general network equation derived in this study.

4. Data from operating plants must be obtained to further refine and develop more extensive and meaningful electrical analogue expressions. Although OSW contractors were extremely helpful in providing data presently available on the operations of their plants, it was found that a vast amount of data remain unknown. Knowledge of water analyses and how it varies with stack performance, analyses of electrode streams and water transport data are few or lacking completely. As discussed above, the ohmic polarization factor is one of the most important resistive components. However, only a two-parameter equation based on empirical correlations was found to approximate this factor. Certainly, this phenomenon must be influenced by several factors such as spacer design and hydrodynamics, temperature, nature of the membrane, the presence of certain anions and cations in addition to calcium and magnesium, flow rate, pretreatment, feed method and suspended solids. There are far more variables that should be considered and which require much more plant operating data to more fully understand the ohmic polarization terms.

5. Membrane research must be pursued from the standpoint of reducing both short and long term polarization effects. Membrane resistance is a minor consideration in seeking these improvements. Polarization effects determine cost factors exclusive of the electrical power costs. Scale and floc formation require special operating procedures, pretreatment, pulsing, acid backwashing, membrane breakage, and replacement. Advanced membranes that can aid in the reduction of these costly factors need not exhibit low membrane resistance because of the insignificance of the latter factor compared to total operating cost. The electrical power costs approximate less than ten percent of the total cost picture for electrodialysis processing.(1) Membrane resistance in the first stage at Webster,

South Dakota is about one percent of the total stack resistance. Certainly, sacrifices in membrane conductivity can justifiably be made to reduce the scaling problems.

6. The above recommendations (3) and (4) can be the subjects of an effective advanced study using the electrical analogue approach. Much of the required data for refinement of the study can be obtained using a portable 1000 GPD test stack which can be operated at a number of sites having different feed waters. Completion and refinement of the optimization equations could then be used to optimize a test stack design for each site or water type. Operation and testing the optimized designs at the various sites would be a final phase of the program. The use of any advanced electrodialysis technologies such as inorganic membranes, and special operating procedures such as pulsing and current reversal should definitely be a part of this program.

2.5 Personnel

Astropower personnel who participated in this study are Dr. C. Berger, principal investigator, Dr. G. A. Guter and Mr. G. Belfort. Dr. K. S. Spiegler participated in this study as consultant to Astropower. Mr. Robert Hubata of Astropower assisted with some of the calculations.

3.0 ELECTRICAL ANALOGUE STUDIES

3.1 Phase I — Subcomponent Analysis

A discussion and review of a number of subcomponent factors of the electrodialysis process will be undertaken in this section. For each subcomponent factor, the resistance-analogue (ohms-cm^2/cell pair), will be preceded by a summary of the present state of the art. These resistance values are combined and calculated in Sections 3.2 and 3.3 using data obtained from the electrodialysis plants at Webster, South Dakota, and Buckeye, Arizona.

3.1.1 Membrane Polarization

Extensive experimental work has been,(2) and is being,(3) done to quantitatively explain the phenomena of membrane polarization. The dialyzing current faces a two-fold polarization effect close to the membrane surface. A concentration gradient across the diffusion layer and scale formation are the respective causes of such polarization. The former is termed concentration polarization while the latter is called ohmic polarization. Each is separately discussed and evaluated below.

3.1.1.1 Concentration Polarization

It is possible to estimate the approximate resistance due to concentration polarization that the dialyzing current faces, provided two important system parameters can be calculated. These are the thickness (δ) of and the concentration gradient and profile across the diffusion layer.

Several empirical approaches,(4) such as use of the Chilton-Colburn transfer factors and the flux equation of Fick, are able to predict the diffusion layer thickness for nonspace-filled compartments. Because in all practical electrodialysing plants spacers or turbulent promoters are used, these theoretical equations are not applicable. H. P. Gregor, et. al.(5) have studied and measured experimentally, using various size spacers at different compartment flow rates and Reynolds numbers, the relation of the diffusion layer-thickness with flow rates. Figure 2 depicts this relationship, while Table V provides the channel and spacer dimensions.

For flow rates greater than half a gallon per minute, δ, the diffusion layer thickness, can be predicted from the straight line relationship obtained from the lower curve in Figure 2, viz,

$$\delta = 30 - 10.7\ Q \text{ microns} \tag{2}$$

where

Q = superficial volumetric flow rate, G. P. M. /compartment

$$Q = 0.00138 \left(\frac{\text{G. P. D.}_p}{M_s} \right) \text{, gal/min, channel} \tag{3}$$

M_s = membranes/stack

G. P. D._{pw} = gal/day of product water

To calculate the diffusion layer resistance that the dialysing current must pass through, an average resistivity calculated as an average salt concentration within the diffusion layer must be obtained. Refer to Figure 3 for the diagrammatic explanation. The resistivity at the bulk inlet $(\rho_b)_i$ and bulk outlet $(\rho_b)_o$ are known. The resistivity at the surface inlet and outlet is now obtained by estimating the salt concentration at these coordinates. Most empirical(2) and theoretical(6) equations available to do this are not applicable to spacer filled configurations and so the Nernst idealized equation will be used as an approximation. Together with several simplifying assumptions,(2) the Nernst equation also presupposes a linear concentration gradient.

$$\frac{dc}{dx} = \frac{i(\bar{t} - t)}{FD} = \frac{(c - c^1)}{\delta} \tag{4}$$

where

δ = diffusion layer thickness, cm

$\bar{t}, t$ = transference numbers of counter ion in membrane in bulk solution respectively

i = current density, amp/cm^2

F = Faradays constant, coulombs/gm equiv.

D = Diffusion coefficient of electrolyte

c^1, c = Concentration of ions at membrane surface and in bulk solution respectively, gm equiv/cc

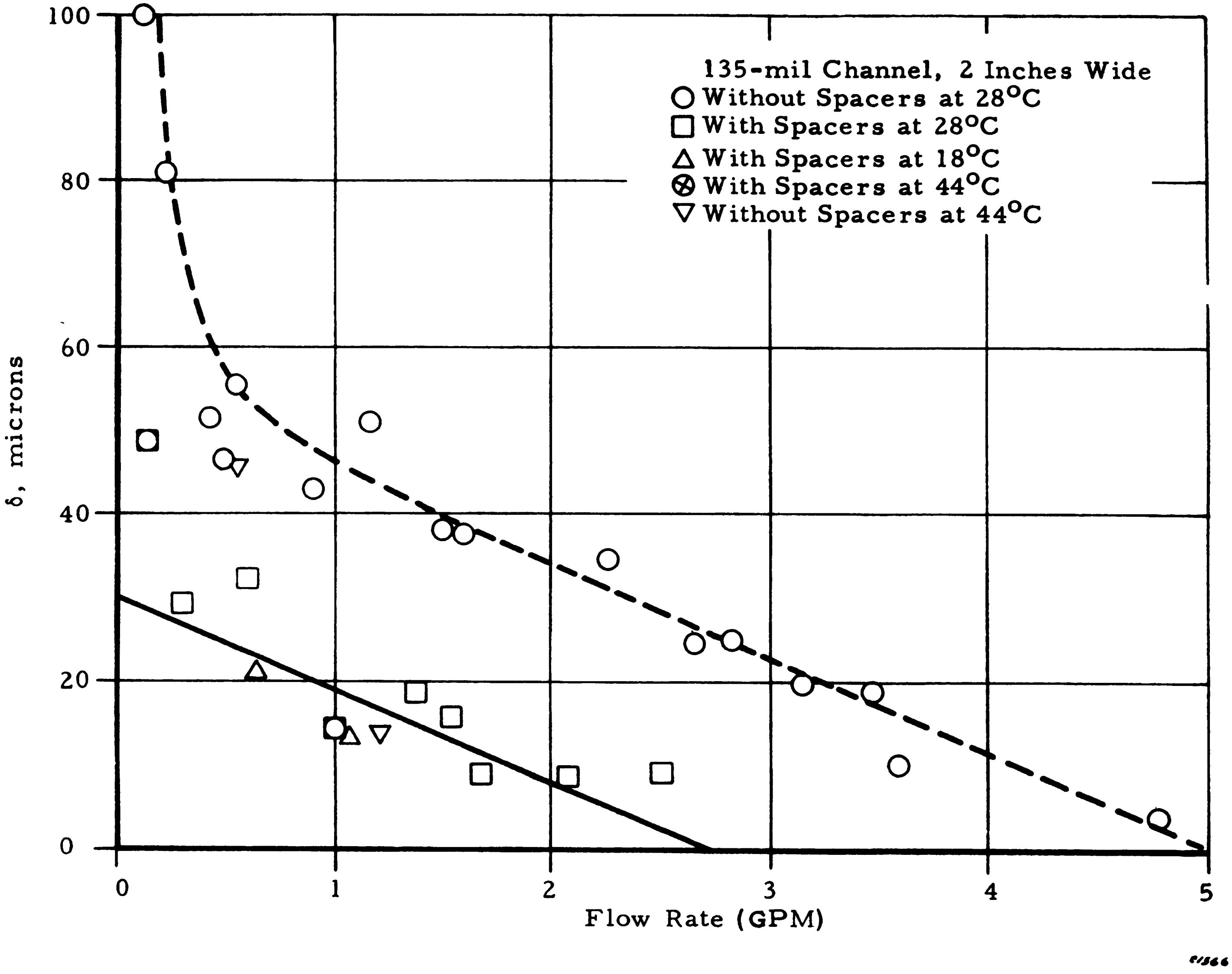

Figure 2. Boundary Film Thickness as a Function of Volumetric Rate of Flow

TABLE V

SEPARATOR AND CHANNEL DIMENSIONS

Channel Thickness, Mils	Separator Designation	Hydraulic Radius Ft. x 10^{+3}	Area Sq. Ft. x 10^{+3}	ν_o/ν [(b)]
42	1/11-inch mesh, 1.00-mm OAT[(a)]	1.72	0.58	1.90
72	1/11-inch mesh, 1.75-mm OAT	2.89	1.00	1.38
135	1/1-inch mesh, 1/1-inch OAT; 1/11-inch mesh, 0.15-inch strand	5.27	1.85	1.41
270	1/1-inch mesh, 1/1-inch strand; 1/11-inch mesh, 1.75-mm OAT	9.91	3.70	1.26

(a) Overall thickness

(b) Ratio of the volume of water displaced per unit length of compartment without a separator, to the volume of water displaced per unit length of compartment with a separator.

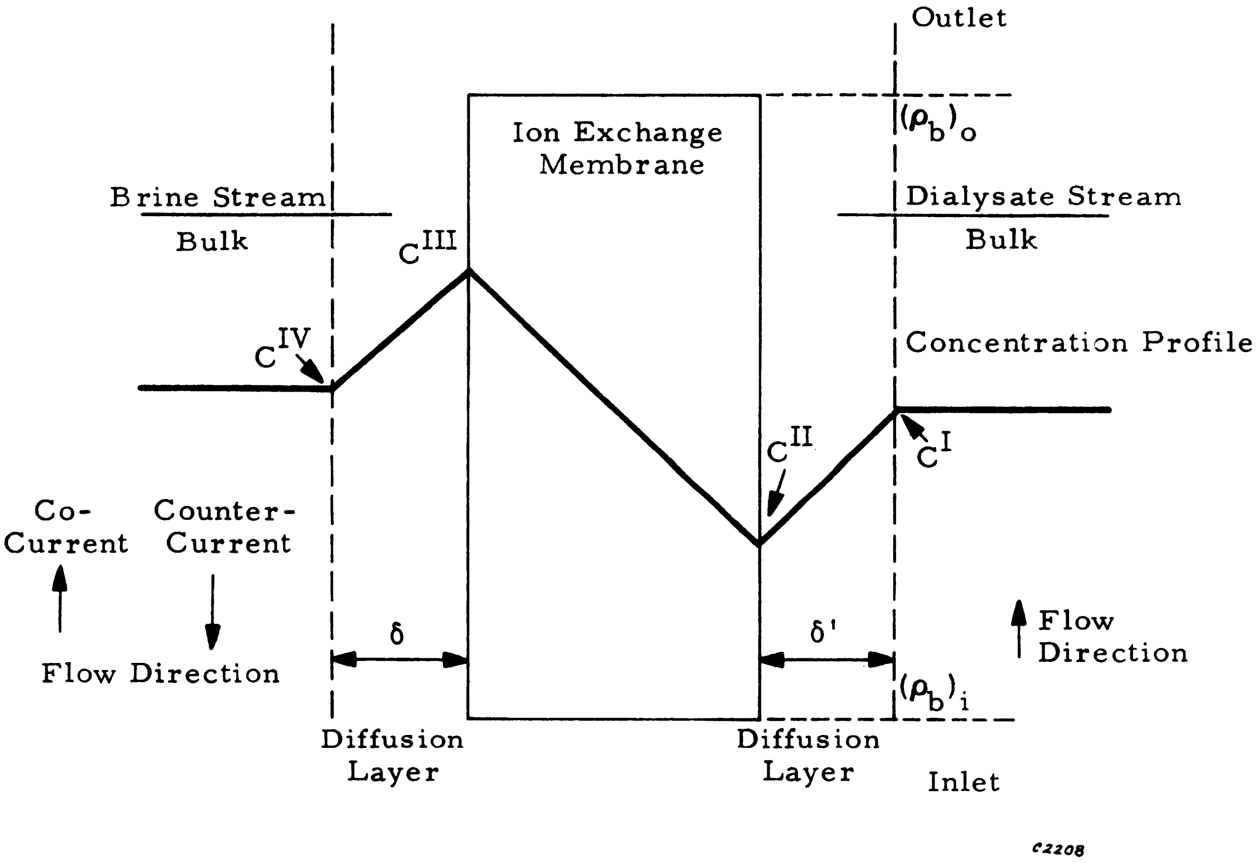

Figure 3. Diagram of the Concentration Profile and the Diffusion Layer on Each Side of an Electrodialysis Ion Exchange Membrane

The current density, i, must be estimated before the Nernst equation can be used. Limiting current density (i_{lim}) will occur when the exit concentration of the dilute stream $(\rho_m)_o$ shown in Figure 3, reaches zero, providing the fluid velocity and diffusion layer thickness are constant.

$$\left(\frac{i}{C}\right)_{lim} = \frac{FD}{\delta(\bar{t} - t)} \tag{5}$$

E. A. Mason and T. A. Kirkham$^{(7)}$ use the following experimental relationship to determine the operating current density with varying flow rates.

$$\left(\frac{i}{C_d}\right)_{lim} = 590\,(v)^{0.6} \tag{6}$$

where

i = current density, ma/cm^2

C_d = dialysate concentration, gm equiv/l

v = dialysate linear velocity, cm/sec

Since Equation (6) is peculiar to the Ionics membranes (Nepton Ar-111 and CR-61), a short experiment similar to that described by Mason and Kirkham$^{(7)}$ would have to be undertaken to determine the operating current density for the particular membranes under study.

The Asahi Chemical Company$^{(8)}$ has correlated the polarization factor with linear velocity of the dialysate stream for their particular membranes with sea water.

$$\left(\frac{i}{C}\right)_{lim} = 72.3\,(v)^{0.947} \text{ at } 20^\circ\text{C} \tag{7}$$

where

i = current density, amps/cm^2

C = log mean concentration between inlet and outlet, desalting stream, gm equiv/cm^3

v = dialysate linear flow velocity, cm/sec (valid for v = 3 to 10 cm/sec)

Since the equations above all apply to conditions at room temperature (25°C), $\left(\frac{i}{C}\right)_{lim}$ will be corrected using a temperature correction derived from the recent work done at the Sea Water Conversion Laboratory in Berkeley.(9) Refer to Figure 4. At a given product concentration, the correction factor at some temperature t°C will be,

$$\text{C. F.} = \left[\frac{\left(i_{\text{lim}}\right)_{t^\circ C}}{\left(i_{\text{lim}}\right)_{25^\circ C}} \right] \tag{8}$$

Therefore, the new, or temperature corrected, limiting current density will be

$$\left(i_{\text{lim}}\right)_{t^\circ C} = \left(i_{\text{lim}}\right)_{25^\circ C} \times \text{C. F.} \tag{9}$$

In a hypothetical plant, the K ratio ($= i_{\text{oper}}/i_{\text{lim}}$), which appears in many of the following analogue derivations, can be optimized, but in this treatment, because the equation will be derived and applied to two existing electrodialysis plants, the K ratio per stage is fixed as each stage capacity (salt transferred/unit time) is given. Using Faraday's Law and a material balance, the capacity is defined as,

$$\text{Cap} = \frac{ieA_p n}{F} = F_d n C_{di} f \qquad \frac{\text{gm equiv transferred}}{\text{sec.}} \tag{10}$$

Since,

$$i_{\text{oper}} = \frac{F\,F_d C_{di} f}{eA_p} \qquad \text{Amps/m}^2 \tag{11}$$

where

F = Faraday's constant, coul/gm equiv.

F_d = volumetric flow rate, l/sec, channel

C_{di} = inlet dialysate concentration, gm equiv. / l

f = fraction desalted

e = coulomb efficiency

A_p = desalination area, cms.

Two methods, concerning the prediction of the average resistivity using the Nernst Equation(4) diffusion layer, present themselves. Refer to Figure 3. The first method requires the average

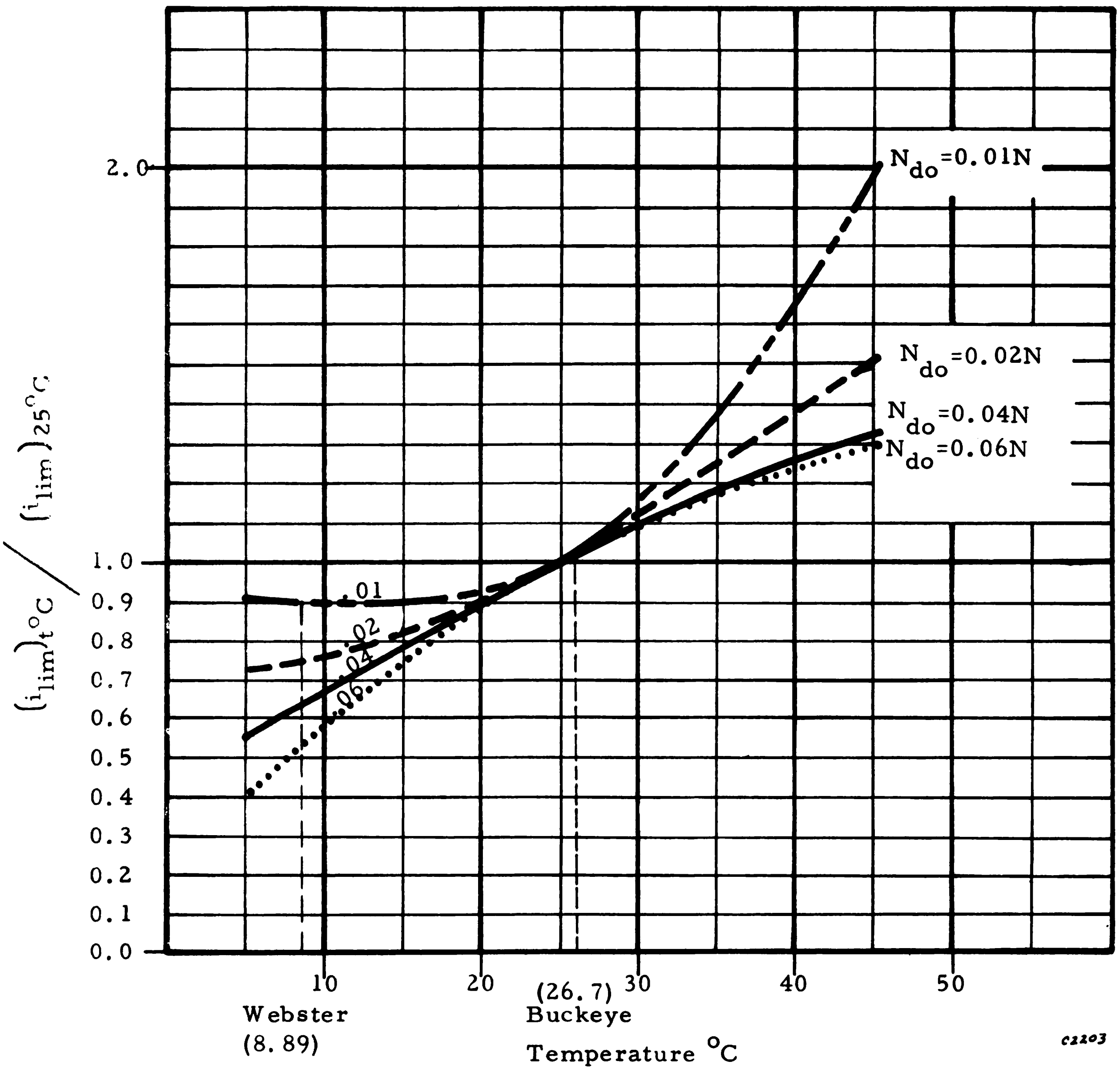

Figure 4. Plot of the correction Factor $\left[\text{C.F.} = \frac{(i_{lim})\ t^\circ C}{(i_{lim})25^\circ C} \right]$ Versus Temperature of Fluids at Various Product Concentrations
Exit Dialysate Concentration≡N_{do}

resistivity (surface and bulk) at the inlet and outlet to be evaluated from the general equation,

$$p = \frac{1000}{\Lambda C} \quad \text{ohms-cms} \tag{12}$$

where

C = concentration, gms/liter

Λ = equivalent conductance.

This simple average resistivity can be refined by replacing it with a double integrated value. This is the second and far more accurate method. Here a straight-line concentration profile is not assumed (see Equation 17).

The double integration will be performed across the diffusion layer (x co-ordinate) and along the flow path (z co-ordinate).

$$\frac{1}{R_{\text{total}}} = \frac{1}{h} \int_{z=0}^{m} \left[\frac{I}{\int_{x=0}^{\delta} \rho_{x,z}\, dx} \right] dz \tag{13}$$

From the basic definition of resistivity and the Onsager equation, we get

$$(\Lambda_V)_{t^oC} = (\Lambda_\infty)_{t^oC} - (A + B\,(\Lambda_\infty)_{t^oC}\sqrt{C} \tag{14}$$

$$\rho_{x,z} = \frac{1000}{(\Lambda_V)_{t^oC}\, C_{x,z}} = \frac{1000}{(\Lambda_\infty)_{t^oC}\, C_{x,z} - C_{x,z}^{3/2}\,(A + B\,(\Lambda_\infty)_{t^oC}} \tag{15}$$

After $\rho_{x,z}$ is substituted in Equation (13), $C_{x,z}$ as a function of x and z has to be evaluated from the boundary conditions. Note also that the surface concentration, C^{II}, is related to the bulk stream concentration, C^{I}, as follows:

$$C^{II} = (1 - K)\, C^{I} \tag{16}$$

where

$K = i_{oper}/i_{lim}$

The following general equation for $C_{x,z}$ can be written

$$C_{x,z} = ax + bz + cxz + d \tag{17}$$

The four constants, a, b, c, d can be evaluated in terms of the surface and bulk concentrations at the inlet and outlet. If we assume a constant, K, the four constants above are readily evaluated. The validation of this assumption is based on the fact that both the operating and the limiting current vary similarly with the concentration (i. e., along the flow path, z).

The concentration polarization resistance component is evaluated for the dialysate stream and anion exchange membrane,

$$R_{c.p.} = R_{total} \text{ from Equation (13)}$$

A slightly different surface to bulk relationship from Equation (16) exists for the bulk stream. Refer to Figure 3.

$$\begin{aligned} C^{III} &= (C^{IV} - C^{I}) + (C^{I} - C^{II}) \\ &= C^{IV} - C^{II} \\ &= C^{IV} - (1 - K)\, C^{I} \end{aligned} \tag{18}$$

We obtain Λ, the equivalent solution conductance, from the Onsager Equation at various temperatures and concentrations.

$$(\Lambda)_{t^{o}C} = (\Lambda_{\infty})_{t^{o}C} - \left[A + B\,(\Lambda_{\infty})\right]_{t^{o}C} \sqrt{C} \tag{14}$$

$$(\Lambda_{\infty})_{t^{o}C} = (\Lambda_{\infty})_{25^{o}C} \left[1 + 0.023\,(t - 25)\right] \tag{19}$$

$$\begin{aligned} (\Lambda_{a})_{25^{o}C} &= \frac{1}{2}\left[(\Lambda_{\alpha})_{25^{o}C,\ \text{Feed}} + (\Lambda_{\alpha})_{25^{o}C,\ \text{Product}}\right] \\ &= \frac{1}{2}\Big[(\iota^{\alpha}_{\frac{1}{2}Ca^{++}}\,(f_{p} + f_{f})_{\frac{1}{2}Ca^{++}} + \iota^{\alpha}_{\frac{1}{2}Mg^{++}}\,(f_{p} + f_{f})_{\frac{1}{2}Mg^{++}} + \\ &\qquad \iota^{\alpha}_{Na^{+}}\,(f_{p} + f_{f})_{Na^{+}} \text{ etc.}\Big] \end{aligned}$$

$$= \frac{1}{2}\left\{\left[59.5\,(f_p + f_f)_{\frac{1}{2}Ca^{++}} + 53.06\,(f_p + f_f)_{\frac{1}{2}Mg^{++}} + 50.11\,(f_p + f_f)_{Na^{+}}\right] + \left[76.34\,(f_p + f_f)_{Cl^{-}} + 44.48\,(f_p + f_f)_{HCO_3^{-}} + 79.8\,(f_p + f_f)_{\frac{1}{2}SO_4^{=}}\right]\right\} \quad (20)$$

where

$(\Lambda)_{t^oC}$ = equivalent conductance at the existing concentration and t^oC

$(\Lambda_\alpha)_{t^oC}$ = equivalent conductance at infinite dilution and t^oC

$(f_p)_x$, $(f_f)_x$ = fraction in product and feed streams in e.p.m. of ionic species X

C = average concentration of salts in the water, equivalent/liter

A, B = temperature and ionic species dependent constants (see Figure 5 for plot of A, B, versus temperature)

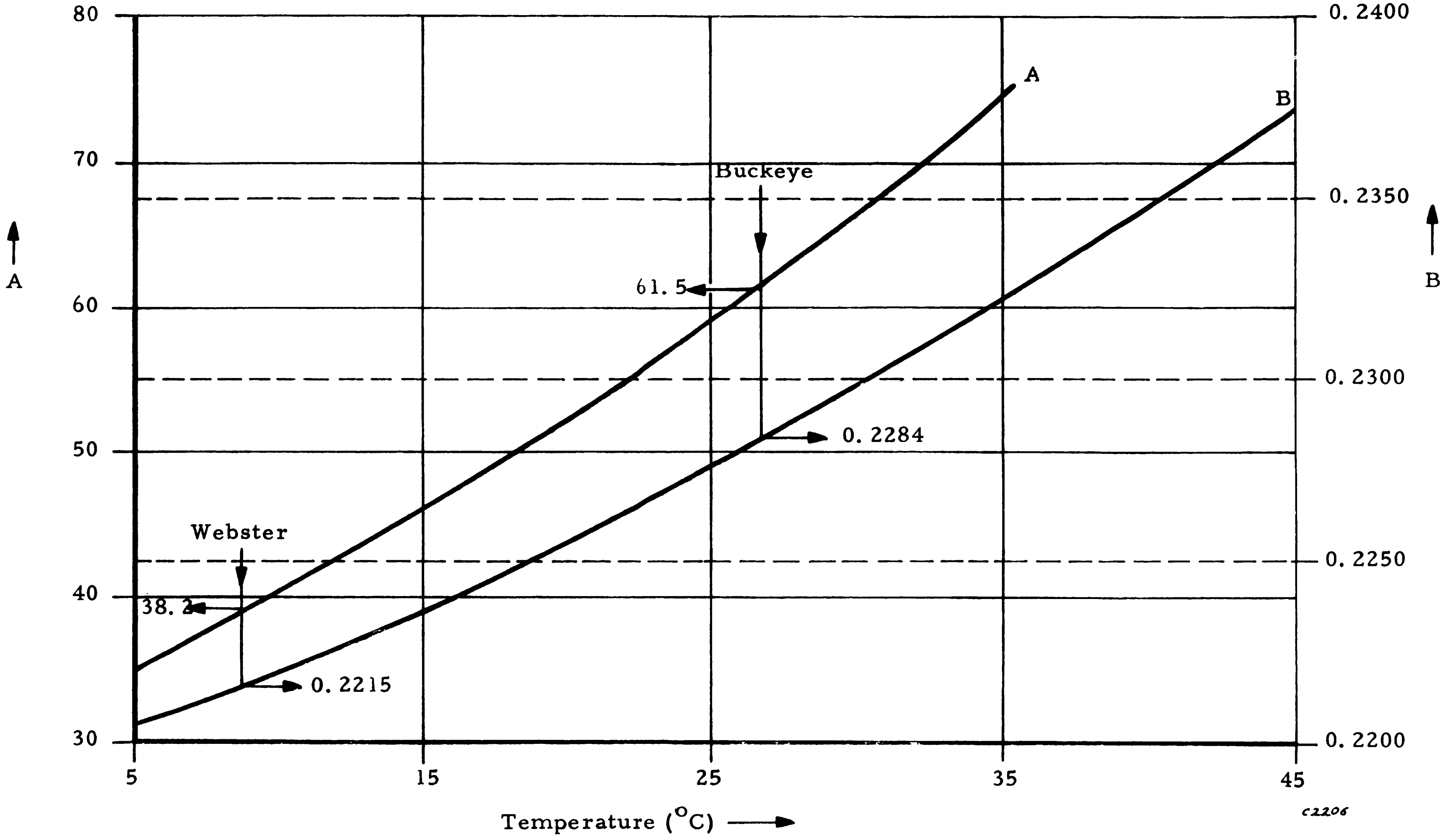

Figure 5. Constants A and B (From Onsager Equation) Versus Temperature °C

3.1.1.2 Estimation of Ohmic Polarization

Ohmic polarization involves a number of complex and interrelated factors. It is associated with scale formation and other effects that contribute to resistance rise with operating time in the order of hours and days. Scales differ in their chemical and physical character as well as the processes by which they are formed. Certain scales are loosely formed and can be removed by simply flushing the stack. Other scales are hard and can be removed only by removing and scrubbing membranes, a frequent cause of breakage. Scale formation can also occur within a membrane and greatly shorten its lifetime. Flocs and other membrane deposits can occur. Calcium sulfate and other insolubles can come out of solution as local concentrations rise on a membrane surface. Trace organic materials can also dissolve in the membranes over a long period of time and change the conductivity drastically.

Calcium carbonate scaling of anion permeable membranes is closely associated with concentration polarization. Operation near and above the limiting current density results in water breakdown into H_3O^+ and OH^- ions at the membrane interface and transfer of OH^- ions through the anion membrane. The OH^- ions convert biocarbonate ions to carbonate, which in turn combines with calcium to form a scale.

$$HCO_3^- + OH^- \longrightarrow H_2O + CO_3^=$$

$$Ca^{++} + CO_3^= \longrightarrow CaCO_3 \text{ (scale)}$$

Ohmic polarization can thus be expected to vary with electrolyte composition, current density, limiting current density, concentration polarization, local hydrodynamic conditions as influenced by spacer design and flow velocity, and pretreatment procedures. It has also been suggested that membranes can undergo an orientation polarization which is an internal polarization by reorientation of the polar groups and thereby setting up a potential opposing the applied potentials.(8)

The task of writing a resistance analogue expression for the ohmic polarization factor is further encumbered by a lack of plant and experimental data on this phenomenon. Some data have been collected using a small test stack at the Webster plant. Figure 6 shows the rate of resistance change with continuous operating current. The influence of current is obvious. This data was obtained using Webster water which had not been treated with sulfuric acid. Resistance buildup is due to deposition of calcium carbonate and calcium sulfate scales as well as ferric hydroxide floc and inorganic materials which evade the pretreatment filters. The orientation polarization may also be operative. The data of Figure 6 were found to satisfy an equation of the general type

$$\frac{dR}{dt} = ae^{bK} \tag{21}$$

where a and b are constants. This correlation is represented in Figure 7 where log (dR/dt) shows a linear relationship with I, the stack current.

The ohmic polarization values in Table I through IV were calculated using Equation (22) which is equivalent to Equation (23)

$$\log R_{ohmic} = 0.150 + 0.92K \tag{22}$$

$$R_{ohmic} = 1.41\ e^{2.12K} \tag{23}$$

where

R_{ohmic} is rate of rise in ohm cm^2 per cell pair per hour

K is the ratio of operating current to limiting current

These constants in Equations (22) and (23) were chosen to give the best fit of these equations to the available data. A comparison of calculated values and observed values for ohmic polarization is given in Table VI. The observed values for the Webster and Buckeye Plant were calculated by assuming that the major differences between observed cell pair resistance and the value calculated using all factors other than ohmic polarization were due to the latter factor.

The equation gives surprisingly good results based on the theory and data limitations. It should be pointed out, however, that Equation (23) isonly an approximation at best. It should also be noted that

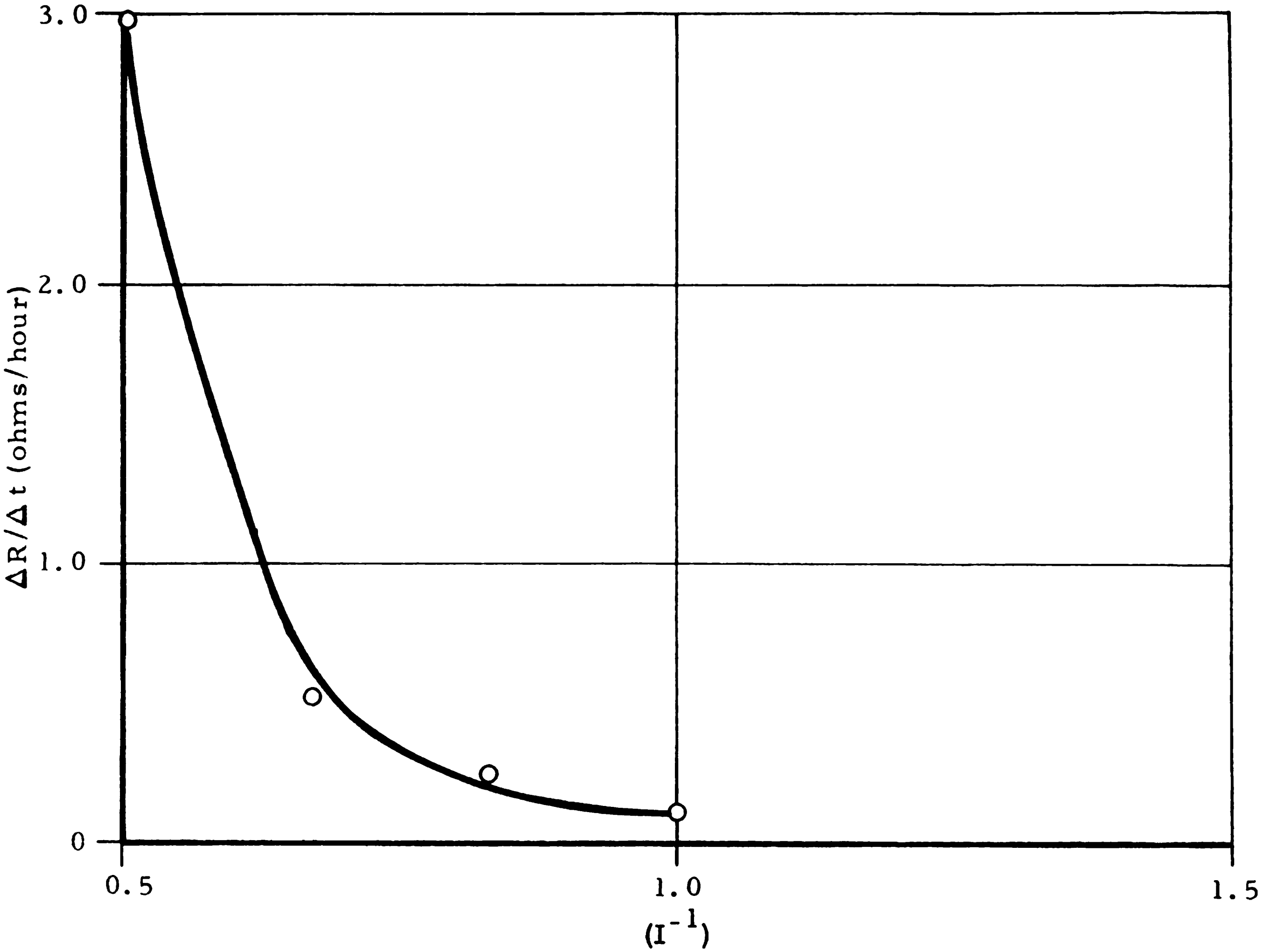

Figure 6. Relationship Between Rate of Resistance Change and Reciprocal of Stack Current

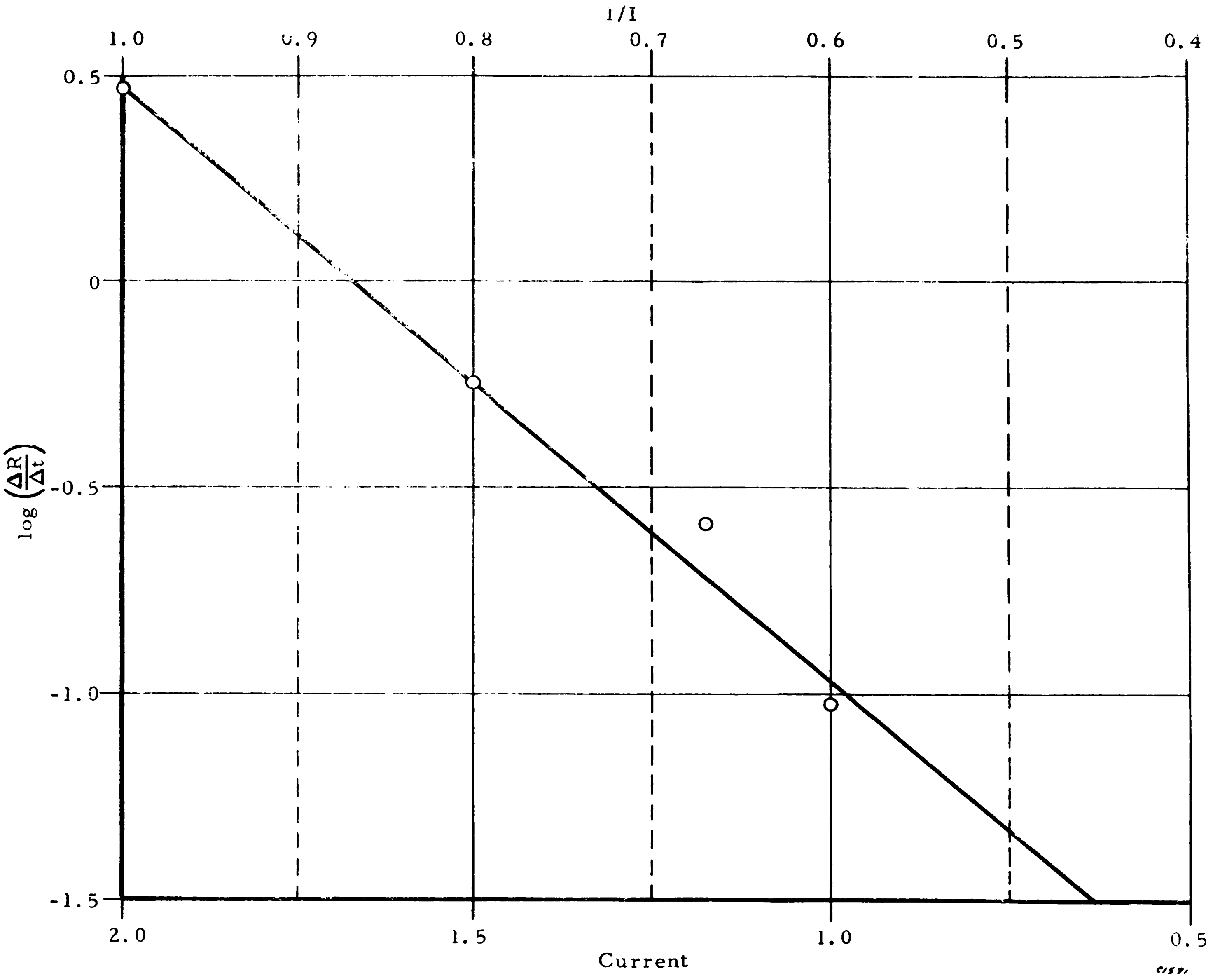

Figure 7. Linear Relationship Between Rate of Resistance Change and Stack Current

TABLE VI

COMPARISON OF CALCULATED AND OBSERVED OHMIC RESISTANCE CHANGE WITH TIME

	R_{ohmic}[a]	
	Observed	Calculated
	Webster Test Stack(b)	
i/i_{lim}		
203	156	105
1.52	29	35
1.21	13	18
1.00	4.9	12
	Webster Plant	
.64	7.6	5.5
.63	7.3	5.4
.52	5.8	4.3
.56	4.1	4.6
	Buckeye Plant	
.20	2.1	2.2
.18	2.1	2.1

a) ohms cm^2 per hour per cell pair

b) Five pair test stack, 260 cm^2 membranes.
Data supplied by Dr. John Nordin.

R_{ohmic} is very sensitive to i/i_{lim}. This ratio can vary from time to time during stack operation. It is also probable that i_{lim} can change during this time.

Three general methods are used to prevent the increase of electrical and flow resistance in the stack.

1. Pretreatment to slow or prevent scale formation
2. pH adjustments to acid conditions, preventing the precipitation of the carbonates and the hydroxides
3. Removal of the partially or fully formed deposits by a reversal of polarity and a reversal of the flow streams.

The importance of polarity reversal techniques is the ability to control the place, form, and time of scale formation during a continuous operation. The mechanism can be explained as follows. (10)

Refer to Figure 8. Before the voltage is applied (Figure 8a), the concentration profile is horizontal for both streams. After about 30 seconds, (11) steady state is reached (Figure 8b), and the concentratia's maximum and minimum is at the surfaces. When a short reversal of polarity is imposed on the system, for a short time Δt_p, concentration minima and maxima move (Figure 8c) a short distance away from the membrane surface where the fluid flow is not stagnant but can flush the precipitate deposited at the minima and maxima out of the compartment. In a short time the concentration gradients will smooth out on reversal to normal polarity (Figure 8d).

3.1.2 Electrode Polarization (12, 13)

It is proposed to develop an electrode analogue resistance ($R_{anode\ and\ cathode}$), that will describe the various resistive components within the electrode compartment due to the bulk solution, the diffusion layer and kinetic phenomena at the electrode surface. A short general electrode discussion on each overpotential will now follow and thereafter, the equations developed, will be specifically applied to the cathode and anode cases that occur in electrodialysis.

The passage of current through each of the electrode compartments involves three steps:

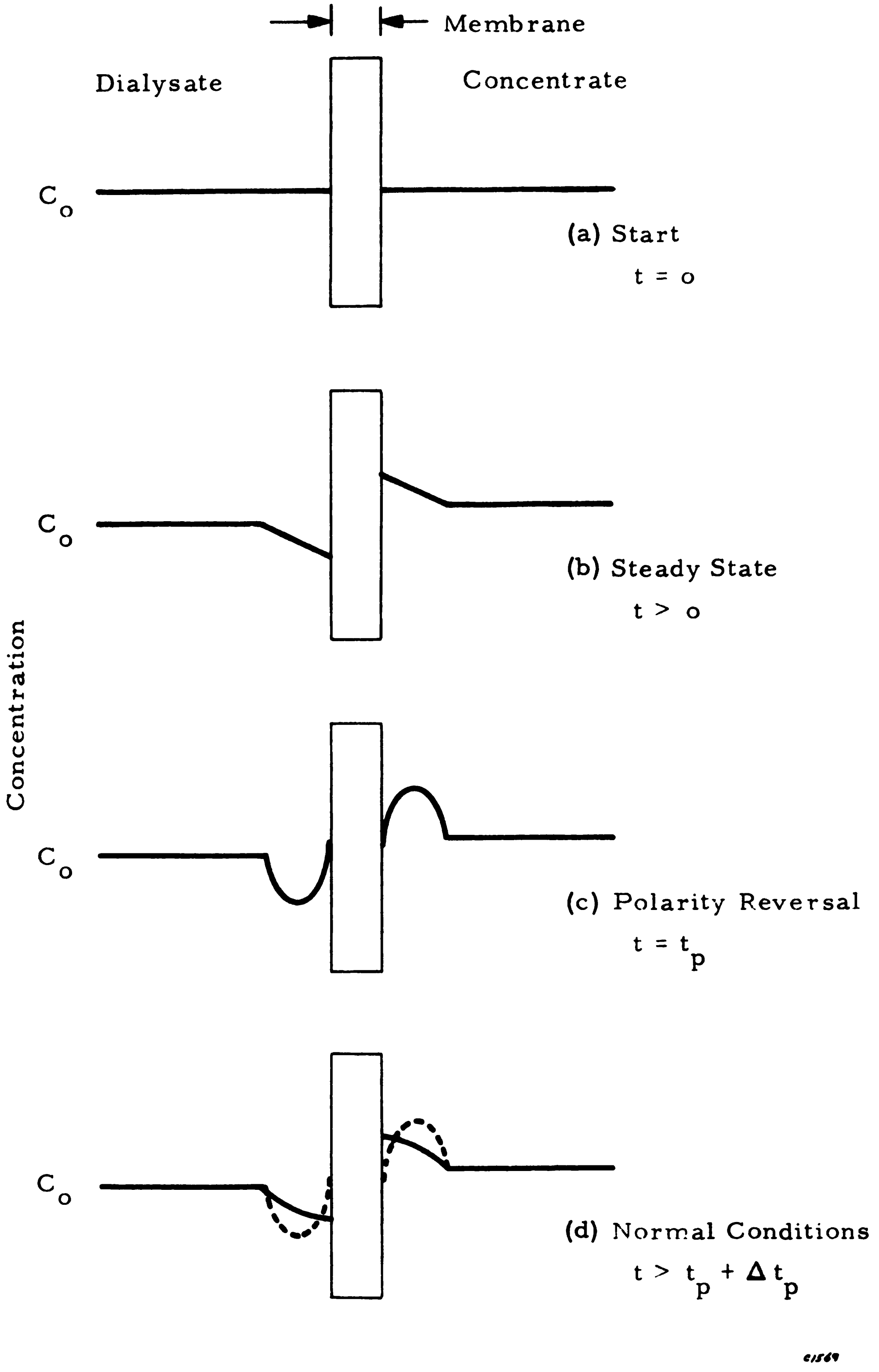

(a) Start
$t = o$

(b) Steady State
$t > o$

(c) Polarity Reversal
$t = t_p$

(d) Normal Conditions
$t > t_p + \Delta t_p$

Figure 8. Development of Membrane Polarization
(▬▬ Concentration Profile)

1. The transfer of ions from the bulk of the solution to the surface of the electrode.
2. The electrochemical reaction at the electrode.
3. The formation of the final products of the reaction and their removal from the electrode surface.

3.1.2.1 Concentration Overpotential

When the current is flowing the ions that discharge migrate towards the electrode and cause a concentration gradient across the thin diffusion layer at the electrode surface. This phenomenon is exactly analogous to the concentration gradient that occurs at the ion exchange membranes. The concentration gradient leads to a change in electrode potential of

$$\eta_{conc} = \frac{-RT}{F} \ln \frac{c_{bulk}}{c_{surface}} \tag{24}$$

Differentiating (24) with respect to i, and noting that

$$\frac{c_{bulk}}{c_{surface}} = \frac{1}{1 - K} = \frac{1}{1 - i/i_{lim}} = \left(\frac{i_{lim}}{i_{lim} - i} \right) \tag{25}$$

(See Section 3.1.1.1.1.)

we get

$$R_{conc} = \frac{RT}{F} \frac{\alpha}{\alpha_i} \ell n \frac{i_{lim} - i}{i_{lim}}$$

$$= - \frac{RT}{F} \cdot \frac{i_{lim}}{i_{lim} - i} \frac{1}{i_{lim}} = - \frac{RT}{F} \left(\frac{1}{i_{lim} - i} \right) \tag{26}$$

3.1.2.2 Chemical Overpotential

The chemical overpotential η_{chem} is defined to be that potential in excess of the discharge potential for the given reaction which must be applied to the cell in order to maintain a finite rate of discharge. Chemical overpotential occurs as a result of steps (2) and (3) above. The value of η_{chem} for the electrode reaction is given by Tafel's Formula:

$$\eta_{chem} = a + \frac{RT}{\alpha F} \ell n\, i, \tag{27}$$

where

$\alpha \approx \frac{1}{2}$, and

a = constant (depends on nature of cathode).

Differentiating (27) with respect to i;

$$R_{chem} = \frac{RT}{\alpha F}\left(\frac{1}{i}\right) \tag{28}$$

3.1.2.3 Ohmic Overpotential

The ohmic overpotential ($\Delta\varphi_{ohm}$) consists of two parts, namely the voltage drop which occurs in the bulk solution of constant concentration plus the voltage drop across the diffusion layer where the concentration gradient varies linearly with the current density.

$$\Delta\varphi_{ohm} = \Delta\varphi_{sol} + \Delta\varphi_{\delta} \tag{29}$$

Differentiating (29) with respect to i,

$$R_{ohm} = R_{sol} + R_{\delta} \tag{30}$$

The first term R_{sol}, is evaluated by the same procedure as in Section 3.1.3, providing the bulk solution chemical analysis is known.

$$R_{sol} = \frac{\rho_{mean}\,\ell}{A_p} \tag{31}$$

R_{δ} may be evaluated by specifying the resistivity at any point within the diffusion layer as a function $\rho(x, y)$ and by computing the double integral of this function as was done in Section 3.1.1 for the case of membrane polarization. The relationship between each resistance component and current density is shown in Figure 9.

3.1.2.4 Cathodic Resistance Analogue

Consider first the passage of current in the cathode compartment. The total change in potential across the cathode compartment is

$R_{ohm} = R_{sol} + R_{diff}$

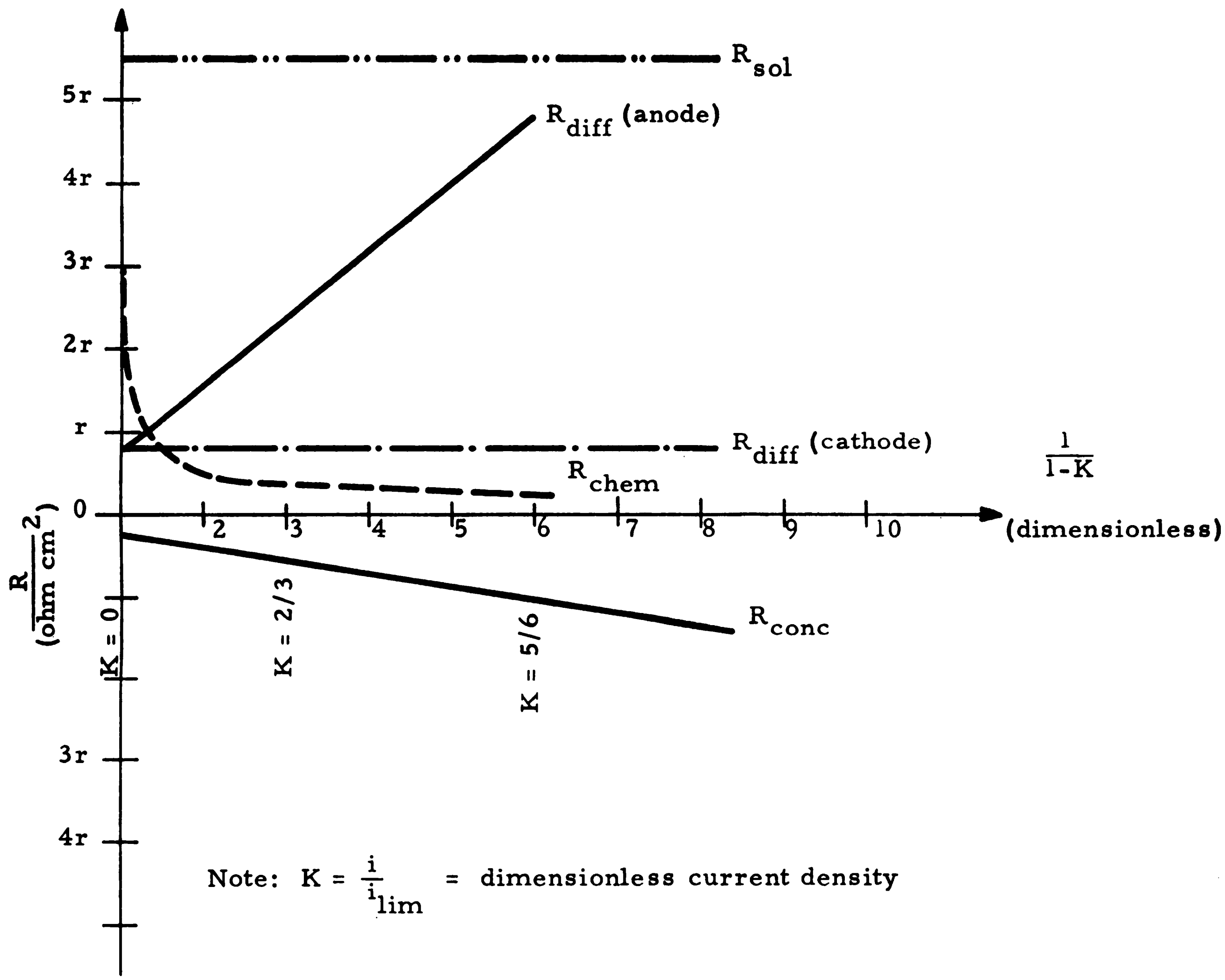

Note: $K = \frac{i}{i_{lim}}$ = dimensionless current density

c2209

Figure 9. Comparison of Resistances in Electrode Compartments

$$\Delta\varphi_{cathode} = \Delta\varphi_o + \Delta\varphi_{ohm} + \eta_{conc} + \eta_{chem} \tag{32}$$

Differentiating with respect to i, we obtain the total effective resistance R of the cathode compartment...

$$R_{cathode} = (R_{sol} + R_\delta)_{ohm} + R_{conc} + R_{chem} \tag{33}$$

R_{sol} = resistance of the bulk solution = constant

R_δ = resistance of the diffusion layer (varies with i)

$R_{conc} = -\frac{RT}{F}\left(\frac{1}{i_{lim} - i}\right)$

$R_{chem} = \frac{RT}{\alpha F}\left(\frac{1}{i}\right)$

In the case of the cathode compartment, the bulk solution contains H_2SO_4 and NaCl at given influent and effluent concentrations. Since the discharge potential for Na^+ upon the stainless steel cathode is substantially higher than that for H^+ ions in electrodialysis, we may consider the NaCl present to be a supporting or "neutral" electrolyte. The transfer of ions to the surface of the electrode is therefore accomplished by the migration of H^+ ions from the bulk solution.

The following electrochemical reaction occurs at the cathode:

$$H^+ + e^- \rightarrow \frac{1}{2} H_2$$

Because of the "neutral" electrolyte, R_δ is negligible in the cathode compartment, and (33) becomes

$$\begin{aligned} R_{cathode} &= R_{sol} + R_{conc} + R_{chem} \\ &= R_{sol} - \frac{RT}{F}\left(\frac{1}{i_{lim} - i}\right) + \frac{RT}{\alpha F}\left(\frac{1}{i}\right) \end{aligned} \tag{34}$$

where

R_{sol} = evaluated as in Section 3.1.1.1.

3.1.2.5 Anodic Resistance Analogue

At the anode, as can be seen from Figure 10, the discharge of Cl^- will occur preferentially to that of H_2O. The transfer of ions to the anode surface is therefore accomplished by the migration of Cl^- ions from the bulk solution. In this case no supporting electrolyte is present, and hence R_δ must be included in evaluating the ohmic effect. The anodic resistance analogue is calculated from

$$R_{an} = (R_{sol} + R_\delta)_{ohm} + R_{conc} + R_{chem}$$

$$= R_{sol} + R_\delta - \frac{RT}{F}\left(\frac{1}{i_{lim} - i}\right) + \frac{RT}{\alpha F}\left(\frac{1}{i}\right) \tag{35}$$

where

R_{sol} = evaluated as in Section 3.1.3

R_δ = evaluated as in Section 3.1.1.

3.1.3 Composite Cell Pair Resistance

The cell pair resistance is defined as the sum of the anion exchange membrane resistance R_{an}, the cation exchange membrane resistance R_{cat}, and the dialysate R_d, and brine R_b stream resistances, all calculated at some position along the flow path length.

$$\left(R_p\right)_z = R_{an} + R_{cat} + R_d + R_b \tag{36}$$

where R_{an}, R_{cat}, the membrane resistances can be obtained from literature or evaluated (see Section 3.1.3 on membrane resistance) at some average concentration, C_a.

$$\left(R_p\right)_z = p^a t_-^a + p^c t_+^c + \frac{1000\, y_d}{\Lambda_d C_d} + \frac{1000\, y_b}{\Lambda_b C_b} \tag{37}$$

where

p^a, p^c membrane resistivities are evaluated at C_a

Λ_c, Λ_b equivalent conductance of dialysate and brine streams.

Integration over the membrane area (pa) available for desalination of the cell pair resistance $(R_p)_z$ at chosen path length, z, from

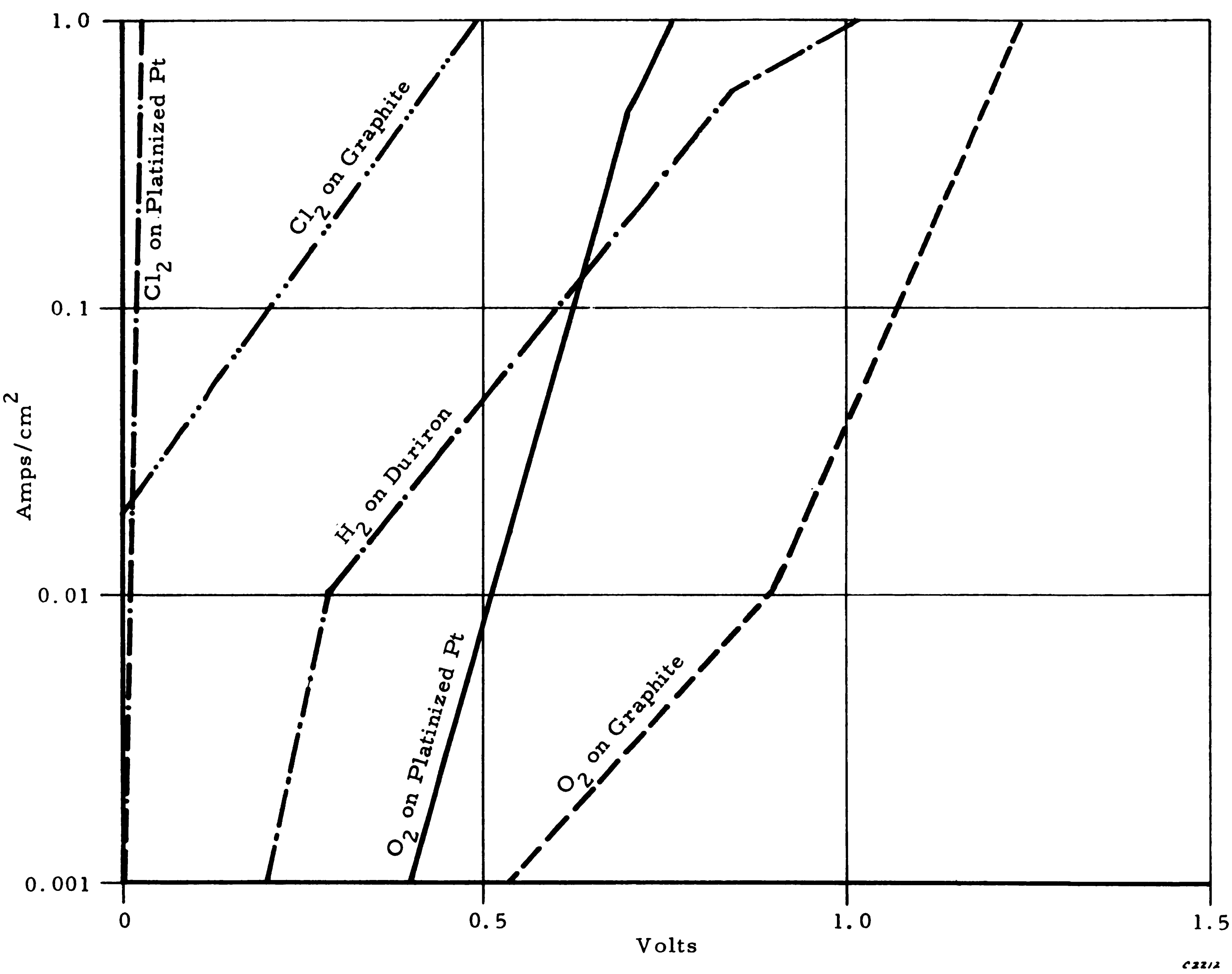

Figure 10. Various Overvoltages at Electrodes (13)

the bottom of the stack, will result in the total resistance per cell pair.

$$\left\{\begin{array}{l}\text{Note: } p = \text{fraction of usable area} \\ \qquad a = \text{total membrane area}\end{array}\right\}$$

$$\frac{1}{R_p} = \int_o^a \frac{da}{(R_p)_z} \qquad \text{cell pair}/\Omega \tag{38}$$

If we assume that $(R_p)_z$ is constant in the lateral direction (perpendicular to the z direction), then the area equals,

$$pa = pnz \qquad cm^2$$

$$pda = pndz$$

$$\left\{\begin{array}{l}\text{Note: fraction of usable area } p = .77 \\ \qquad n = \text{overall membrane width}\end{array}\right\}$$

substituting,

$$\frac{1}{R_p} = pn \int_o^m \quad (R_p)_z \tag{39}$$

According to E. A. Mason and T. A. Kirkham,(7) cell pair resistance at coordinate z, can be expressed in terms of some average concentration C_z

$$\frac{1}{C_a} = \frac{1}{2}\left(\frac{1}{C_d} + \frac{k}{C_b}\right) \tag{40}$$

where

$$k = y_{b/y_d} = \frac{\text{brine compartment thickness}}{\text{dialysate compartment thickness}}$$

and

$$(R_p)_z = \frac{K_1}{C_a} + K_2 - K_3 C_a \tag{41}$$

Variation of C_d and C_d with z, will let C_a be a function of z.

$$C_a = f(z) \tag{42}$$

$$(R_p)_z = \left[\frac{K_1}{f(z)} + K_2 - K_3 f(z)\right] \tag{43}$$

Substituting Equation (43) into Equation (39),

$$\frac{1}{R_p} = pn \int_o^m \frac{dz}{\left[\frac{K_1}{f(z)} + K_2 - K_3\, f(z)\right]} \tag{44}$$

$$= pn \int_o^m \frac{f(z)\, dz}{\left\{K_1 + K_2\, f(z) - K_3\, [f(z)]^2\right\}} \tag{45}$$

The general form of which is:

$$\frac{1}{(R_p)_z} = K \int_o^m \frac{(\alpha z + \beta)\, dz}{(z^2 + \gamma z + \delta)} \tag{46}$$

Equation (46) can be evaluated using standard integration table, viz, first, manipulating

$$\frac{1}{R_p} = \frac{Ka}{2} \int_o^m \frac{(2z + \gamma)\, dz}{(z^2 + \gamma z + \delta)} + \frac{Ka}{2}\left(\frac{2\beta}{a} - \gamma\right) \int_o^n \frac{dz}{x^2 + \gamma z + \delta} \tag{47}$$

integrating (from tables, as both parts are standard forms)

$$\frac{1}{R_p} = \frac{Ka}{2}\Big[\log\,(z^2 + \gamma z + \delta)\Big]_o^n + \frac{Ka}{2}\ \frac{2\beta}{a} - \gamma\ \ \frac{1}{-q}\left[\log \frac{2z + \gamma - \sqrt{-q}}{2z + \gamma - \sqrt{-q}}\right]_o^n \tag{48}$$

where

$$q = 4\delta - y^2$$

Hence, R_p, the composite cell pair resistance can be evaluated. If we sum the various other resistances due to membrane polarization, duct losses, etc., the total result could be compared with the actual plant cell pair resistance.

Equation (46) can also be solved with a computer, by replacing the integral by a summation, viz,

$$\left(\frac{1}{R_p}\right)_z = K \sum_{z=0}^{z=m} \frac{(\alpha z + \beta)}{(z^2 + \gamma z + \delta)}\ \Delta z \tag{49}$$

3.1.4 Parasitic Electrical Duct Losses

Because of the inherent engineering design of electrodialysis units, each concentration stream within the stack is connected, via the ducts in the manifolding, to all other concentration streams. The same applies for the dilution streams. Since the concentration stream is more conductive to electricity than the dilute stream, it would be expected that most of the nonproductive-leakage current would flow through the concentration stream.

Wilson(14) in his monograph describes these losses and bases his evaluation and equation derivations on a hypothetical model. An expression for the effective leakage current is obtained, using a representative electrical network (Figure 11) which can be reduced to that shown in Figure 12. The mathematical procedure consists of first evaluation i_n^ℓ, leakage current through the n^{th} loop in terms of ÷ N, total number of cells; i_o, stack current; and

N = total number of cells

$$r = \frac{\text{total leakage resistance}}{\text{overall cell resistance}} = \frac{R_\ell}{R_p N}$$

$$\Psi = \frac{\text{total channel resistance}}{\text{overall cell resistance}} = \frac{\overline{R}}{R_p N}$$

Refer to Figure 13.

$$i_n = \frac{[N/2 - n + 1]\, i_o}{[r + (1 + \Psi)] \sum_{n=1}^{n=N/2}} \tag{50}$$

and secondly evaluation I_ℓ, effective leakage current, by summing all the leakage loops of the stack.

$$I_\ell = \sum_{n=1}^{n=N/2} i_n^\ell \frac{(N - 2n + 2)}{N} \tag{51}$$

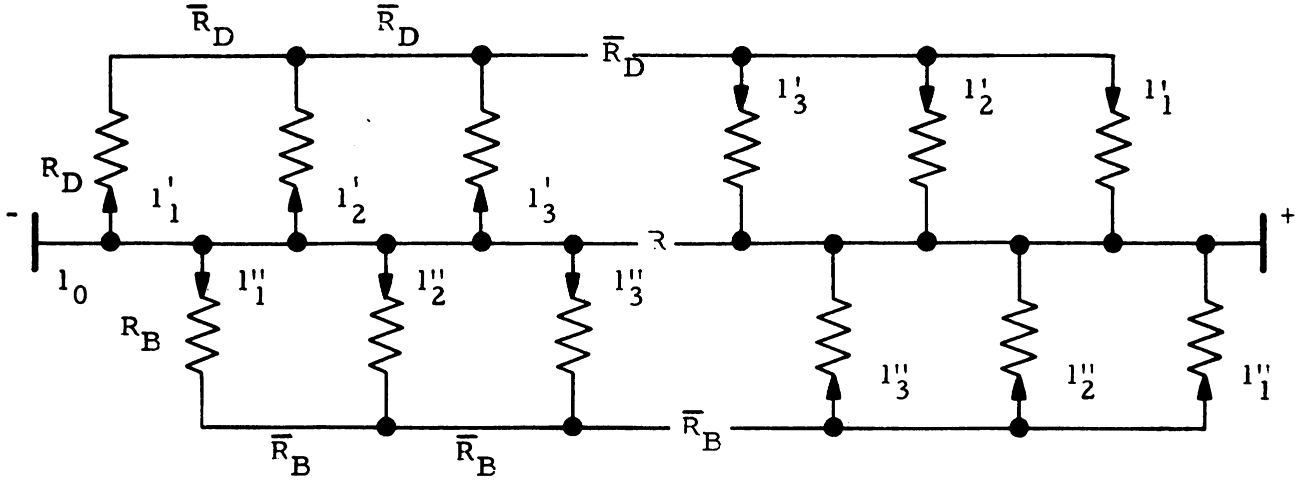

C/578

Figure 11. Representative Electrical Network of a Multicompartment Electrodialysis Unit

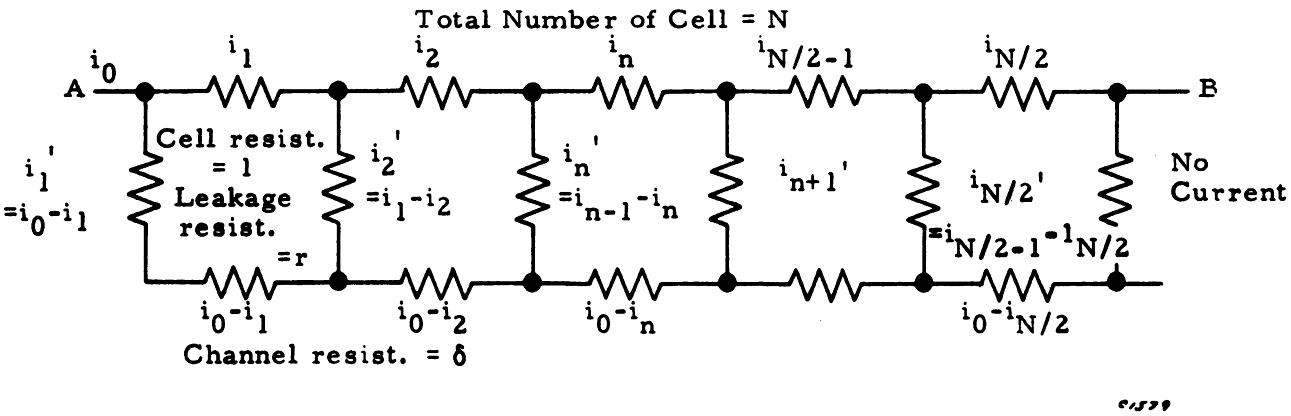

Figure 12. "Reduced" Electrical Network of a Multicompartment Electrodialysis Unit

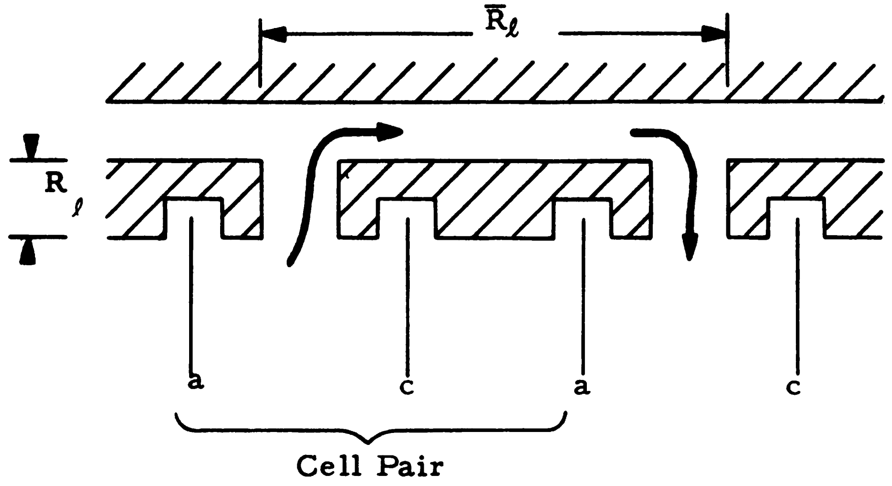

c = cationic membrane

a = anionic membrane

c/848

Figure 13. Schematic View of Current Leakage

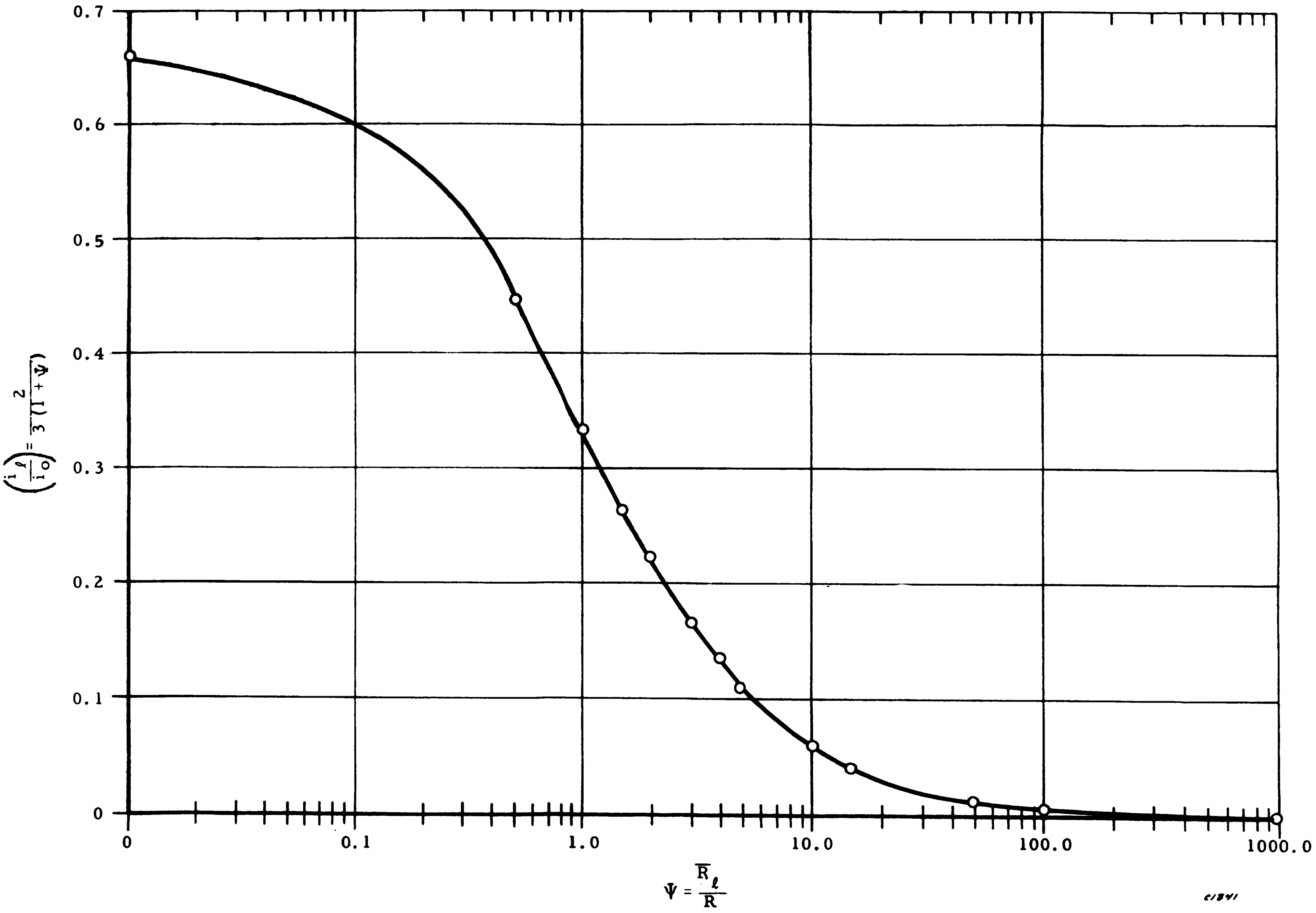

Figure 14. Plot of the Leakage Fraction $\left(\frac{i_\ell}{i_o}\right)$ Versus the Normalized Channel Resistance Ratio (Ψ)

Substitute i_n from Equation (51) into Equation (50), we get

$$I_\ell = i_o \sum_{n=1}^{n=N/2} \left[\frac{n^2}{\left\{ \frac{N}{2} \; r + (1 + \Psi) \sum_{n=1}^{N/2} n \right\}} \right] \tag{52}$$

$$\frac{1}{R_L} = \frac{1}{R_D} + \frac{1}{R_B} \tag{53}$$

Equation (52) is an exact derivation using the hypothetical model proposed (see Figures 11, and 12). Looking at Equation (52), if N is large, r is negligible, compared with

$$(1 + \Psi) \sum_{n=1}^{n=N/2} n$$

If we expand the summation and cancel terms

$$\frac{i_\ell}{i_o} = \frac{(2/N(N + 1)}{3(1 + \Psi)}$$

and again, if N is large, (2/N) (N + 1) term reduces to 2,

$$\frac{i_\ell}{i_o} = \frac{2}{3(1 + \Psi)} \tag{54}$$

See Figure 14 for plot of $\frac{i_\ell}{i_o}$ versus Ψ.

Hence, we need only calculate Ψ ratio in order to estimate the current leakage as a function of the total stack current. To calculate Ψ, we must evaluate $\bar{R}_\ell$, channel resistance, and R, cell pair resistance. (See Figure 15 for nomenclature.)

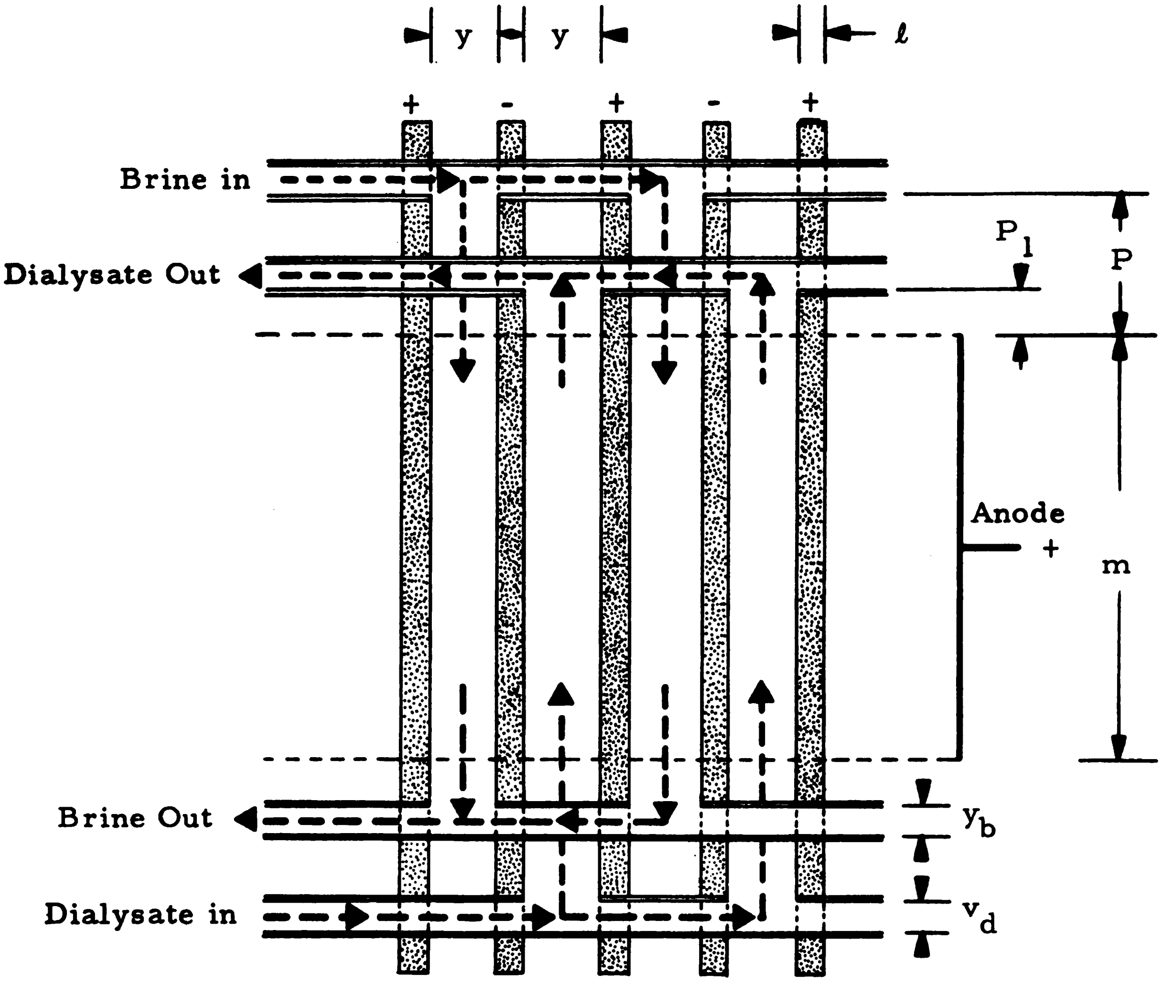

c/580

Figure 15. Dimensions of Electrodialysis Unit Required for Electrical Leakage Model

3.1.4.1 Total Channel Resistance, $\bar{R}_\ell$

The total channel resistance is obtained from $\bar{R}_b$ and $\bar{R}_d$ where

$$\bar{R}_b = \text{Brine channel resistance} = \frac{2\rho_b\,(\ell + Y)\,N}{(\pi/4)\,Y_b^{\,2}}\,,\quad \Omega/\text{stack} \tag{55}$$

$$\bar{R}_d = \text{Dialysate channel resistance} = \frac{2\rho_d\,(\ell + y)\,N}{u_d \times v_d}\,,\quad \Omega/\text{stack} \tag{56}$$

and $\bar{R}_\ell$ is obtained from the following parallel resistance relationship,

$$\frac{1}{\bar{R}_\ell} = \frac{1}{\bar{R}_d} + \frac{1}{\bar{R}_b} \tag{57}$$

Note that in Equations (55) and (56), besides the solution resistivities ρ_b and ρ_d, all other factors are of geometric consequence. (See Nomenclature, Appendix D.)

3.1.4.2 Cell Pair Resistance, R_p

The cell pair resistance $(R_p)_z$ is defined as the sum of the anion exchange membrane resistance R_{an}, the cation exchange membrane resistance R_{cat}, and the dialysate R_d and brine R_b stream resistances (see Section 3.1.3).

where

$$\left.\begin{aligned} (R_p)_z &= R_{an} + R_{cat} + R_d + R_b \\ (R_p)_z &= \rho^a t^a_- + \rho^c t^c_+ + \rho^d y_d + \rho^b y_b \end{aligned}\right\} \tag{58}$$

By multiplying the cell pair resistance R_p, by the number of cell pairs N, the total stack resistance is obtained. Three methods can be employed in calculating R_p. Two are based on Kirkham and Mason's(7) choice of an average cell pair concentration C_a at various path positions, z, up the stack. The first method uses the equations in Appendix B (the porosity method) while the second method uses the following relationship,

$$(R_p)_z = \frac{K_1}{C_a} + K_2 - K_3 C_a, \qquad \Omega - cm^2 \qquad (59)$$

Assuming the concentration profiles (straight line or a logarithmic relationship) of the brine and dialysate streams, then calculating the average concentration at pre-chosen distances (z) from the bottom of the channel, C_a and thus $(R_p)_z$ can be evaluated at each z. Either an arithmetic mean R_p can be obtained by

$$R_p = \frac{1}{2}\left[(R_p)_{\substack{\text{bottom}\\ z=o}} + (R_p)_{\substack{\text{top}\\ z=m}}\right], \qquad \Omega - cm^2 \qquad (60)$$

or $(R_p)_z$, as a function of z, can be integrated over the desalination area of the membrane to obtain the cell pair resistance R_p, (Section 3.1.4, the integration method).

$$\frac{1}{R_p} = \int_o^m \left(\frac{1}{R_p}\right)_z dz, \qquad \Omega^{-1}\, cm^{-2} \qquad (62)$$

The third method to obtain R_p, relies on membrane data supplied by the manufacturer for R_{an} and R_{cat}. The solution resistivities are found as follows.

$$\rho^d = \frac{1}{2}\left[\frac{1000}{\Lambda C_{b,o}} + \frac{1000}{\Lambda C_{b,i}}\right]_{\text{dialysate}} \qquad \Omega - cm \qquad (63)$$

$$\rho^b = \frac{1}{2}\left[\frac{1000}{\Lambda C_{b,o}} + \frac{1000}{\Lambda C_{b,i}}\right]_{\text{brine}} \qquad \Omega - cm \qquad (64)$$

Note: lower subscript b denotes bulk solution
lower subscript i denotes inlet of channel
lower subscript o denotes exit of channel

$$R_p = R_{an} + R_{cat} + y\,(\rho^d + \rho^b)$$

if $y_d = y_b = y$ = channel thickness, cms.

3.1.4.3 Resistance Analogue of Electrical Duct Losses

Once $\Psi, = \frac{\bar{R}_\ell}{R_p}$ has been evaluated, $\frac{i_\ell}{i_o}$ can be obtained from Equation (54) or the plot of Equation (54) in Figure 14. The analogue duct leakage resistance can now be evaluated, knowing i_o, E, the stack current and potential difference, respectively.

$$R_{d.\ell.} = \frac{E}{i_o \left[\frac{2}{3(1+\Psi)}\right]} \quad \text{ohms - cm}^2\text{/stack}$$

$$= \frac{E}{i_o N \left[\frac{2}{3(1+\Psi)}\right]} \quad \text{ohms - cm}^2\text{/cell pair} \qquad (65)$$

3.1.5 Water Transfer Processes

3.1.5.1 Discussion

Water transfer accompanying electrodialysis can be divided into two classes (Figure 16), "primary hydration" of ions — either by counter or co-ion transport — and the excess above this value. The latter has been termed electroosmosis. The effect of osmotic water transfer may become excessive at very low dialysate concentrations unless the brine is of low concentration. This effect is shown in Figure 17.(27) Studies(28) have also been carried out with reference to the effect current density has on the water transport occurring with a cationic membrane. Water transfer increases significantly at very low current densities (Figure 18). The explanation given is that at low current densities, water transport occurs through the larger pore holes only, while at high current densities, the water transfer values are averaged for all pore sizes.

Many writers(14) have found that the water transport numbers (w_c and w_a moles/Faraday) of cation and anion-exchange membranes, respectively, are close to the primary hydration numbers.

e.g. Na^+ $w_c = 8$

Cl^- $w_a = 4$

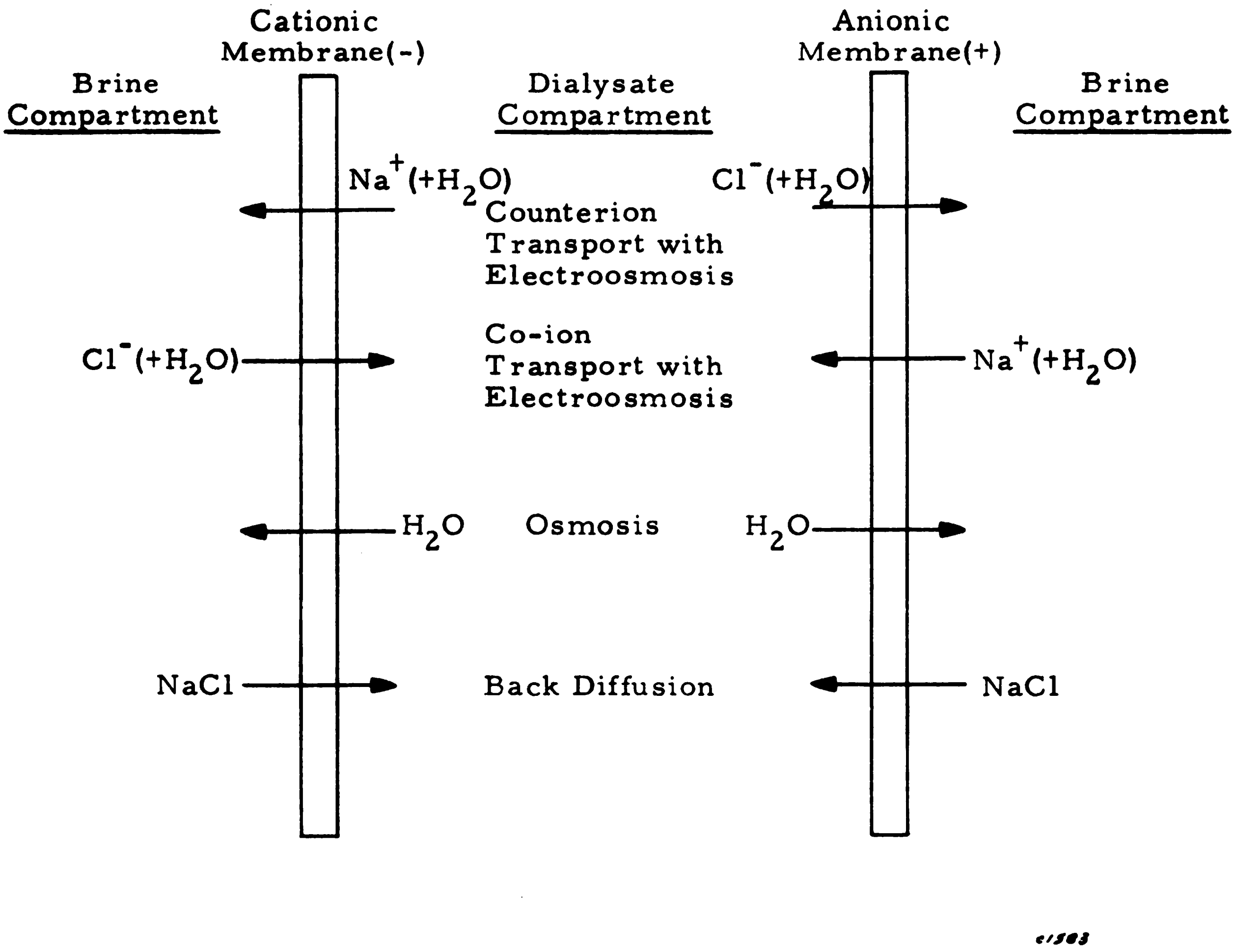

Figure 16. Various Simultaneous Processes Occurring During Electrodialytic Separation

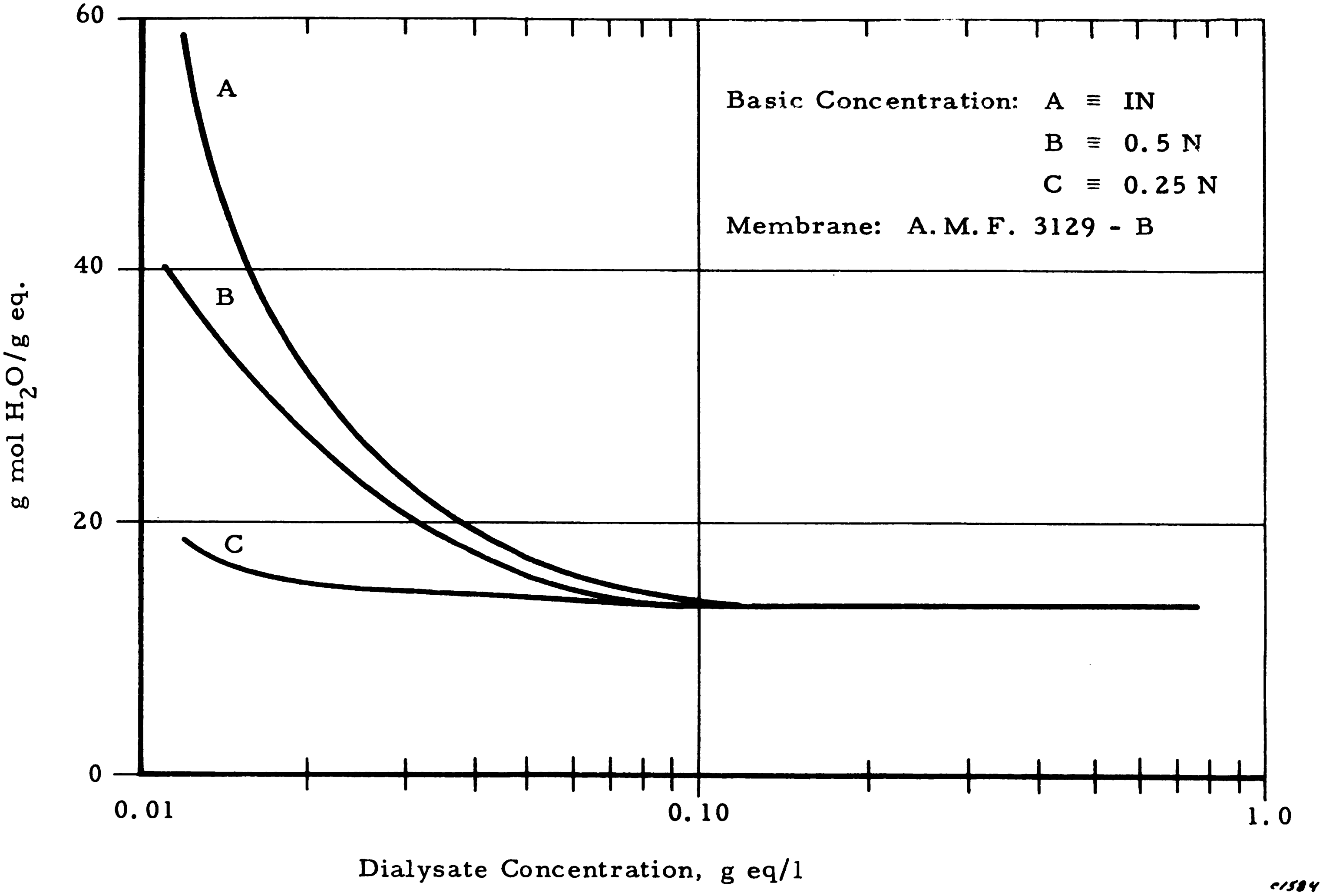

Figure 17. Water Transfer From Dialysate to Brine per Gram Equivalent of Salt Transport (Reference 29)

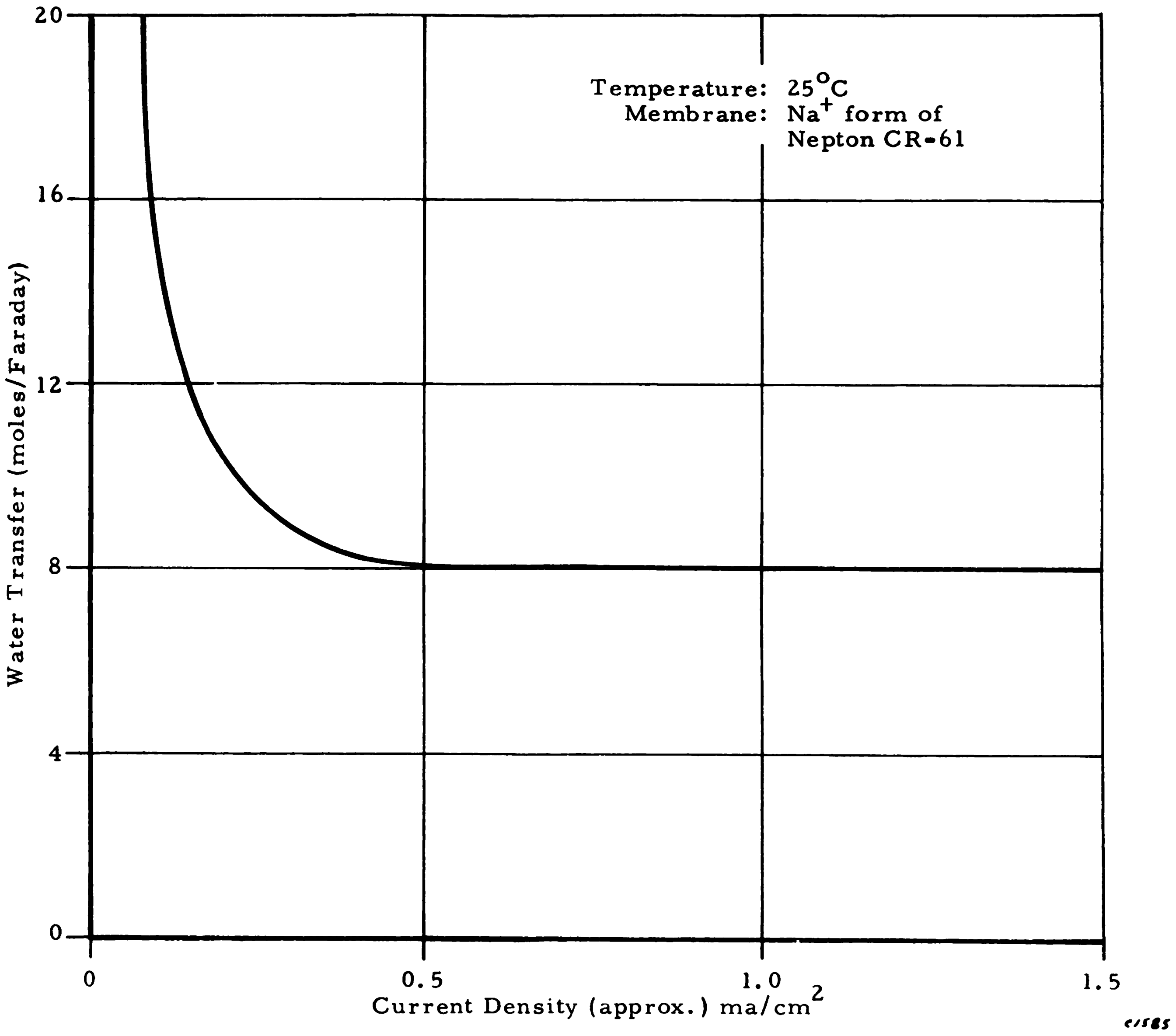

Figure 18. Water Transfer as a Function of Current Density in a Cationic Membrane (Reference 30)

Thus, a membrane pair with NaCl present will have a total water transport number ($w_t = w_c + w_a$) of 12 moles/Faraday.

The deleterious effect of water transport from the diluate to the brine streams results in a lowering of the coulomb efficiency. Wilson et al$^{(14)}$ have aptly described this effect mathematically, using apparent coulomb efficiencies η_D and η_C and actual coulomb efficiency η.

$$\eta = \eta \frac{\text{numbers of equivalents transported (transport numbers)}}{\text{(number of Faradays passed in process) (number of membrane pairs)}}$$

$$\eta_D = e = \eta\left[1 - 18\, W_t (C_d)_i\right] = \frac{F_D\left[(C_d)_i - (C_d)_o\right]F}{I} \qquad (66)$$

based on the dilute solution

$$\eta_C = \eta\left[1 - 18\, W_t (C_b)_i\right] = \frac{F_B\left[(C_b)_o - (C_b)_i\right]F}{I} \qquad (67)$$

based on the concentrated solution where

η = true coulomb efficiency
W_t = moles of water transported per equivalent of NaCl transfer
$(C_d)_i$ = incoming dilute solution concentration (equiv/ml)
$(C_b)_o$ = outgoing dilute solution concentration (equiv/ml)
$(C_b)_i$ = incoming concentrate solution concentration (equiv/ml)
$(C_b)_o$ = outgoing concentrate solution concentration (equiv/ml)
F_D = dilute solution outgoing flow rate (ml/sec)
F_B = concentrate solution outgoing flow rate (ml/sec)
F = Faraday constant
n = number of membrane pairs
I = current (amp)

The membrane manufacturer supplies data on W_t, water transport number, at various concentrations. Because different and varying concentrations exist on either side of the membrane, the average concentration (C_a) concept can be used (Equation 40).

Mandersloot$^{(15)}$ mathematically describes the detrimental effect water losses have on the coulomb efficiency with the following equation,

$$\frac{\eta}{\eta_o} = \frac{\left[\dfrac{(1 - 2\,W_t C_o) - (1 - 2\,W_t C_T)}{\ln(1 - 2\,W_t C_o)/(1 - 2\,W_t C_T)}\right]}{(1 - W_t C_T)} = \frac{(1 - 2\,W_t C)_{\ln \text{mean}}}{(1 - W_t C_T)} \qquad (68)$$

where

C_T = product concentration = $(C_d)_o$

C_o = inlet concentration = $(C_d)_i$

Mandersloot$^{(15)}$ has plotted η/η_D versus W_t for various desalination ranges. This enables us to get η immediately from Figure 19 or Equation (68). The true coulombic efficiency, η, is used to correct the coulombic efficiency (η_D) obtained from the membrane manufacturer.

Hence, no actual analogue resistance to represent the water transfer losses is envisaged. The correction and replacement of η_D by η will represent the effect water transfer has on the system as a whole.

3.1.6 Membrane Potential

Membrane potentials arise from the concentration cell potentials which can exist across both types of membranes. In the derivation of the equations for membrane potentials a concentration cell with reversible electrodes and with transference of ions through the membrane is considered. The membrane potential is then obtained by subtracting the electrode potentials from the potential of such a cell.

To derive the anion membrane potential, a concentration cell with electrodes reversible to the cation is considered. If a concentration difference exists across the membrane with $a_2 > a_1$ the net spontaneous

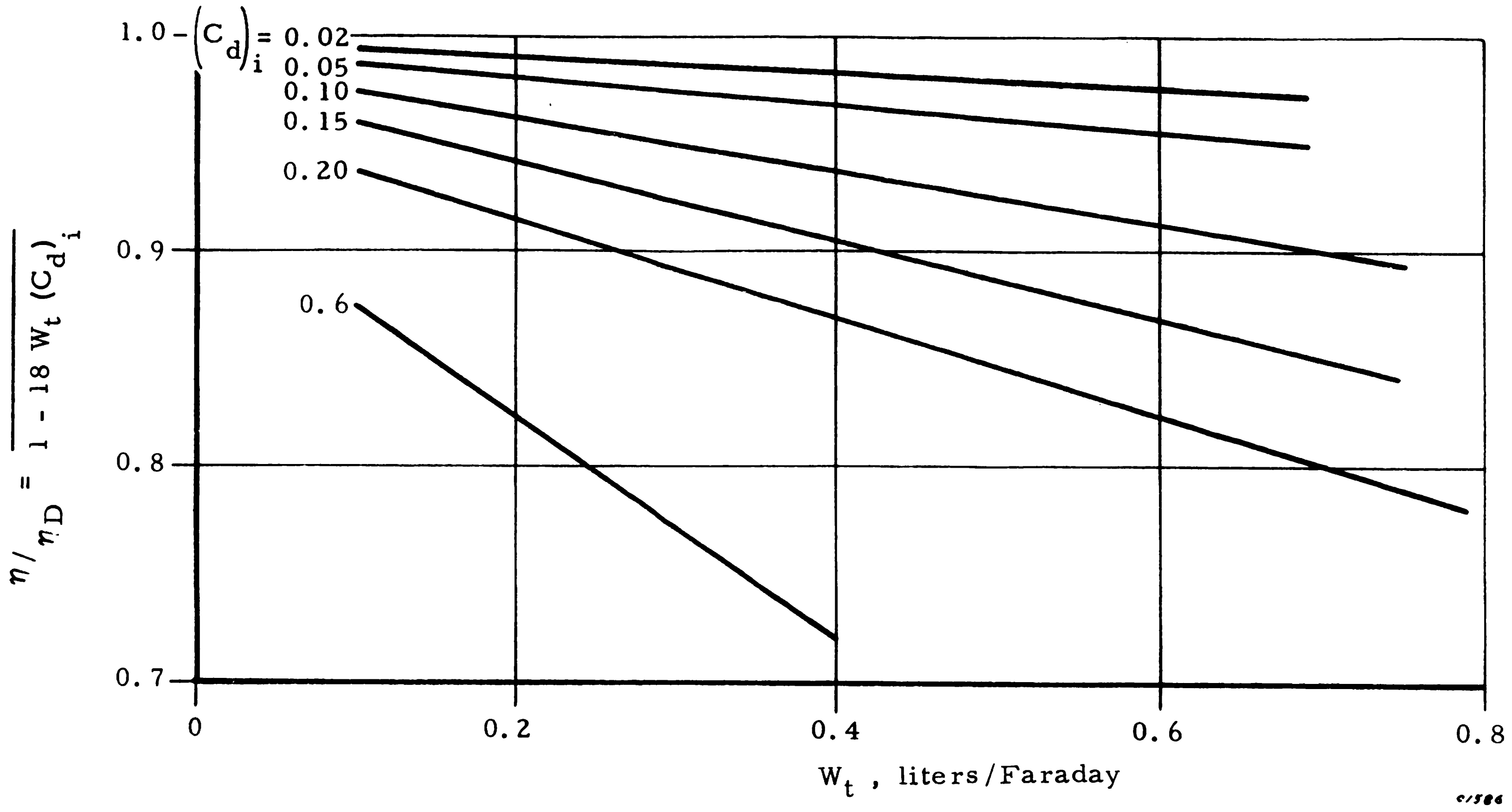

Figure 19. Ratio η/η_D, for Various Values of Water Transferred (W_t) and Dialysate Concentration at Start, $(C_d)_i$ when $C_{product}$ = 0.01 (drinking water) (Reference 15) [Equation (68)]

reaction which can occur is

$$t_{-} \text{ electrolyte } (a_2) \rightarrow t_{-} \text{ electrolyte } (a_1)$$

The potential of the concentration cell is

$$E_{cell} = \frac{RT}{F} \ln \left(\frac{a_2}{a_1} \right)^{t_{-}} \tag{69}$$

substituting mean activity coefficients

$$E_{cell} = 2 t_{-} \frac{RT}{F} \ln \frac{(a_{\pm})_2}{(a_{\pm})_1} \tag{70}$$

The electrode potentials of the concentration cell with electrodes reversible for the cation is

$$E_{el} = \frac{RT}{F} \ln \frac{(a_{+})_2}{(a_{+})_1} \tag{71}$$

Since $t_{+} + t_{-} = 1$ and $(a_{\pm})^2 = a_{+} a_{-}$ and the assumption is made that

$$\frac{(a_{+})_2}{(a_{+})_1} = \frac{(a_{-})_2}{(a_{-})_1} = \frac{(a_{\pm})_2}{(a_{\pm})_1}$$

Equation (71) can be subtracted from (70) to obtain the anion membrane potential, $E_{m,a}$

$$E_{m,a} = \frac{RT}{F} (t_1 - t_{+}) \ln \frac{(a_{\pm})_2}{(a_{\pm})_1} \tag{72}$$

Substituting electrolyte concentrations for activities

$$E_{m,a} = \frac{RT}{F} (t_{-} - t_{+}) \ln \frac{(C_{b,m})_z}{(C_{d,m})_z} \tag{73}$$

where $(C_{b,m})_z$ and $(C_{d,m})_z$ are the concentrations of electrolyte at the membrane boundary layer on the brine side and dialysate side respectively and at position, z, along the flow path of the membrane.

A parallel derivation for the cation membrane potential gives

$$E_{m,c} = \frac{RT}{F} (t_+ - t_-) \ln \frac{(C_{b,m})_z}{(C_{d,m})_z} \tag{74}$$

In a concentration cell operating in a spontaneous fashion, the flow of ions is from higher to lower concentrations and a potential is set up accordingly. The direction of flow of ions and the potential set up in each case opposes the direction of ion flow and the potential applied when the electrodialysis process operates. Consequently Equations (73) and (74) represent potentials which oppose the applied electrodialysis potential.

The total resistance of a membrane stack due to membrane potential then becomes

$$(R_{m,p})_{total} = \frac{N_a E_{m,a}}{I} + \frac{N_c E_{m,c}}{I} \quad \Omega/\text{stack} \tag{75}$$

where

N_a = number of anion membranes
N_c = number of cation membranes
I = total current passing through stack

In resistance-area units per cell pair,

$$R_{m,p} = \frac{(R_{m,p})_{total} \; A_p}{M_s/2} \quad \Omega - \text{cm}^2/\text{cell pair} \tag{76}$$

3.1.7 Membrane Selectivity

3.1.7.1 Discussion

Basic definitions defining selectivity are available$^{(16)}$ in order to compare various membranes on a relative basis.

$$P = \frac{\bar{t}_{R^+} - t_{R^+}}{1 - t_{R^+}} \tag{77}$$

where

P = selectivity (of a cationic membrane)
$\bar{t}_{R^+}$ = transference number of cations (R^+) in the membrane
t_{R^+} = transference number of cations (R^+) in free solution

For an ideal selective membrane $\bar{t}_{R^+} = 1$ and $P = 1$.
For a complete nonselective membrane $\bar{t}_{R^+} = t_{R^+}$ and $P = 0$.

The theoretical explanation of ionic transport in permselective membranes is in the embryonic stage. Unexplained anomalies occur. For example, at current densities above the critical value, it is expected that hydrogen ions (H^+), resulting from "water-splitting," would start to carry the current through the cationic membranes, but this is not the case.(17)

Qualitative treatment of permselective membrane phenomena, uses the M.S.T.(18, 19) "fixed charged" model and Donnan equilibrium as a basis. The application of the general classical theory to experimental cells is one of the main tasks of the basic electrochemistry of membranes.(21)

In as much as the practical electrodialysis unit is concerned, empirical experimental analysis(22) has been the mainstay in choosing membranes for various waters.

3.1.7.2 Resistance Analogue of Membrane Selectivity

The fact that the selectivity, P, in practice is not equal to one suggests that some hypothetical resistance R_s could be placed in parallel with the current effecting separation, so as to lower the coulomb efficiency.

$$R_s = \frac{E_s}{I_L} \tag{78}$$

where I_L is the co-ion or leakage current.

$I_L = I t_m \, [D(c)]$

I = total stack current

t_m = co-ion transport number

$D(c)$ = Donnan equilibrium expression as a function of concentration.

Until the Donnan expression, $[D(c)]$, can be theoretically predicted, the following relationship between leakage current, (I_L), due to co-ion transport can be used to calculate R_s.

$$\eta = \frac{I - I_L}{I} = 1 - (t_-^c + t_+^a) \tag{79}$$

where η is the coulomb efficiency, considering losses due only to co-ion transport.

I is the total stack current

t_-^c and t_+^a are transport numbers of the co-ions in the cation and anion exchange membrane, respectively.

Solving Equation (79) for I_L and substituting in Equation (78) we obtain

$$R_s = \frac{E_s}{I_L} = \frac{E_s}{I(1 - \eta)} = \frac{E_s}{I(t_-^c + t_+^a)} \tag{80}$$

3.1.8 Temperature Effects

The performance of electrodialysis units increase with an increase in temperature. The change in electrical resistance of the membrane system has been found to be similar to the change in resistance of solutions. Many of the membrane parameters vary with temperature rise, due to membrane swelling. Salt leakage and conductance both rise with a temperature increase. How each of these properties affect the membranes use and final performance is not yet quantitatively explained. How high a temperature the membrane can withstand before degradation occurs, depends on the type of membrane, its preparation and duration at the given temperature. Polarization, one of the major factors limiting practical performance of electrodialysis, is a function of many variables, including temperature. (See Section 3. 1. 1.) The temperature dependance of the power consumption has been studied(9) and with feeds more concentrated than 2000 p. p. m., the power expended at 5°C rises far more rapidly than at 40°C.

With sea water, the precipitation of calcium sulphate is a major problem. In some temperature ranges, $CaSO_4$ has a negative temperature coefficient of solubility.

Other problems such as vapor pressure of the streams, internal leakage caused by expansion of the stack itself, are also influenced by temperature changes.

C. Forgacs(21) has suggested the possibility of preheating the streams so as to utilize the benefits of high-temperature operation. He delves thoroughly into the various aspects of such a possibility and suggests that a thorough economic analysis is required to justify such operation.

Finally, K. S. Spiegler(22) has suggested that for each 1°C rise in temperature, the resistance of an electrodialysis system is reduced by 2%. Mason and Kirkham(7) have developed the following type of relationship,

$$(R_p)_T = \frac{(R_p)_{T_o}}{1 + m(T - T_o)} \qquad (81)$$

when temperatures are measured in Fahrenheit, $T_o = 70°F$, $m = 0.012$ for strong electrolytes and the Ionic's nepton membranes. This relationship predicts for each 1°C rise in temperature, the same 2% resistance reduction as Spiegler suggests.

Study of the temperature effects on electrodialysis is only just beginning. Now that each subcomponent of the electrodialysis process can quantitatively be estimated, the effect of temperature on each individual subcomponent is possible. This will enable the parameters which are most affected by temperature to be isolated.

3.2 Phase II — Integration of Subcomponent Mathematical Elements into a General Analytical Expression

3.2.1 Development of General Mathematical Analogue

To develop a general mathematical equation the individual resistance analogues can be combined as parallel or series resistances as expressed in the following equations.

$$R_{\text{cell pair}} = \frac{1}{\dfrac{1}{R_{\substack{\text{series}\\\text{equiv}}}} + \dfrac{1}{R_{\substack{\text{parallel}\\\text{equiv}}}}} \tag{82}$$

$$\frac{1}{R_{\substack{\text{parallel}\\\text{equiv}}}} = \frac{1}{R_S} + \frac{1}{R_L} \tag{83}$$

$$R_{\substack{\text{series}\\\text{equiv}}} = R_{AP} + R_E + R_{AE} + \ldots. + R_{CM} + R_{CE} + R_{CP} \tag{84}$$

Where each component, R_S, R_{BD}, etc., is independently evaluated. For a list of the nomenclature in above equations, refer to Figures 20 and 21.

Resistance due to water transfer effects are included in the expression for the figure of merit. The resistances in the network shown in Figures 20 and 21 can be used to calculate total overall stack resistance $(R_{CP})_T$ is multiplied by the total number of cell pairs in the stack and added to the resistances associated with the two electrodes. An example of the calculation of each resistive component and stack resistance is given in Section 3.3.

3.2.2 Power Index

One of the objectives of this study is to predict the operating stack power cost (excluding pumping cost). The power required to treat 1000 gallons of water as dialysate is given in Equation (85).

$$\text{Kw-hrs} = \frac{0.0015\ i\ R_p\ \Delta C}{1000\ \eta}$$

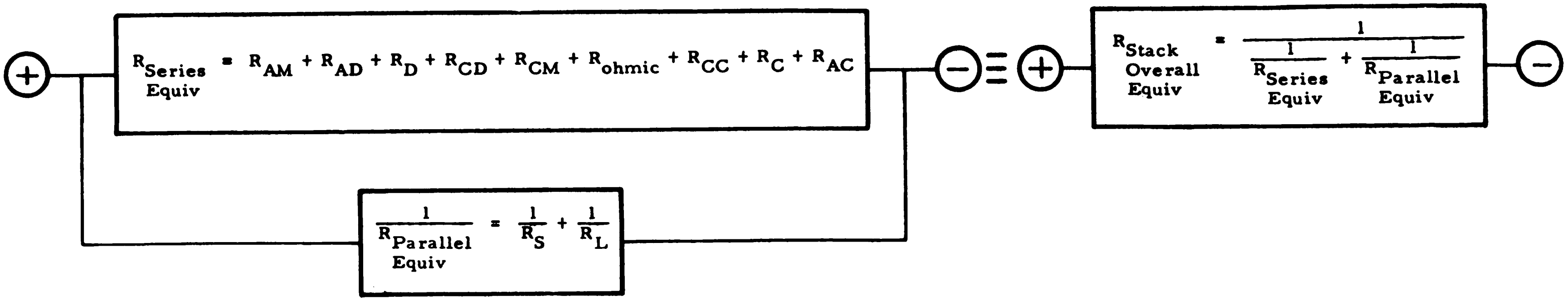

$$(R_{CP})_T = \frac{1}{\frac{1}{R_{Series}} + \frac{1}{R_{Parallel}}}$$

KEY

R_{AP} = Electrode polarization effect, anode
R_E = Electrode bulk stream
R_{AE} = Diffusion layer (DL) of anion membrane (AM), electrode stream side
R_{AM} = Bulk AM
R_{AD} = DL of AM, dilute stream side
R_D = Dilute bulk stream
R_{CD} = DL of cation membrane (CM), dilute stream side
R_{CM} = Bulk CM
R_{CC} = DL of CM, concentrate stream side
R_C = Concentrate bulk stream

R_{AC} = DL of AM, concentrate stream side
R_{CE} = DL of CM, electrode stream side
R_{CP} = Electrode polarization effect, cathode
R_L = Electrical leakage through dilute stream ducts
Electrical leakage through concentrate stream ducts
R_{BD} = Back diffusion of electrolyte
R_S = Membrane Selectivity
$(R_{CP})_T$ = Resistance for single cell pair
R_{ohmic} = Ohmic polarization

c2223

Figure 20. Equivalent Resistance Circuits For a Single Cell Pair

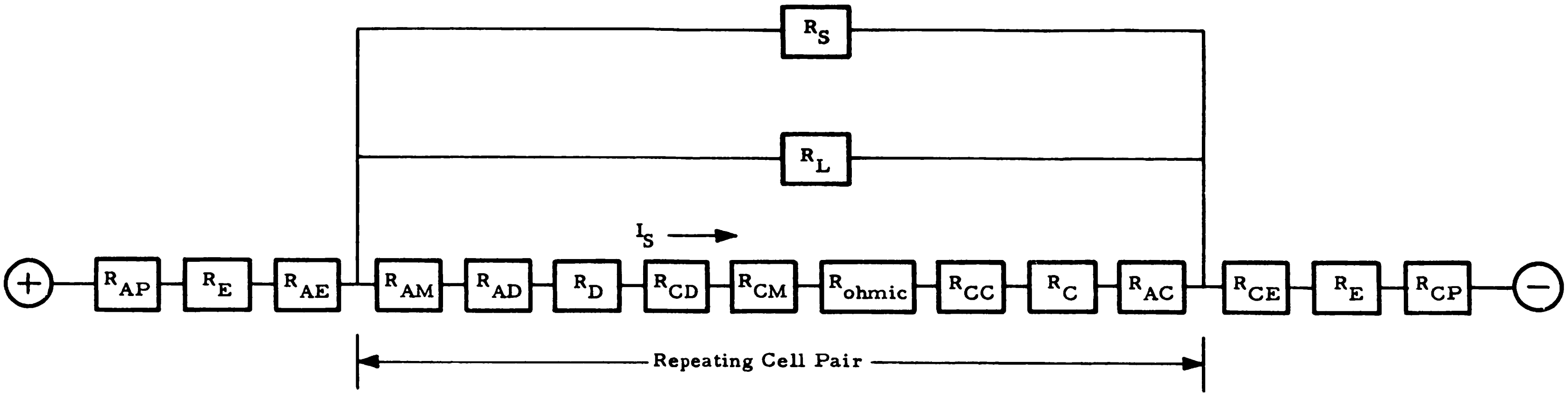

NOTE: Each R is an equivalent resistance

I_S = Effective current for salt transfer
R_{AP} = Electrode polarization effect, anode
R_E = Electrode bulk stream
R_{AE} = Diffusion layer (DL) of anion membrane (AM), electrode stream side
R_{AM} = Bulk AM
R_{AD} = DL of AM, dilute stream side
R_D = Dilute bulk stream
R_{CD} = DL of cation membrane (CM), dilute stream side
R_{CM} = Bulk CM
R_{CC} = DL of CM, concentrate stream side
R_C = Concentrate bulk stream
R_{AC} = DL of AM, concentrate stream side

R_{CE} = DL of CM, electrode stream side
R_{CP} = Electrode polarization effect, cathode
R_L = Electrical leakage through dilute stream ducts
Electrical leakage through concentrate stream ducts
R_S = Membrane selectivity
R_{ohmic} = Resistance due to ohmic polarization

C2224

Figure 21. Equivalent Circuit for Electrodialysis Process

where

Kw-hrs = kilowatt-hours to treat 1000 gallons as dialysate

$i^{\cdot}$ = mean stack current density, ma cm^{-2}

R_p = area resistance of single cell pair ohms cm^2 per cell pair

ΔC = change in dialysate concentration through the stack in gram equivalents per liter

A power index, P_i, is defined as

$$P_i = \frac{iR_p\Delta C}{\eta}$$

which can be combined with the constants in Equation (85) to give power costs per stack.

Define $(i_o\Omega/\eta)$ as the figure of merit. All other factors in equation (85) are given or easily evaluated.

Refer to Figure 22 and it can be seen that the actual total current required i_o, is equal to

$$i_o = i_1 + i_2 + i_3 \qquad (86)$$

(Note: i_4 and i_5 are a measure of the amount of back diffusion and water losses that occur and are never recovered by the system. These could be called pseudo currents.) $(R_p)_T$, the actual measureable cell pair resistance, is obtained from:

$$\frac{1}{(R_p)_T} = \frac{1}{R_1} + \frac{1}{R_2} + \frac{1}{R_3} \qquad (87)$$

where the R's are obtained from the various subcomponent analysis. Ω, the total cell resistance, is defined as:

$$\Omega = (R_p)_T N + \text{resistance component of the electrodes}$$

where

N = number of cell pairs.

The definition of η, the coulomb efficiency, includes the various water transfer losses, whereas, in Section 3.1.5, η_D is defined as the coulomb efficiency not including these water losses. Therefore, i_5 in Figure 22

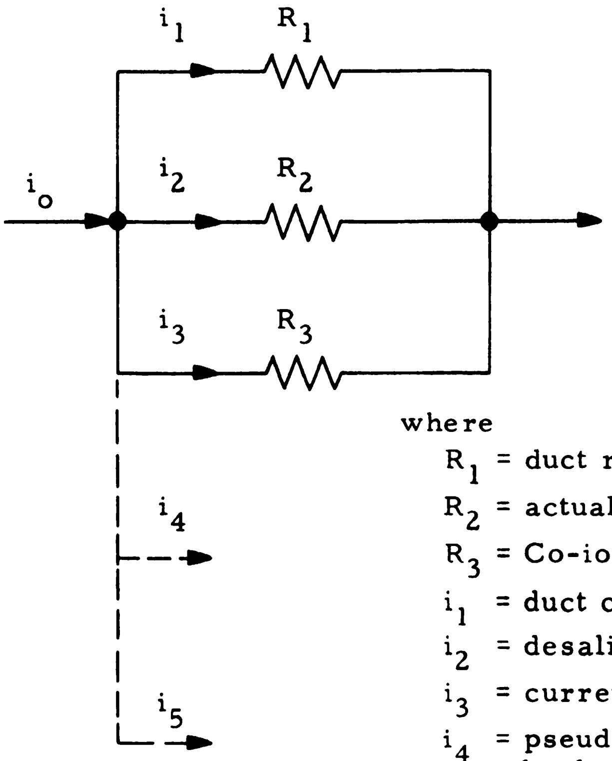

where

R_1 = duct resistance loss

R_2 = actual cell pair resistance

R_3 = Co-ion leakage resistance

i_1 = duct current loss

i_2 = desalinating current

i_3 = current carried by co-ions

i_4 = pseudo current loss due to back diffusion of salt

i_5 = pseudo current loss due to water transfer processes

C/839

Figure 22. Electrical Schematic of Current Resistance Losses in a Membrane Cell Pair

need note be calculated because by including η in the power equation (85), water transfer losses are automatically taken care of. η is obtained by the procedure suggested in Section 3.1.5, which requires first η_D to be calculated from:

$$\eta_D = \frac{i_2}{i_o + i_4} \tag{89}$$

(Note: If the denominator in the above equation included i_5, then

$$\eta = \frac{i_2}{i_o + i_4 + i_5} \tag{90}$$

3.3 Phase III — Application of Generalized Mathematics Solution to Specific Situations

The mathematical equations derived in Section 3.1 will be applied to and compared with the actual operating data for two electrodialysis plants at Webster, South Dakota and Buckeye, Arizona. Most of the plant data for Webster was obtained from Dr. J. Nordin(8) and M. Seko(23) and for Buckeye from Dr. E. J. Parsi(24) and W. E. Katz(25) of Ionics, Inc.(26) The equations will also be used for the design of a hypothetical sea water plant, and finally assuming various technological advances, the plants at Webster and Buckeye will be recalculated so as to compare the projected or future plant with the present one. Equations from Section 3.1 will not be repeated but only referred to in the following Sections. Table VII summarizes the important equations to be used.

As an example, Stage IV at Webster, South Dakota, will be used to illustrate the application of the calculations. All other stages were calculated by the same method. One very important difference between the plants at Buckeye and Webster is that they are operated with the dialysate and brine streams co- and counter-current, respectively. Other differences are recognizable in Figure 23 and Figure 24. Tables VIII, IX and X summarize the input data used to calculate the final analogue resistances (shown in Tables I, II, III and IV) for the Webster, Buckeye, sea water and projected plants.

TABLE VII

SUMMARY OF THE IMPORTANT MATHEMATICAL RELATIONSHIPS USED IN PHASE III (DERIVED IN SECTION 3.1) – APPLICATION OF GENERALIZED MATHEMATICAL EQUATIONS TO SPECIFIC SITUATIONS

Subcomponent Description	Important Preliminary Equations	Equation Number	Final Electrical Analogue Equation (ohms-cm^2 per cell pair)	Equation Number
1. Concentration Polarization	$\delta = 30 - 10.7\,Q$	(2)	$R_{c.p.} = \dfrac{m}{\int_{z=0}^{m}\left[\dfrac{dz}{\int_{x=0}^{\delta}\rho_{x,z}\,dx}\right]}$	(13)
	$(i/C)_{lim} = \dfrac{FD}{\delta(\bar{t} - t)}$	(5)		
	$(i/C_d)_{lim} = \text{Const}\,(\nu)^n$	(6), (7)		
	$(i_{lim})_{t^\circ C} = (i_{lim})_{25^\circ C} \times \text{C.F.}$	(9)		
	$i_{oper} = \dfrac{F\,F_d C_{di} f}{e\,Ap}$	(11)		
	$\rho = 1000/\Lambda_v C$	(12)		
	$(\Lambda_v)_{t^\circ C} = (\Lambda_\alpha)_{t^\circ C} - (A + B\,\Lambda_\alpha)_{t^\circ C}\sqrt{C}$	(14)		
2. Ohmic Polarization	–		$R_{ohmic} = 24.656\,e^{2.847\,K}$	(23)
3. Electrode Polarization	$\eta_{conc} = -\dfrac{RT}{F}\ln(C_{bulk}/C_{surface})$	(24)	$R_{cath\ \text{or anodic}} = (R_{sol} + R_\delta)_{ohm} + R_{conc} + R_{chem}$	(33), (35)
	$\eta_{chem} = a + \dfrac{RT}{\alpha F}\ln i$	(27)		
	$\Delta\varphi_{ohm} = \Delta\varphi_{sol} + \Delta\varphi_\delta$	(29)		
4. Composite Cell Pair Resistance	$1/C_a = \dfrac{1}{2}\left(\dfrac{1}{C_d} + \dfrac{h}{C_b}\right)$	(40)	$R_p = \dfrac{1}{K'\int_{z=0}^{n}\dfrac{dz}{(R_p)_z}}$	(39), (49)
	$(R_p)_z = \dfrac{K_1}{C_a} + K_2 - K_3 C_a$	(41)		
	$(R_p)_z = 1/\left(\dfrac{\alpha z + \beta}{z^2 + \gamma z + \delta}\right)_z$	(46)		
5. Parasitic Electrical Duct Losses	$\dfrac{i_\ell}{i_o} = \dfrac{2}{3(1 + \Psi)}$	(54)	$R_{d.\ell} = \dfrac{E}{Ni_o\left[\dfrac{2}{3(1 + \Psi)}\right]}$	(65)
	$\Psi = \bar{R}/R_p N$	(50)		
6. Water Transfer Processes	$\eta_D = \dfrac{F_D\left[(C_d)_i - (C_d)_o\right]F}{I}$	(66), (67)	$\eta = \eta_D\left\{\left[\dfrac{(1-2\omega_t C_o)-(1-2\omega_t C_T)}{\ln(1-2\omega_t C_o)/(1-2\omega_t C_T)}\right]/(1-\omega_t C_T)\right.$ (coulomb efficiency)	(68)
7. Membrane Selectivity	–		$R_s = \dfrac{E}{i_o(t_-^c + t_+^a)}$	(80)
8. Membrane Potential	$E_{m.p.} = \dfrac{RT}{F}(t_- - t_+)\ln\left[(a_\pm)_2/(a_\pm)_1\right]$	(72)	$R_{m.p.} = \dfrac{2RT}{i_o F}\ln\left(\dfrac{C_{b,m}}{C_{d,m}}\right)_2\left[1 - t_+^a - t_-^c\right]$	(75), (76)

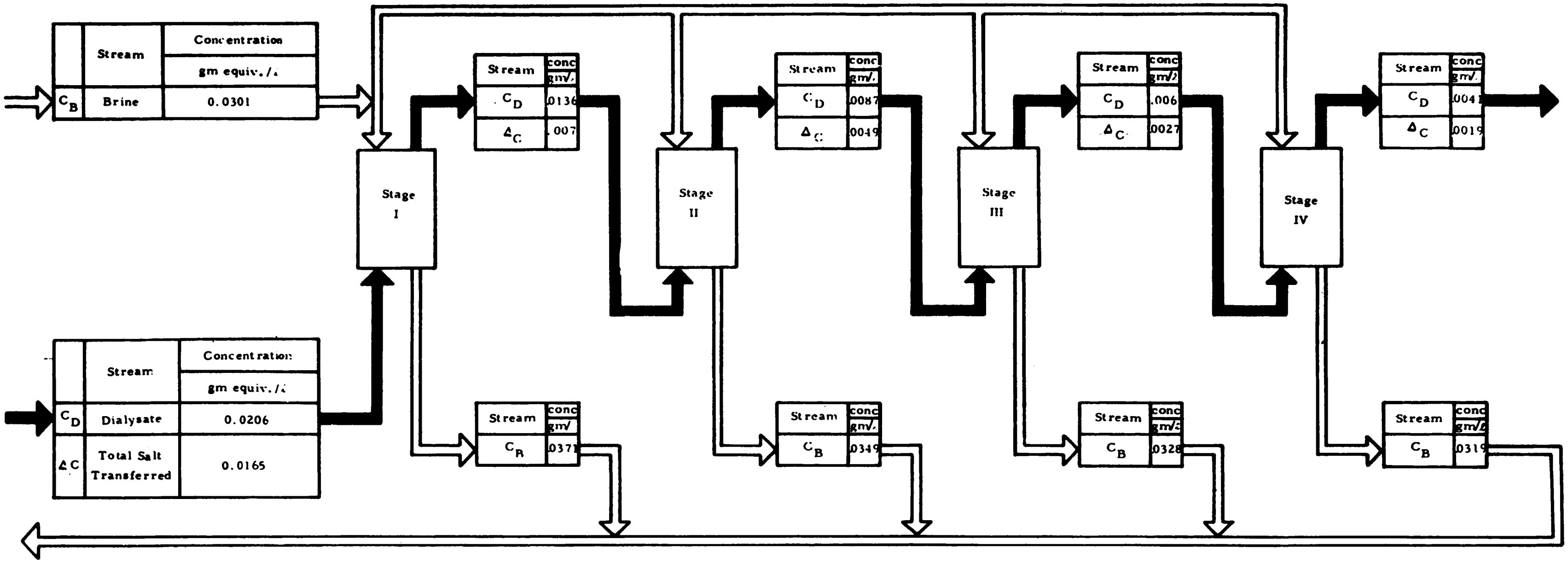

C2204

Operating Conditions

Temperature: 8.89°C
Stacks per stage: 1
Usable area per membrane: 9,574 cm^2
Dialysate flow rate: 0.779 gal/min, channel
Type of ion exchange membranes:
cation - asahi - DK-1 (thickness 0.023 cms)
anion - asahi - DA-1 (thickness 0.023 cms)
Power Requirements:

	Volts	Amp	Current Efficiency
Stage I	240	35.0	98.2
Stage II	200	24.0	99.3
Stage III	145	14.0	96.8
Stage IV	128	10.0	91.4

Figure 23. Flow Sheet and Material Balance for Electrodialysis Plant at Webster So. Dakota

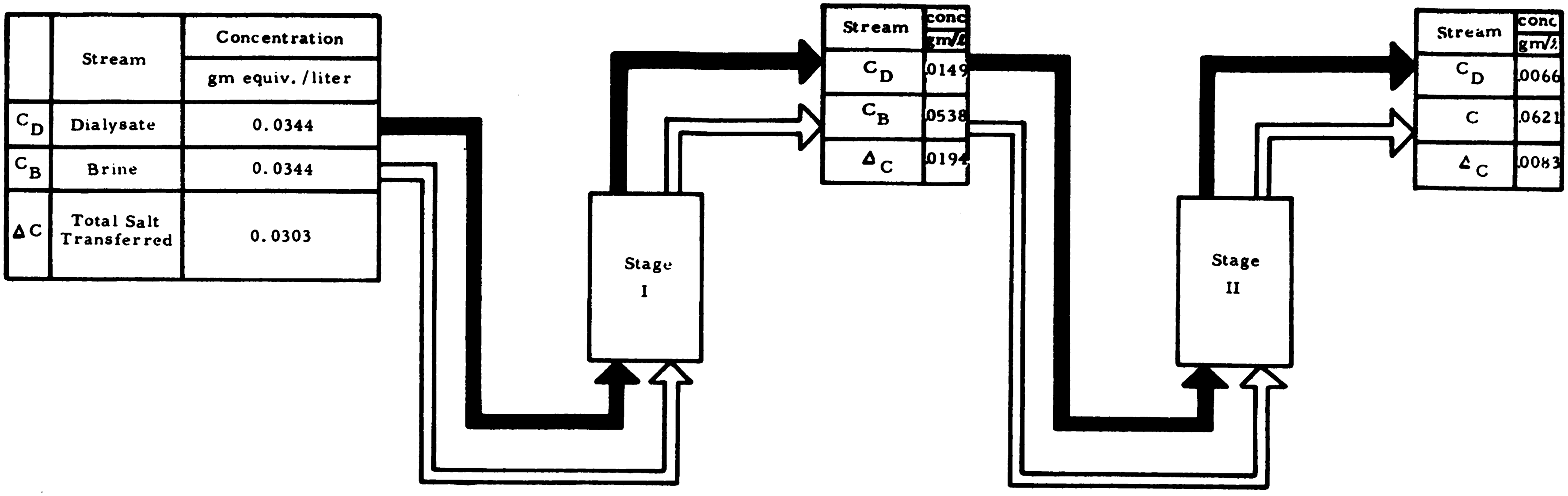

	Stream	Concentration gm equiv./liter
C_D	Dialysate	0.0344
C_B	Brine	0.0344
ΔC	Total Salt Transferred	0.0303

Stream	conc gm/ℓ
C_D	.0149
C_B	.0538
ΔC	.0194

Stream	conc gm/ℓ
C_D	.0066
C	.0621
ΔC	.0083

Operating Conditions

Temperature: 26.7°C
Stacks per stage: 3
Membranes per stack: 550
Usable area per membrane: 3,252 cm^2
Dialysate flow rate: 0.3252 gal/min, channel
Type of ion exchange membranes:
  cation - Ionics #61AZL183 (thickness 0.06 cm)
  anion - Ionics #111BZL183 (thickness 0.06 cm)
Power Requirements:

	Volts	Amp
Stage I	400	40.1
Stage II	355	21.73

C2205

Figure 24. Flow Sheet and Material Balance for Electrodialysis Plant at Buckeye, Arizona

TABLE VIII

ARRAY OF DATA USED AS INPUTS FOR THE ELECTRODIALYSIS ELECTRICAL ANALOGUE MODEL FOR THE PRESENT WEBSTER PLANT

	Stage I	Stage II	Stage III	Stage IV
RAY (1) = K = i_{op}/i_{lim} =	0.6447	0.6333	0.5287	0.5674
RAY (2) = $(C_d)_o$ = outlet dial. conc. gm eq/ℓ	0.0136	0.0087	0.0060	0.0041
RAY (3) = $(C_d)_i$ = inlet dial. conc. gm eq/ℓ	0.0206	0.0136	0.0087	0.0060
RAY (4) = $(C_b)_o$ = outlet brine conc. gm eq/ℓ	0.0371	0.0349	0.0328	0.0319
RAY (5) = $(C_b)_i$ = inlet brine conc. gm eq/ℓ	0.0301	0.0301	0.0301	0.0301
RAY (6) = $E.P.M._{total}$ = total outlet equiv per million (dial.)	20.6	13.6	8.7	6.0
RAY (7) = m = stack path length, cm	111.76	111.76	111.76	111.76
RAY (8) = n = stack path width, cm	111.76	111.76	111.76	111.76
RAY (9) = p = fraction usable desalination area	0.77	0.77	0.77	0.77
RAY (10) = δ = diffusion layer thickness, cm	0.00214	0.00214	0.00214	0.00214
RAY (11) = A = const. from the Onsager Eq.	38.2	38.2	38.2	38.2
RAY (12) = B = const. from the Onsager Eq.	0.2215	0.2215	0.2215	0.2215
RAY (13) = t^oC = temperature, centigrade	8.89	8.89	8.89	8.89
RAY (14) = FPCA = 1/2 Ca^{++} fraction in product (epm units)	0.495	0.465	0.44	0.41
RAY (15) = FFCA = 1/2 Ca^{++} fraction in feed	0.507	0.495	0.465	0.44
RAY (16) = FPMG = 1/2 Mg^{++} fraction in product	0.321	0.324	0.316	0.30
RAY (17) = FFMG = 1/2 Mg^{++} fraction in feed	0.313	0.321	0.324	0.32
RAY (18) = FPNA = Na^+ fraction in product	0.183	0.211	0.244	0.29
RAY (19) = FFNA = Na^+ fraction in feed	0.180	0.183	0.211	0.24
RAY (20) = FPCl = Cl^- fraction in product	0.011	0.009	0.008	0.007
RAY (21) = FFCl = Cl^- fraction in feed	0.013	0.011	0.009	0.008
RAY (22) = $FPHCO_3$ = HCO_3^- fraction in product	0.296	0.324	0.360	0.41
RAY (23) = $FFHCO_3$ = HCO_3^- fraction in feed	0.280	0.296	0.324	0.36
RAY (24) = $FPSO_4$ = 1/2 $SO_4^=$ fraction in product	0.693	0.667	0.634	0.58
RAY (25) = $FFSO_4$ = 1/2 $SO_4^=$ fraction in feed	0.707	0.693	0.667	0.64
RAY (26) = CF = current dens. temp. correction	0.85	0.85	0.85	0.85
RAY (27) = M = const. in limiting current equation	72.3	72.3	72.3	72.3
RAY (28) = n = const. in limiting current equation	0.947	0.947	0.947	0.947
RAY (29) = M_s = membranes per stack	432.0	432.0	432.0	432.0
RAY (30) = y = spacer thickness, cm	0.023	0.023	0.023	0.023
RAY (31) = ℓ = membrane thickness, cm	0.075	0.075	0.075	0.075
RAY (32) = Ap = usable area, cm^2	9574.0	9574.0	9574.0	9574.0
RAY (33) = w_a = water transport, ℓ/F (anion)	0.168	0.2333	0.349	0.466
RAY (34) = w_b = water transport, ℓ/F (cation)	0.24	0.3333	0.499	0.666
RAY (35) = η_D = uncorrected coul. efficiency	0.982	0.993	0.968	0.914
RAY (36) = E = stack voltage, volts	240.0	200.0	145.0	128.0
RAY (37) = I = current, amps	35.0	24.0	14.0	10.0
RAY (38) = y_b = brine manifold width, cms	2.818	2.818	2.818	2.818
RAY (39) = x_b = brine manifold height, cms	—	—	—	—
RAY (40) = u_d = dialysate manifold width, cm	4.246	4.246	4.246	4.246
RAY (41) = V_d = dialysate manifold height, cm	3.77	3.77	3.77	3 77
RAY (42) = t_-^a = anion transference no. in anion exchanger	0.9806	0.9806	0.9806	0.9806
RAY (43) = t_+^c = cation trans. no. in cation exchanger	0.9518	0.9542	0.9557	0.9573
RAY (44) = i = constant in equation (100)	0.3838	0.3838	0.3838	0.3838
RAY (45) = j = constant in equation (101)	0.0817	0.0817	0.0817	0.0817
RAY (46) = k = constant in equation (100)	48.0	48.0	48.0	48.0
RAY (47) = q = constant in equation (101)	160.0	160.0	160.0	160.0
RAY (48) = $(C_E^C)_o$ = outlet catholyte conc. (I) gm eq/ℓ	0.1879	0.1879	0.1879	0.1879
RAY (49) = $(C_E^C)_i$ = inlet catholyte conc. (I) gm eq/ℓ	0.1884	0.1884	0.1884	0.1884
RAY (50) = $(C_E^A)_o$ = outlet anolyte conc. (I) gm eq/ℓ	0.1879	0.1879	0.1879	0.1879
RAY (51) = $(C_E^A)_i$ = inlet anolyte conc. (I) gm eq/ℓ	0.1884	0.1884	0.1884	0.1884
RAY (52) = $(C_B^C)_o$ = outlet cathode buffer conc.gm eq/ℓ	0.03026	0.03026	0.03026	0.03026
RAY (53) = $(C_B^C)_i$ = inlet cathode buffer conc. gm eq/ℓ	0.04005	0.04005	0.04005	0.04005

TABLE IX

ARRAY OF DATA USED AS INPUTS FOR THE ELECTRODIALYSIS ELECTRICAL ANALOGUE MODEL FOR THE PRESENT BUCKEYE PLANT

	Stage I	Stage II
RAY (1) = K = i_{op}/i_{lim} =	0. 1987	0. 1819
RAY (2) = $(C_d)_o$ = outlet dial. conc. gm eq/ℓ	0.0149	0.0066
RAY (3) = $(C_d)_i$ = inlet dial. conc. gm eq/ℓ	0. 0344	0. 0149
RAY (4) = $(C_b)_o$ = outlet brine conc. gm eq/ℓ	0. 0538	0. 0621
RAY (5) = $(C_b)_i$ = inlet brine conc. gm eq/ℓ	0. 0344	0. 0538
RAY (6) = E. P. M.$_{total}$ = total outlet equiv per million (dial)	14. 9	6. 6
RAY (7) = m = stack path length, cm	402.5	402.5
RAY (8) = n = stack path width, cm	8.08	8.08
RAY (9) = p = fraction usable desalination area	0. 700	0. 700
RAY (10) = δ = diffusion layer thickness, cm	0.00265	0.00265
RAY (11) = A = const. from the Onsager Eq.	61.5	61.5
RAY (12) = B = const. from the Onsager Eq.	0. 2284	0. 2284
RAY (13) = t°C = temperature, centigrade	26. 7	26. 7
RAY (14) = FPCA = 1/2 Ca^{++} fraction in product (epm units)	0. 11	0. 06
RAY (15) = FFCA = 1/2 Ca^{++} fraction in feed	0. 17	0. 11
RAY (16) = FPMG = 1/2 Mg^{++} fraction in product	0. 02	0. 01
RAY (17) = FFMG = 1/2 Mg^{++} fraction in feed	0. 04	0. 02
RAY (18) = FPNA = Na^+ fraction in product	0. 88	0. 94
RAY (19) = FFNA = Na^+ fraction in feed	0. 80	0. 88
RAY (20) = FPCl = Cl^- fraction in product	0. 89	0. 88
RAY (21) = FFCl = Cl^- fraction in feed	0. 87	0. 89
RAY (22) = $FPHCO_3$ = HCO_3^- fraction in product	0. 04	0. 05
RAY (23) = $FFHCO_3$ = HCO_3^- fraction in feed	0. 04	0. 04
RAY (24) = $FPSO_4$ = 1/2 $SO_4^=$ fraction in product	0. 06	0. 04
RAY (25) = $FFSO_4^=$ 1/2 $SO_4^=$ fraction in feed	0. 09	0. 06
RAY (26) = CF = current dens. temp. correction	1.05	1.05
RAY (27) = M = const. in limiting current equation	590. 0	590. 0
RAY (28) = n = const. in limiting current equation	0. 6	0. 6
RAY (29) = M_s = membranes per stack	550. 0	550. 0
RAY (30) = y = spacer thickness, cm	0. 1016	0. 1016
RAY (31) = ℓ = membrane thickness, cm	0. 06	0. 06
RAY (32) = Ap = usable area, cm^2	3252. 0	3252. 0
RAY (33) = w_a = water transport, ℓ/F (anion)	0. 205	0. 21
RAY (34) = w_b = water transport, ℓ/F (cation)	0. 28	0. 30
RAY (35) = η_D = uncorrected coul. efficiency	0. 925	0. 965
RAY (36) = E = stack voltage, volts	400. 0	355. 0
RAY (37) = I = current, amps	40. 1	21. 73
RAY (38) = y_b = brine manifold width, cms	5. 0	5. 0
RAY (39) = x_b = brine manifold height, cms	4. 0	4. 0
RAY (40) = u_d = dialysate manifold width, cm	5. 0	5. 0
RAY (41) = V_d = dialysate manifold height, cm	4. 0	4. 0
RAY (42) = t_-^a = anion transference no. in anion exchanger	0. 9922	0. 9961
RAY (43) = t_+^c = cation transf. no. in cation exchanger	0. 9939	0. 9939
RAY (44) = i = constant in equation (100)	0. 1060	0. 1060
RAY (45) = j = constant in equation (101)	0. 1014	0. 1014
RAY (46) = k = constant in equation (100)	125. 0	125. 0
RAY (47) = q = constant in equation (101)	67. 0	67. 0
RAY (48) = $(C_E^c)_o$ = outlet catholyte conc. (I) gm eq/ℓ	0. 1692	0. 169
RAY (49) = $(C_E^c)_i$ = inlet catholyte conc. (I) gm eq/ℓ	0. 1694	0. 1692
RAY (50) = $(C_E^A)_o$ = outlet anolyte conc. (I) gm eq/ℓ	0. 1189	0. 1175
RAY (51) = $(C_E^A)_i$ = inlet anolyte conc. (I) gm eq/ℓ	0. 1192	0. 1189

TABLE X

ARRAY OF DATA USED AS INPUTS FOR THE ELECTRODIALYSIS ELECTRICAL ANALOGUE MODEL FOR THE SEA WATER PLANT

	Stage I	Stage II	Stage III	Stage IV	Stage V
RAY (1) = K = i_{op}/i_{lim} =	0.0208	0.0208	0.0208	0.0208	0.0208
RAY (2) = $(C_d)_o$ = outlet dial. conc. gm eq/ℓ	0.242	0.098	0.04	0.0162	0.0066
RAY (3) = $(C_d)_i$ = inlet dial. conc. gm eq/ℓ	0.594	0.242	0.098	0.04	0.0162
RAY (4) = $(C_b)_o$ = outlet brine conc. gm eq/ℓ	0.652	0.444	0.358	0.3238	0.3096
RAY (5) = $(C_b)_i$ = inlet brine conc. gm eq/ℓ	0.300	0.300	0.300	0.300	0.300
RAY (6) = $E.P.M._{total}$ = total outlet equiv per million (dial.)	242.0	98.0	40.0	16.2	6.6
RAY (7) = m = stack path length, cm	4025.0	4025.0	4025.0	4025.0	4025.0
RAY (8) = n = stack path width, cm	8.08	8.08	8.08	8.08	8.08
RAY (9) = p = fraction usable desalination area	0.7000	0.7000	0.7000	0.7000	0.7000
RAY (10) = δ = diffusion layer thickness, cm	0.00265	0.00265	0.00265	0.00265	0.00265
RAY (11) = A = const. from the Onsager Eq.	61.5	61.5	61.5	61.5	61.5
RAY (12) = B = const. from the Onsager Eq.	0.2284	0.2284	0.2284	0.2284	0.2284
RAY (13) = t^oC = temperature, centrigrade	26.7	26.7	26.7	26.7	26.7
RAY (14) = FPCA = 1/2 Ca^{++} fraction in product (epm units)	0.0207	0.0265	0.0168	0.0105	0.0061
RAY (15) = FFCA = 1/2 Ca^{++} fraction in feed	0.0336	0.0207	0.0265	0.0168	0.0105
RAY (16) = FPMG = 1/2 Mg^{++} fraction in product	0.0992	0.0561	0.0320	0.0185	0.0106
RAY (17) = FFMG = 1/2 Mg^{++} fraction in feed	0.1762	0.0992	0.0561	0.032	0.0185
RAY (18) = FPNA = Na^+ fraction in product	0.8801	0.9173	0.9513	0.9710	0.9833
RAY (19) = FFNA = Na^+ fraction in feed	0.7901	0.8801	0.9173	0.9513	0.9710
RAY (20) = FPCl = Cl^- fraction in product	0.9008	0.9031	0.9025	0.9012	0.9031
RAY (21) = FFCl = Cl^- fraction in feed	0.9031	0.9008	0.9031	0.9025	0.9012
RAY (22) = $FPHCO_3$ = HCO_3^- fraction in product	0.0062	0.0041	0.0050	0.0061	0.0039
RAY (23) = $FFHCO_3$ = HCO_3^- fraction in feed	0.0039	0.0062	0.0041	0.005	0.0061
RAY (24) = $FPSO_4$ = 1/2 $SO_4^=$ fraction in product	0.0930	0.0928	0.0925	0.0926	0.0929
RAY (25) = $FFSO_4$ = 1/2 $SO_4^=$ fraction in feed	0.0929	0.0930	0.0928	0.0925	0.0926
RAY (26) = CF = current dens. temp. correction	1.05	1.05	1.05	1.05	1.05
RAY (27) = M = const. in limiting current equation	590.0	590.0	590.0	590.0	590.0
RAY (28) = n = const. in limiting current equation	0.6	0.6	0.6	0.6	0.6
RAY (29) = M_s = membranes per stack	550.0	550.0	550.0	550.0	550.0
RAY (30) = y = spacer thickness, cm	0.1016	0.1016	0.1016	0.1016	0.1016
RAY (31) = ℓ = membrane thickness, cm	0.06	0.06	0.06	0.06	0.06
RAY (32) = Ap = usable area, cm^2	32520.0	32520.0	32520.0	32520.0	32520.0
RAY (33) = w_a = water transport, ℓ/F (anion)	0.17	0.18	0.19	0.205	0.21
RAY (34) = w_b = water transport, ℓ/F (cation)	0.22	0.24	0.26	0.28	0.30
RAY (35) = η_D = uncorrected coul. efficiency	0.95	0.95	0.95	0.95	0.95
RAY (36) = E = stack voltage, volts	4500.0	2500.0	1300.0	700.0	300.0
RAY (37) = I = current, amps	0.02298	0.00934	0.003794	0.001544	0.000627
RAY (38) = y_b = brine manifold width, cms	5.0	5.0	5.0	5.0	5.0
RAY (39) = x_b = brine manifold height, cms	4.0	4.0	4.0	4.0	4.0
RAY (40) = u_d = dialysate manifold width, cm	5.0	5.0	5.0	5.0	5.0
RAY (41) = V_d = dialysate manifold height, cm	4.0	4.0	4.0	4.0	4.0
RAY (42) = t_-^a = anion transference no. in anion exchanger	0.995	0.995	0.995	0.995	0.995
RAY (43) = t_+^c = cation trans. no. in cation exchanger	0.995	0.995	0.995	0.995	0.995
RAY (44) = i = constant in equation (100)	0.1060	0.1060	0.1060	0.1060	0.1060
RAY (45) = j = constant in equation (101)	0.1014	0.1014	0.1014	0.1014	0.1014
RAY (46) = k = constant in equation (100)	125.0	125.0	125.0	125.0	125.0
RAY (47) = q = constant in equation (101)	67.0	67.0	67.0	67.0	67.0

3.3.1 Calculation of the Concentration Polarization at the Membrane Surfaces

(a) δ, diffusion layer thickness

At the Webster, South Dakota plant, the volumetric flow rate is approximately 250,000 gal/day, stack and the membranes per stack are 432. Substituting these values into equation (3)

$$Q = .00138 \times \frac{250,000}{432} = 0.799, \text{ gal/min, channel.}$$

Substituting this value of Q into equation (2) we get the diffusion layer thickness

$$\delta = [30 - 10.7\,(0.799)]\ 10^{-4} = 21.4 \times 10^{-4}, \text{ cms.}$$

At the Buckeye, Arizona, plant, the volumetric flow rate is approximately 90 gal/min through each of the three parallel stacks per stage. The number of membranes per stack is 550. Substituting into equation (3),

$$Q = .00138\ \frac{90 \times 60 \times 24}{550} = .3252 \text{ gal/min, channel.}$$

Substituting this value of Q into equation (2), we get the diffusion layer thickness,

$$= [30 - 10.7\,(.3252)]\ 10^{-4} = 26.52 \times 10^{-4} \text{ cms.}$$

(b) i, operating current density

At Webster, Q = 0.779 gal/min, channel, and the cross-sectional area to flow, $A = 0.075 \times 98\ \text{cm}^2$, the dialysate linear flow velocity, as shown in equation (7). (Note the dimensions for the Buckeye flow channel are given in Figure 25.)

$$\frac{V = 3.7853 \times 10^3 \times Q}{60 \qquad\qquad A} = 6.69 \text{ cm/sec}$$

and

$$C = \frac{(C_d)_i - (C_d)_o}{\ln (C_d)_i/(C_d)_o} = \frac{.006 - .0041}{\ln(.006/.0041)} = .005 \text{ gm eq/cc}$$

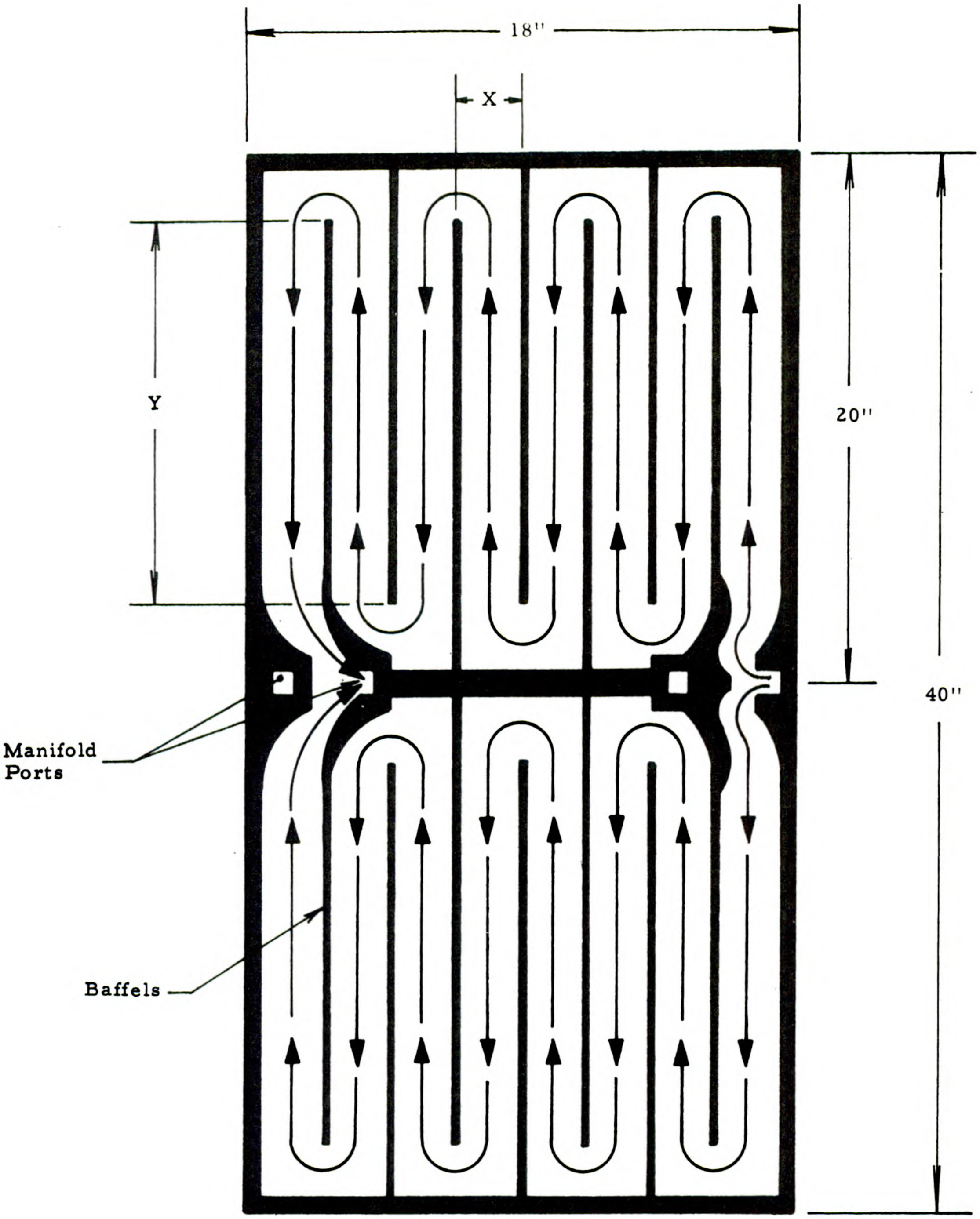

The top half of the spacer; Y = 17.7 "

Approximate path length = 8 x Y + 17 = 158.5" (402.5 cms)

Path width = x = 1.59" (4.04 cms)

$$\% \text{ area utilization} = \frac{158.5 \times 1.59}{18 \times 20} = \frac{252}{360} = 70.0\%$$

Figure 25. Schematic of the Mark III (Ionics Inc.) Spacer

Substituting into equation (7)

$$i_{lim} = (0.005 \times 10^{-3}) \times 72.3\ (6.69)^{0.947} = 0.002165 \text{ amp/cm}^2$$

from Figure 4, $(C.F.)_{9^oC} = 0.9285$

$$(i_{lim})_{9^oC} = .002176 \times .9285 = 0.00202 \text{ amps/cm}^2$$

From equation (10) and (11)

$$\text{Capacity} = \left(\frac{Q \times 3.7853}{60}\right) \left(\frac{M_s}{2}\right) \quad (C_d)_i \left(\frac{(C_d)_i - (C_d)_o}{(C_d)_i}\right)$$

$$= 0.031544 \times Q \times M_s \times (C_d)_i - (C_d)_o \text{ gm equiv/sec}$$

$$i_{oper} = \frac{\text{Capacity} \times F}{A_p \times e \times n} = \frac{\text{Cap} \times 193{,}000}{A_p \times e \times M_s}$$

For Stage IV, Webster

$$\text{Capacity} = 0.031544 \times .799 \times 432 \quad (.0060 - .0041)$$

$$= 0.0207 \text{ gms salt transf/sec}$$

$$i_{oper} = \frac{0.0207 \times 193{,}000}{9574 \times 0.914 \times 432} = 0.0011 \text{ amp/cm}^2$$

$$\text{Current Ratio} = K = 0.001/0.00202 = 0.5674$$

(c) ρ mean, mean resistivity of the diffusion layer

The two methods mentioned in Section 3.1.1.1.1 are outlined. The second is used in Table XI.

(1) The Simple Mean Method

ρ_{mean} is evaluated as the mean resistivity of the diffusion at the entrance and exit of the stream under consideration. The dialysate stream in this case.

$(C_b)_i$ = bulk solution inlet of dialysate = .006 N

$(C_b)_o$ = bulk solution exit of dialysate = .0051 N

TABLE XI

CONCENTRATION POLARIZATION IN THE BRINE AND DIALYSATE STREAMS USING THE COMPUTED DOUBLE INTEGRATION METHOD

		Concentration Polarization(1) $R_{c.p.}$ Ω-cm^2/diffusion layer		Concentration Polarization(2) $R_{c.p.}$ Ω-cm^2/cell pair
Location	Stage No.	Brine	Dialysate	
Webster, South Dakota	I	0.832	2.749	7.162
	II	0.896	4.134	10.060
	III	0.962	5.640	13.204
	IV	1.001	8.557	19.116
Buckeye, Arizona	I	0.518	1.015	3.066
	II	0.420	2.254	5.348

1. $K = i_{operating}/i_{limiting}$ (obtained from Table XV) and the double integral was incremented 150 times/coordinate.
2. In one cell pair, there exists two brine and two dialysate diffusion layers.

From the Nernst Equation (4), the surface concentration is:

$$(C_m)_i = (C_b)_i - \frac{i\delta}{FD_L} (\bar{t} - t)$$

$$(C_m)_i = (C_b)_i - 1 \frac{(21.4 \times 10^{-4}) (.806 - .39) 10^3}{(96,500) \quad (.905 \times 10^{-4})}$$

$$= (C_b)_i - 1.0205 (i_{operating})$$

at operating current $i_o = .0011$ amp/cm^2

$\underline{\text{inlet}} \quad (C_m)_i = .006 - 1.0205(.0011) = .004878$ N

$\underline{\text{outlet}} \quad (C_m)_o = .0041 - 1.0205(.0011) = .002978$ N

Concentration	Inlet	Outlet
surface	.004878	.002978
bulk	.006	.0041

Figures 26, 27, 28 and 29 for Webster and Figures 30 and 31 for Buckeye are all constructed using the Onsager Equation (14) and Equations (19) and (20). The equivalent ionic conductances are obtained from C. F. Prutton and S. H. Maron, "Fundamental Principles of Physical Chemistry," p. 462.

From Figure 5, the following data is obtained,

t = 8.89°C (Webster)	A = 38.2	B = 0.2215
t = 26.7°C (Buckeye)	A = 61.5	B = 0.2284

Equivalent Conductance	Inlet	Outlet
Surface	74.0	75.0
Bulk	71.8	72.0

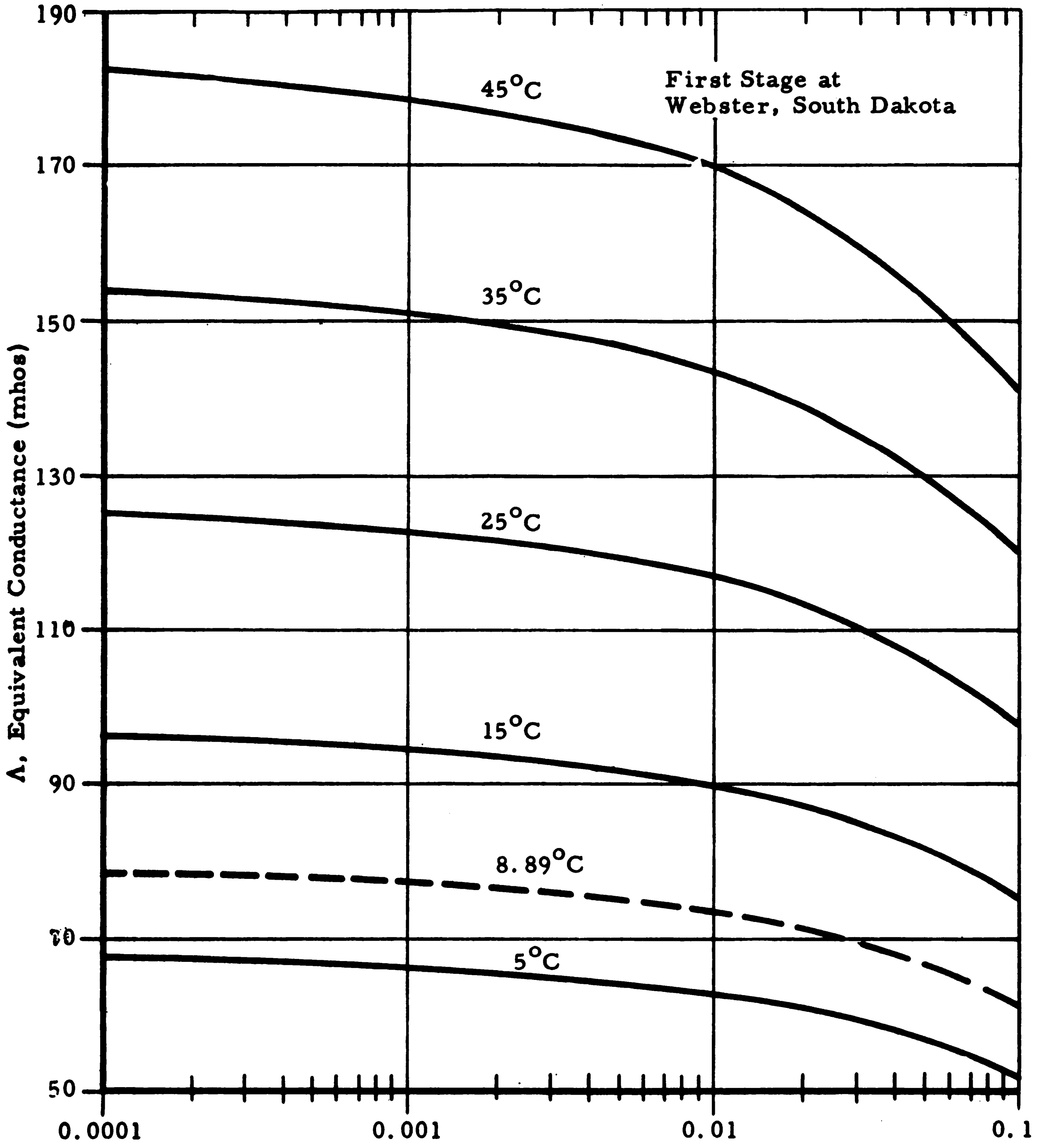

Figure 26. Plot of Equivalent Conductance Versus Average Solution Concentration for Various Temperatures. Derived from the Onsager Equation.

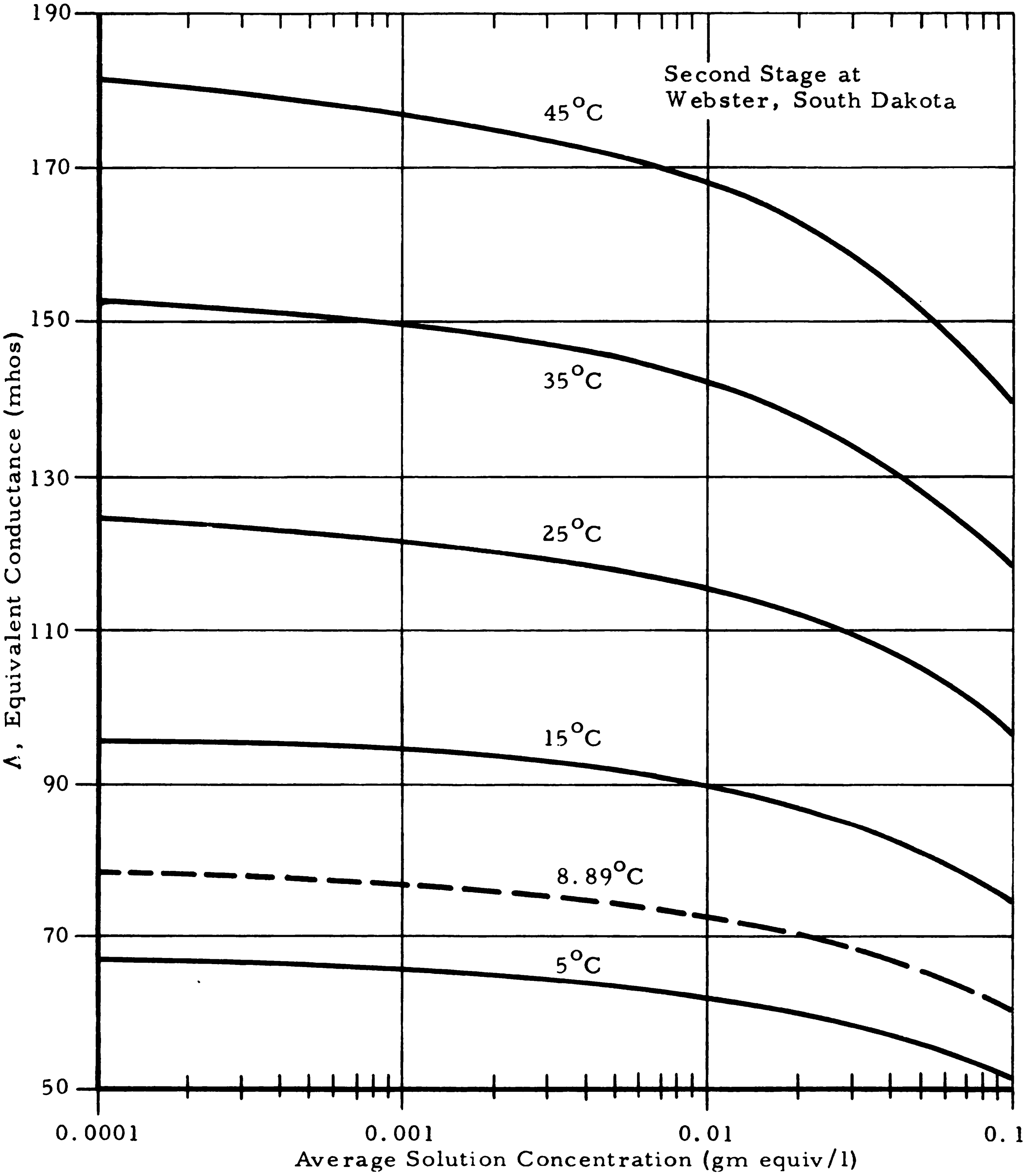

C2214

Figure 27. Plot of Equivalent Conductance Versus Average Solution Concentration for Various Temperatures. Derived from the Onsager Equation.

Then the average resistivity of the diffusion layer at the entrance and exit

$$(\rho_{ave})_i = 1/2 \left\{ \left[\frac{1000}{.004878 \times 74.0} \right] + \left[\frac{1000}{.0060 \times 71.8} \right] \right\} = 1397.0\ \Omega\text{-cm}$$

$$(\rho_{ave})_o = 1/2 \left\{ \left[\frac{1000}{.002978 \times 75.0} \right] + \left[\frac{1000}{.0041 \times 72.0} \right] \right\} = 3932.4\ \Omega\text{-cm}$$

$$\rho_{mean} = \frac{1397.0 + 3932.4}{2} = 2664.6\ \Omega\text{-cm}$$

$$R_{c.p.} = \rho_{mean}\delta = (2664.6 \times 21.4 \times 10^{-4}) = 4.702\ \Omega\text{-cm/diffusion layer}$$

(2) The Integrated Method

In Equation (17), using the four boundary conditions,

BC_1: If $x = 0$, then $C_{x,z} = C_{o,o}$

BC_2: If $x = \delta$, $z = 0$, then $C_{x,z} = C_{\delta,o}$

BC_3: If $x = 0$, $z = m$, then $C_{x,z} = C_{o,m}$

BC_4: If $x = \delta$, $z = m$, then $C_{x,z} = C_{\delta,m}$

it is possible to evaluate a, b, c, and d in terms of the concentration, viz.,

$$a = \frac{(C_{\delta,o} - C_{o,o})}{\delta}$$

$$b = \frac{(C_{o,m} - C_{o,o})}{m}$$

$$c = \left[\frac{(C_{\delta,m} + C_{o,o}) - (C_{\delta,o} + C_{o,L})}{\delta m} \right]$$

$$d = C_{o,o}$$

Thus, $C_{x,z}$ can be evaluated at any x, and z from Equation (17).

$$C_{x,z} = ax + bz + cxz + d \ldots . \qquad (17)$$

Hence, from Equation (15), we find

$$\rho_{x,z} = \text{function of } (x, z)$$

At the same time, $(\Lambda_v)_{t^oC}$ is evaluated at any coordinate x from Equations (14), (19) and (20). Equation (13), the integration can be easily evaluated by summation and iteration on a computer.

$$\frac{1}{R_{total}} = \frac{1}{m} \sum_{z=0}^{m} \left[\frac{\Delta Z}{\sum_{z=0}^{\delta} \rho_{x,z} \Delta X} \right] \qquad (91)$$

(Note: 150 iterations for both coordinates were used.)

At K = 0.5674, $(R_{c.p.})_{Stage\ IV}$ = <u>8.557</u> Ω-cm^2/diffusion layer.

The second method (8.557 compared to 4.702 Ω-cm^2/diffusion layer) is more accurate because it does not assume a linear concentration relationship as does the first. Hence, Table XI is constructed using the second or double integration method. In order to see the effect of varying the K ration, Table XII and Figure 32 were constructed. When optimization of the electrodialysis plant is undertaken, variation of resistance (in this case concentration polarization) could be determined as a function of K or the operating current density, i_o.

To obtain the overall concentration polarization effect of a cell pair, there exists two brine and two dialysate diffusion layers. For the brine stream, the concentration gradient increases from the bulk to the surface and equation (16) is replaced by (18) in the computation.

Table XI summarizes the data obtained for the Webster and Buckeye plants.

3.3.2 Estimation of Ohmic Polarization

The resistance rise due to ohmic polarization was estimated using an Equation (22).

$$\log R_{ohmic} = 0.150 + 0.92K \qquad (22)$$

TABLE XII

CONCENTRATION POLARIZATION COMPUTED USING THE DOUBLE INTEGRATION METHOD[a]

Location	Stage No.	No. of Cell Pairs	Concentration Polarization $R_{c.p.}$ Ω-cm^2/diffusion layer $K^{(b)} = 0.50$	$K = 0.60$	$K = 0.75$	K = 0 80	$K = 0.90$
Webster, South Dakota	I	216	2.206	2.346	2.620	2.736	3.031
	II	216	3.334	3.542	3.944	4.113	4.537
	III	216	5.111	5.457	6.139	6.433	7.187
	IV	216	7.460	7.963	8.952	9.376	10.464
Buckeye, Arizona	I	275	1.083	1.124	1.208	1.240	1.312
	II	275	2.436	2.542	2.731	2.805	2.976

a. The computer program, solving the double integral, was time-optimized with 150 increments per co-ordinate.

b. $K = i_{operating}/i_{limiting}$.

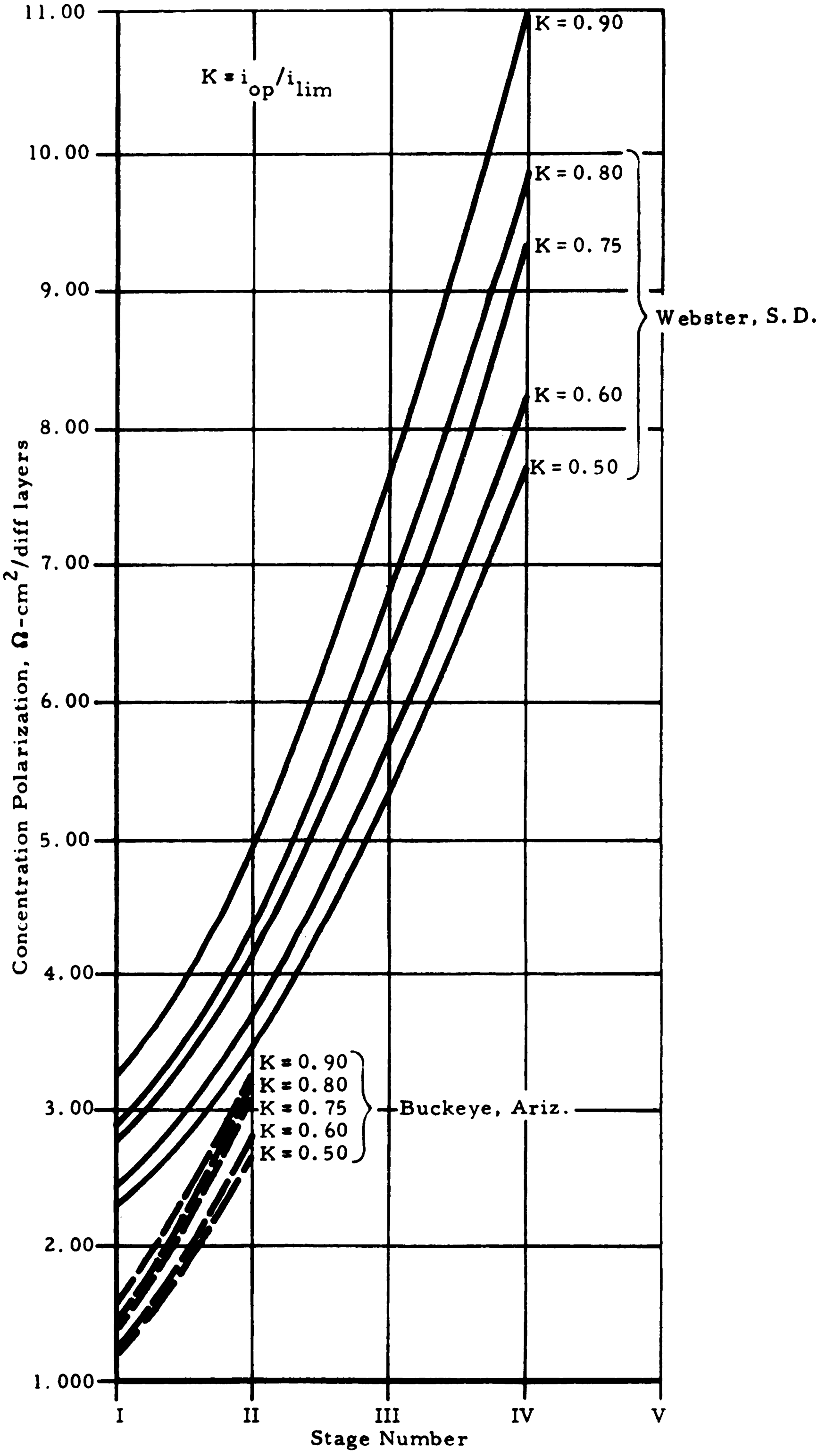

Figure 32. Variation of Concentration Polarization With the Normalized Operating Current Density for the Electrodialysis Plants at Webster, S.D. and Buckeye, Arizona.

For the fourth stage at Webster, South Dakota, K is 0.5674

$$\log R_{ohmic} = 0.150 + 0.92 \times 0.5674 = 0.672$$

$$R_{ohmic} = 4.699 \text{ ohms cm}^2 \text{ per cell pair per hour}$$

R_{ohmic} for a 20 hour period $4.699 \times 20 = 93.98$ ohms cm^2 per cell pair.

3.3.3 Calculation of Electrode Polarization

In addition to the electrode streams, the buffer streams at Webster will also be considered in this section. Figures 33 and 34 depict the approximate concentrations and schematic profiles of both the electrode and buffer streams for Webster and Buckeye. Material balances are shown in Table XIII and Table XIV. .

Cathodic and Anodic Resistances

Equation (33) will be used to evaluate the cathodic and anodic resistance analogue, which will include the catholyte anolyte and buffer bulk stream, the four diffusion layers and the electrode surface resistances. (See Figure 33.) The full equation is,

$$R_{\substack{\text{cath.}\\ \text{or}\\ \text{anode}}} = \left\{ (R_{sol})_{buffer} + (R_{sol})_{\substack{\text{catholyte}\\ \text{or}\\ \text{anolyte}}} + 2(R_{\delta}^{+}) + 2(R_{\delta}^{-}) \right\}_{ohmic} + R_{chem} + R_{conc} \qquad (33)$$

where

(R_{δ}^{+}) = positive sloping diffusion layer

(R_{δ}^{-}) = negative sloping diffusion layer

$$R_{sol} = \frac{M}{\displaystyle\int_0^m \frac{az + B}{(z^2 + yz + \delta)}} \qquad (46)$$

(Section 3.1.3 and 3.3.4)

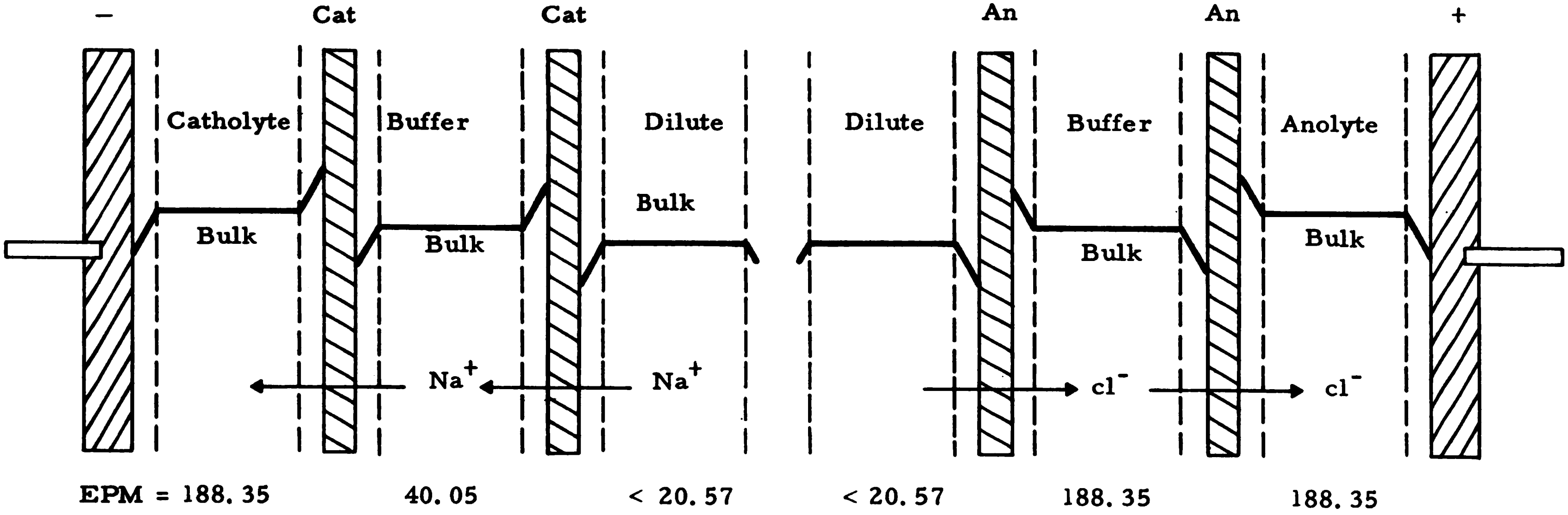

Figure 33. Concentration Profiles of the Electrode, Buffer and Adjacent Streams at Webster, South Dakota

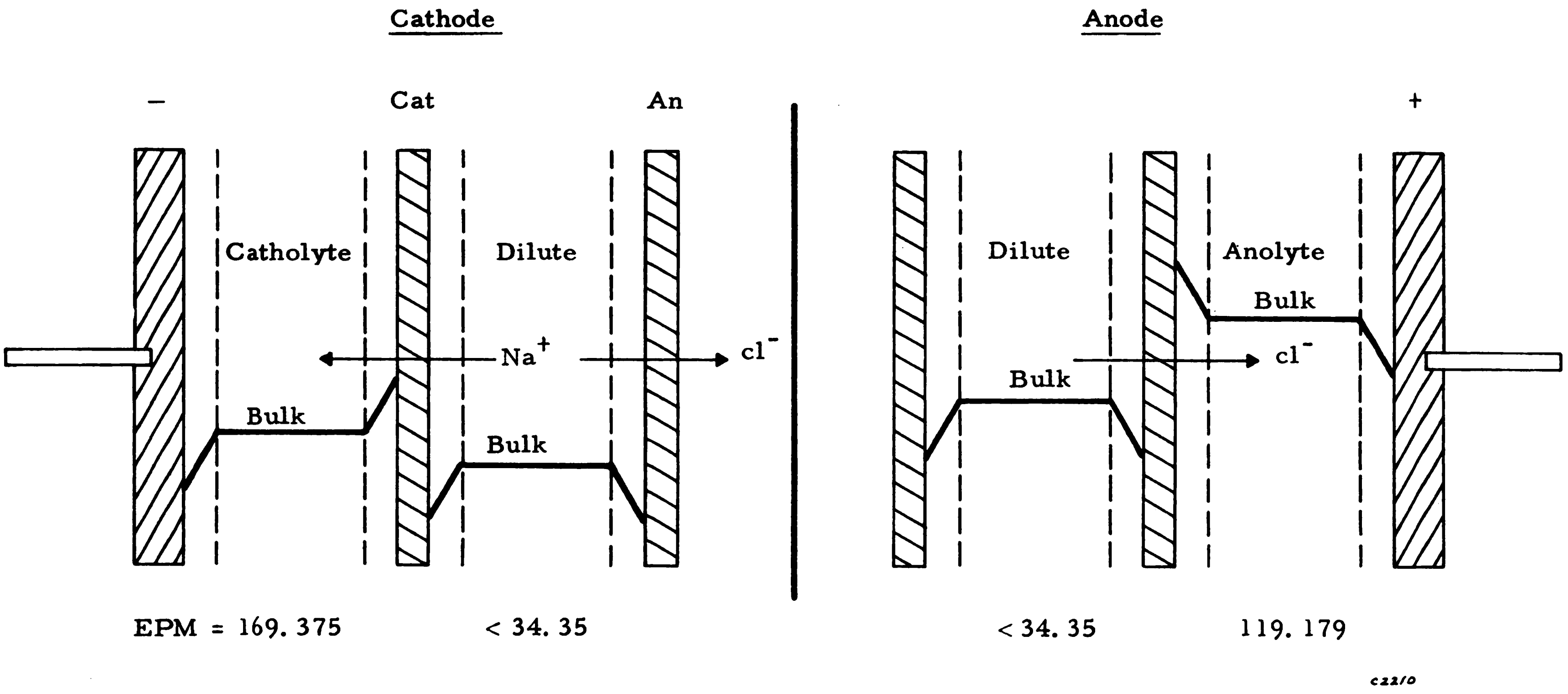

Figure 34. Concentration Profiles of the Electrode and Adjacent Streams at Buckeye, Arizona

TABLE XIII

DETAILED BRINE, CATHOLYTE, ANOLYTE AND BUFFER MATERIAL BALANCES FOR THE ELECTRODIALYSIS PLANT AT WEBSTER, SOUTH DAKOTA(a)(d)

Ionic Composition	Brine to Stage I, II, III and IV (b)		Anolyte, Catholyte and Anode Buffer to Stage I, II, and IV		Cathode Buffer to Stage I, II, III & IV	
	p.p.m.	e.p.m.	p.p.m.	e.p.m.	p.p.m.	e.p.m.
1/2 Ca^{++}	377	18.83	393	19.64	393	19.64
1/2 Mg^{++}	143	11.73	134	11.01	134	11.01
Na^+	117	5.09	147	6.40	147	6.40
H^+	5	5.00	768	152.30	3	3.00
Cl^-	16	0.45	21	0.58	21	0.58
HCO_3^-	540	8.86	561	9.21	561	9.21
1/2 $SO_4^=$	1501	31.24	8625	179.56	1453	30.26
Total dissolved Solids	2699	40.64 (c)	10649	188.35	2712	40.05
Equiv. Weight of Solution	66.41		56.54		67.72	

(a) Since the quantitative chemical analysis of the brine, buffer and electrode streams are not available, the above table is an approximate analysis derived from available data, such as dialysate analysis, pH of streams and salt transfer per stage (Reference 8).

(b) p.p.m. ≡ parts per million, e.p.m. ≡ equivalents per million.

(c) For charge neutrality, the total e.p.m. is equal to either the sum of the e.p.m. of the positive or negative ions in the solution.

(d) The three streams above are fed in parallel through all four stages.

TABLE XIV

DETAILED ELECTRODE MATERIAL BALANCES FOR THE ELECTRODIALYSIS PLANT AT BUCKEYE, ARIZONA (a)

Ionic Composition	Anolyte to Stage I(6)		Anolyte to Stage II		Catholyte to Stage I		Catholyte to Stage II	
	p.p.m.	e.p.m.	p.p.m.	e.p.m.	p.p.m.	e.p.m.	p.p.m.	e.p.m.
1/2 Ca^{++}	409	20.433	408	20.344	409	20.433	513	25.630
1/2 Mg^{++}	53	4.379	53	4.387	53	4.379	68	5.600
Na^+	2076	90.314	2070	90.052	2076	90.314	2853	124.12
H^+	--	0.002	--	--	51	50.200	0	9.689
Cl^-	3562	100.475	3381	95.361	3562	100.475	3558	100.357
HCO_3^-	243	3.994	342	5.607	243	3.994	243	3.994
1/2 $SO_4^=$	901	18.756	1057	22.010	3311	68.954	3309	68.900
Total dissolved Solids	7244	119.179(c)	7311	118.878	9705	169.375	10554	169.145
Equiv. Weight of Solution	60.78		61.50		57.30		62.396	

(a) Since the quantitative chemical analysis of the anolyte and catholyte streams are not available, the above table is an approximate analysis derived from available data, such as dialysate analysis, pH of the streams, kinetics at the electrodes and salt transfer per ion exchange, e.p.m. ≡ equivalents per million.

(b) p.p.m. ≡ parts per million, e.p.m. ≡ equivalents per million.

(c) For charge neutrality, the total e.p.m. is equal to either the sum of the e.p.m. of the positive or negative ions in the solution.

(d) The electrode streams are fed co-currently with the dialysate and brine streams and pass through each stage serially.

$$(R_\delta) = \frac{m}{\int_0^m \left[\frac{dz}{\int_0^\delta \rho_{x,z} dx} \right]} \tag{13}$$

(Section 3. 1. 1. 1. 1 and 3. 3. 1)

$$R_{conc} = \frac{-RT}{F} \left(\frac{1}{i_{lin} - i} \right) \tag{26}$$

$$R_{chem} = \frac{RT}{.5F} \left(\frac{1}{i} \right) \tag{28}$$

(Section 3. 1. 2)

Using the above five equations and referring to the evaluation of the limiting and operating current density in Section 3. 3. 1 (b), Table XV is constructed.

3.3.4 Calculation of Resistance Due to the Overall Cell Pair

Dialysate and Brine Material balances for Webster and Buckeye are given in Tables XVI, XVII, XVIII and XIII.

Assume a straight line relationship from inlet to outlet of brine and dialysate concentrations.

$$C_a = \frac{2C_B C_D}{C_B + C_D} \quad \text{if } k = 1 \tag{40}$$

Two cases occur, co- and counter-current flow of the brine and dialysate streams, both of which will be described below so as to obtain a general equation in the form of equation (46).

I. Counter Current Flow (Figure 35a)

$$C_D = a^1 z + C_i \tag{92}$$

$$C_B = a^1 z + (C_B)_o \tag{93}$$

$$C_a = \frac{Az^2 + Bz + C}{Dz + E} \tag{94}$$

TABLE XV

RESISTANCE ANALOGUE EVALUATION FOR THE ANODE AND CATHODE (PLUS BUFFER STREAM AT WEBSTER, SOUTH DAKOTA) COMPARTMENTS

Location	Stage	Electrode	i (a)	i_{lim} (a)	$i_{lim} - i$	$\frac{1}{i_{lim} - i}$	$\frac{1}{i}$	$\frac{RT}{F}$	R_{chem} $\frac{2RT}{F}(\frac{1}{i})$	R_{conc} $\frac{-RT}{F}(\frac{1}{i_{lim} - i})$	R_{sol}		R_{δ}	$R_{an\ or\ cath}$
			amp/cm^2	amp/cm^2	amp/cm^2	cm^2/amp	cm^2/amp	Volts	Ω -cm^2	Ω -cm^2	Ω - cm^2 (b)		Ω -cm^2 (b)	Ω -cm^2
											Electrode	Buffer		
Webster, South Dakota (8.89°C)	I	Cathode	0.0037	0.0057	0.0020	500.00	270.0	0.0559	30.186	-27.950	2.027	25.622	7.162	0.1715
		Anode									2.027	2.027	7.162	0.0622
	II	Cathode	0.0025	0.0040	0.0015	666.60	400.0	0.0559	44.720	-37.266	2.027	25.622	10.060	0.2091
		Anode									2.027	2.027	10.060	0.0999
	III	Cathode	0.0014	0.0027	0.0013	769.23	714.2	0.0559	79.850	-42.990	2.027	25.622	13.204	0.3597
		Anode									2.027	2.027	13.204	0.2505
	IV	Cathode	0.0011	0.0019	0.0008	1250.00	909.1	0.0559	101.640	-69.870	2.027	25.622	19.116	0.3636
		Anode									2.027	2.027	19.116	0,2543
											Electrode			
Buckeye, Arizona (267°C)	I	Cathode	0.0131	0.0657	0.0526	19.01	76.3	0.0594	9.070	- 1.129	4.080		1.533 (c)	0.0493
		Anode									8.340		1.533	0.0647
	II	Cathode	0.0053	0.0290	0.0237	42.19	188.7	0.0594	22.440	- 2.506	5.734		2.674	0.1031
		Anode									8.410		2.674	0.1128

(a) From equation (11) and (7).

(b) Webster, South Dakota: Two electrode and two buffer streams (two positive and two negative sloping diffusion layer, Figure 35).

(c) Buckeye, Arizona: Two electrode streams (one positive and one negative sloping diffusion layer, Figure 36).

TABLE XVI

DETAILED DIALYSATE MATERIAL BALANCES FOR THE ELECTRODIALYSIS PLANT AT WEBSTER, SOUTH DAKOTA [a]

Ionic Composition	Feed to Stage I[b]		Feed to Stage II		Feed to Stage III		Feed to Stage IV		Product Waste	
	p.p.m	e.p.m.	p.p.m.	e.p.m.	p.p.m.	e.p.m.	p.p.m.	e.p.m.	p.p.m.	e.p.m.
1/2 Ca^{++}	209	10.43	134.7	6.72	81.15	4.05	52.5	2.62	33.7	1.68
1/2 Mg^{++}	78.3	6.44	53.0	4.36	34.29	2.82	22.9	1.88	14.7	1.21
Na^+	85.1	3.70	57.2	2.49	42.3	1.84	33.3	1.45	27.6	1.20
Cl^-	9.22	0.26	5.32	0.15	2.84	0.08	1.8	0.05	1.1	0.03
HCO_3^-	351.4	5.76	245.2	4.02	172.0	2.82	129.9	2.13	101.9	1.67
$1/2SO_4^=$	693.9	14.55	448.3	9.40	277.1	5.81	179.8	3.77	114.0	2.39
Total dissolved solids	1426.92	20.57	943.72	13.57	609.58	8.71	420.2	5.95	293.0	4.09
Equivalent weight of solution	69.37[c]		69.54		69.99		70.62		71.64	

(a) Reference (8)

(b) p.p.m. ≡ parts per million, e.p.m. ≡ equivalents per million

(c) For charge neutrality, the total e.p.m. is equal to either the sum of the e.p.m. of the positive or negative ions in the solution.

TABLE XVII

DETAILED DIALYSATE MATERIAL BALANCES FOR THE ELECTRODIALYSIS PLANT AT BUCKEYE, ARIZONA(a)

Ionic Composition	Feed to Stage I(b)		Feed to Stage II		Product Water	
	p.p.m.	e.p.m.	p.p.m.	e.p.m.	p.p.m.	e.p.m.
1/2 Ca^{++}	116	5.79	32	1.60	9	0.45
1/2 Mg^{++}	15	1.23	4	0.33	1	0.08
Na^{+}	630	27.41	302	13.14	145	6.31
Cl^{-}	1054	29.73	467	13.17	207	5.84
HCO_3^{-}	78	1.28	41	0.67	22	0.36
1/2 $SO_4^{=}$	155	3.25	43	0.90	12	0.25
Total dissolved solids	2048	34.35(c)	889	14.910	396	6.645
Equivalent weight of solution	59.63		59.64		59.59	

(a) Reference (8)

(b) p.p.m.≡parts per million, e.p.m.≡equivalents per million

(c) For charge neutrality, the total e.p.m. is equal to either the sum of the e.p.m. of the positive or negative ions in the solution.

TABLE XVIII

DETAILED BRINE MATERIAL BALANCES FOR THE ELECTRODIALYSIS PLANT AT BUCKEYE, ARIZONA[(a)]

Ionic Composition	Brine to Stage I[(b)] p.p.m.	Brine to Stage I[(b)] e.p.m.	Brine to Stage II p.p.m.	Brine to Stage II e.p.m.	Brine[(d)] Recycle p.p.m.	Brine[(d)] Recycle e.p.m.
1/2 Ca^{++}	409	20.433	493	24.623	516	25.773
1/2 Mg^{++}	53	4.379	64	5.279	67	5.529
Na^{+}	2076	90.314	2404	104.584	2561	111.414
H^{+}	-	0.002	-	0.002	-	0.002
Cl^{-}	3562	100.475	4149	117.035	4409	124.365
HCO_3^{-}	243	3.994	281	4.604	299	4.914
1/2 $SO_4^{=}$	901	18.756	1014	21.106	1045	21.756
Total dissolved Solids	7244	119.179[(c)]	8405	138.617	8897	146.877
Equiv. Weight of Solution	60.78		60.63		60.57	

(a) Since the quantitative chemical analysis of the brine and electrode streams are not available, the above table is an approximate analysis derived from available data, such as dialysate analysis, pH of streams and salt transfer per stage (Reference 8).

(b) p.p.m. ≡ parts per million, e.p.m. ≡ equivalents per million.

(c) For charge neutrality, the total e.p.m. is equal to either the sum of the e.p.m. of the positive or negative ions in the solution.

(d) Brine is fed co-currently with the dialysate and passes through each stage serially.

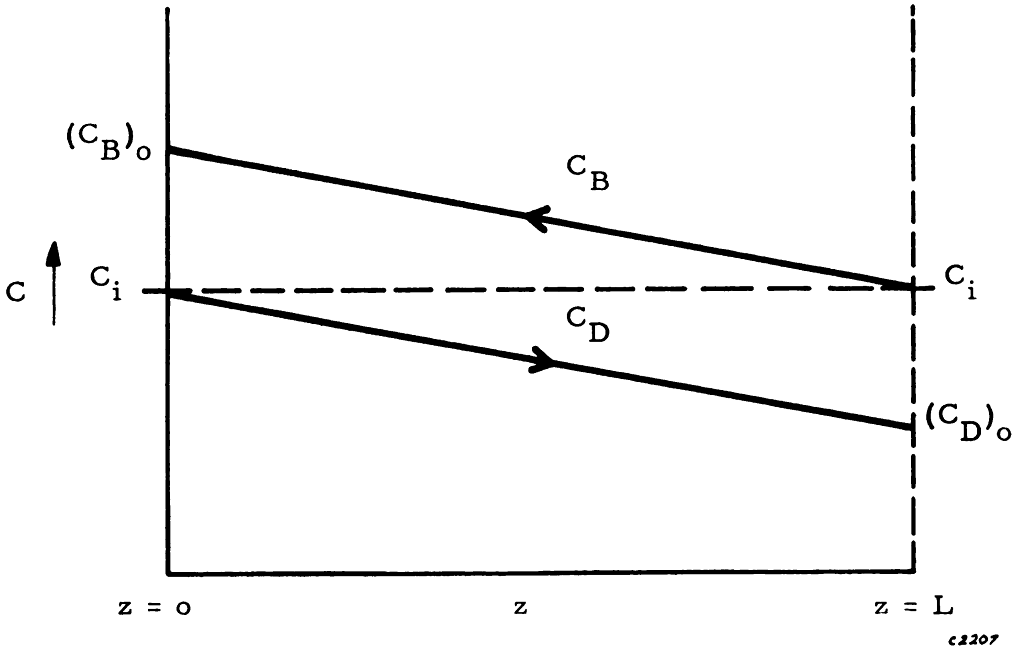

(a) Counter-Current Flow (Webster)

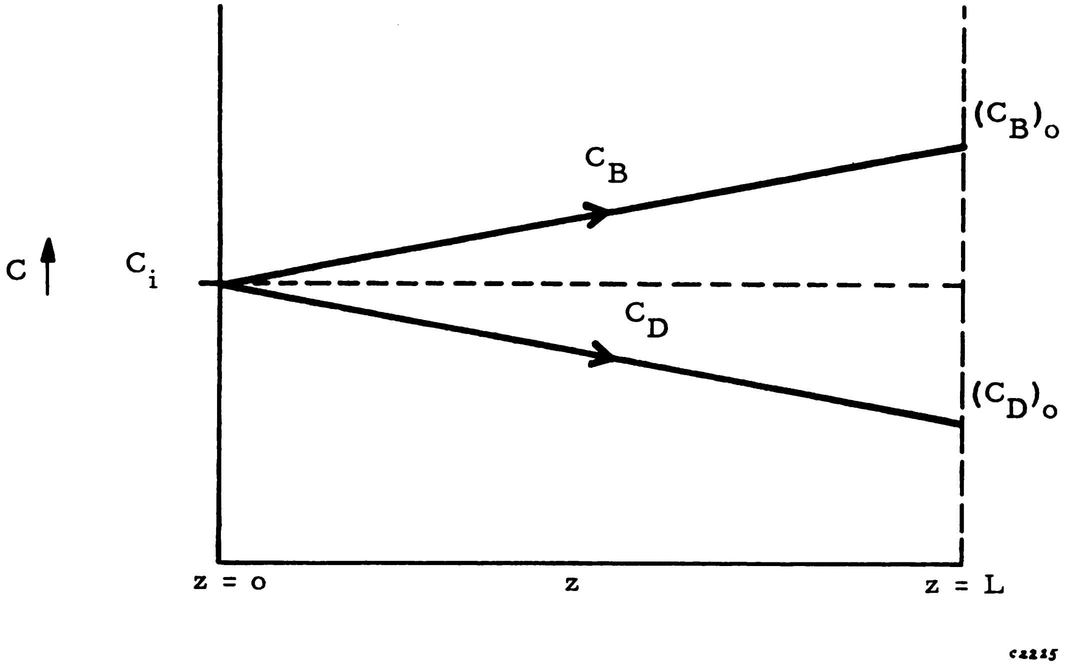

(b) Co-current Flow (Buckeye)

Figure 35. Concentration Profiles of the Dialysate and Brine Streams.

$$\frac{1}{R_p} = K^1 \int_o^m \frac{(z^3 + \alpha z^2 + \beta z + \gamma)\, dx}{(z^4 + \delta z^3 + \theta z^2 + z + \eta)} \qquad (95)$$

II. Co-Current Flow (Figure 35b)

$$C_D = -ax + C_i \qquad (96)$$

$$C_D = +az + C_i \qquad (97)$$

$$C_a = F + Gz^2 \qquad (98)$$

$$\frac{1}{R_p} = K'' \int_o^m \frac{(z^2 + \sigma)\, dx}{(z^4 + \gamma z^2 + \mu)} \qquad (99)$$

The nomenclature for the above eight equations is as follows:

where

$$\alpha = \left(\frac{AE + CB}{DA}\right)$$

$$\beta = \left(\frac{BE + CD}{DA}\right)$$

$$\gamma = \frac{CE}{DA}$$

$$\delta = \left(\frac{K_2AD - K_2 2AB}{K_3A^2}\right)$$

$$\theta = -\left(\frac{K_1D^2 + (AE-BD)K_2 - (2AC+B^2)K_3}{K_3A^2}\right)$$

$$\varphi = -\left(\frac{2\ DEK_1 + (BE + CD)\ K_2 - 2\ BCK_3}{K_3A^2}\right)$$

$$\eta = -\left(\frac{E^2K_1 + ECK_2 - C^2K_3}{K_3A^2}\right)$$

$$K^1 = -\left(\frac{P\eta DA}{K_3A^2}\right)$$

$$\sigma = F/G$$

$$\nu = -\left(\frac{K_2G - K_3FG^2}{K_3G^2}\right) = -\left(\frac{K_2 - 2K_3F}{K_3G}\right)$$

$$\mu = -\left(\frac{K_1 + K_2F - K_3F^2}{K_3G^2}\right)$$

$$K'' = -\left(\frac{pnG}{K_3G^2}\right) = -\left(\frac{pn}{K_3G}\right)$$

where

$A = 2(a')^2$

$B = 2a'(C_i + C_B)_o$

$C = 2C_i(C_B)_o$

$D = 2a'$

$E = C_i + (C_B)_o$

$F = C_i$

$G = \frac{-a^2}{C_i}$

and

$a = \left(\frac{\Delta C}{m}\right)$ slope of C vs. z chart

m = total path length (of desalination area), cms

n = total width of chamber, cms

p = fraction of usable desalination area

$a' = \left(\frac{-\Delta C}{m}\right)$ = slope of C vs. z chart, gm. equiv/l cm

$\Delta C = (C_B)_o - C_i = C_i - (C_D)_o$

C_i = initial feed concentration, gm. equiv/l

$(C_B)_o$ = final brine concentration, gm. equiv/l

$(C_D)_o$ = final dialysate concentration, gm. equiv/l

K_1, K_2, K_3 = constants obtained from $\underline{R_p}\ \underline{C_a}$ vs. $\underline{C_a}$, see following derivation.

In order to evaluate K_1, K_2 and K_3, Equation (43) will be evaluated for three different z-coordinate positions — a quarter, a half, and three quarters of the path length, m. Thus, three simultaneous equations are obtained and the three unknowns can be evaluated provided $(R_p)_z$ is evaluated at each coordinate from the following equation,

$$(R_p)_z = (\rho_{cat} + \rho_{an})\, t_m + \left\{ \frac{1}{(\Lambda_v)_{t^\circ C_D} \times C_D} + \frac{1}{(\Lambda_v)_{t^\circ C_B} \times C_B} \right\} 10^3 y \qquad (37)$$

$$\rho_{cat} = (C_a)^i + k \qquad (100)$$

$$\rho_{an} = (C_a)^j + q \qquad (101)$$

where

t_m = membrane thickness, cms

y = spacer thickness, cms

Ca, C_D, C_B = obtained from Equations (92), (93) and (94)

$(\Lambda_v)_{t^\circ C}$ = obtained from Section 3. 1. 1. 1. 1

i, j, k, q = obtained from manufacturer for given membrane.

(See Figure 36 for the constant values.)

The results of the above method is presented in Table XIX. It must be emphasized that using equation (47) and (48) result in the exact answer, but are more tedious to use than the summation Equation (49).

For Stage IV Webster,

$$\left.\begin{aligned} K_1 &= 1.9687 \\ K_2 &= 14.3605 \\ K_3 &= 86.3433 \end{aligned}\right\} \text{ and } R_p = 249.79\ \Omega\text{-cm}^2/\text{cell pair}$$

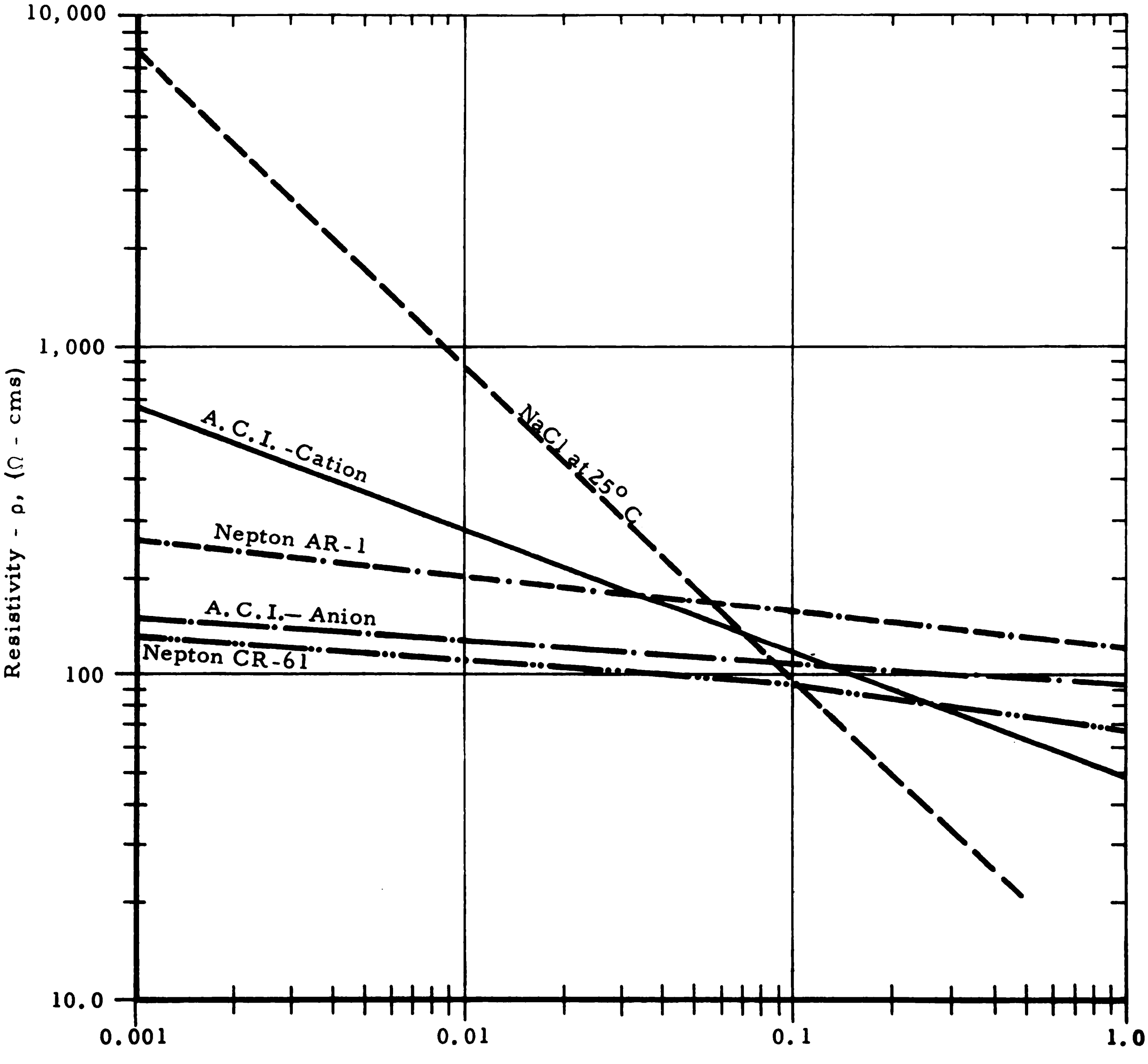

Figure 36. **Resistivity of Ion Exhange Membranes and Sodium Chloride Solutions**

TABLE XIX

SUMMARY OF THE SOLUTION AND MEMBRANE RESISTANCES PER CELL PAIR

		Present Buckeye Plant		Sea Water Plant					Projected Plant (Buckeye)		Present Webster Plant			
		Stage		Stage					Stage		Stage			
	Units	I	II	I	II	III	IV	V	I	II	I	II	III	IV
(R_p) Composite Cell Pair Resistance	$\Omega\text{-cm}^2$/cell pair	68.68	107.67	18.322	21.85	29.597	47.402	89.871	62.884	101.78	102.25	136.42	185.16	249.79
R_{Membrane} Path Position*	$\Omega\text{-cm}^2$										Not Calculated			
.25 m		11.6044	11.5974	11.633	11.623	11.614	11.606	11.598	5.844	5.847		4.806	4.804	4.804
.50 m		11.6039	11.5969	11.633	11.623	11.613	11.605	11.598	5.844	5.847		4.805	4.804	4.803
.75 m		11.6029	11 5961	11.631	11.621	11.612	11.604	11.596	5.843	5.836		4.805	4.804	4.803
R_{Solution}	$\Omega\text{-cm}^2$													
.25 m		52.3493	83.0379	6.482	9.287	15.551	30.075	65.033	52.349	83.038		116.765	163.862	223.638
.50 m		55.4473	94.7128	6.426	9.930	17.544	35.104	77.239	55.447	94.713		126.738	176.541	241.246
.75 m		61.5978	112.2080	6.712	11.089	20.647	42.821	95.896	61.598	112.208		138.957	191.770	262.507

*m = total path length.

3.3.5 Calculation of the Parasitic Duct Loss Resistance

(a) Cell Pair Resistance, R

$$R = R_{an} + R_{cat} + R_d + R_b \qquad (58)$$

From Equation (56), ρ^d and ρ^b are evaluated using the data from Stage IV Webster, S. D. Refer to mass balance in Figure 37 for concentrations and Figure 29 for equivalent conductance at 48°F.

(i) Dialysate

$$p^d = \frac{1}{2}\left\{\left[\frac{1000}{\Lambda C}\right]_{b,o} + \left[\frac{1000}{\Lambda C}\right]_{b,i}\right\} = \frac{1}{2}\left\{\left[\frac{1000}{73.0 \times .0041}\right] + \left[\frac{1000}{72.0 \times .0060}\right]\right\} \qquad (63)$$

$$= 2.828 \times 10^3 \ \Omega\text{-cm}$$

where $\underline{b}$ refers to bulk stream, $\underline{o}$ to stream outlet and $\underline{i}$ the stream inlet.

(ii) Brine

$$p^b = \frac{1}{2}\left\{\left[\frac{1000}{C}\right]_{b,o} + \left[\frac{1000}{C}\right]_{b,i}\right\} = \frac{1}{2}\left\{\left[\frac{1000}{64.8 \times .0427}\right] + \left[\frac{1000}{65.0 \times .0406}\right]\right\} \qquad (64)$$

$$= 0.370 \times 10^3 \ \Omega\text{-cm}$$

We now evaluate

$$R_d + R_b = \frac{y}{(mxn)p}\left[\rho^d + \rho^b\right] \qquad (58)$$

where

$msn = 44 \text{ in.} \times 44 \text{ in.} = 111.76 \times 111.76 \text{ cm}^2$

$y = .075$ cm

p = fraction of area for ion transfer = .77

Substituting into above equation

$$R_d + R_b = \frac{.075}{(111.76)^2 \times 0.77}\left[2.828 \times 10^3 + 0.370 \times 10^3\right]$$

$$= 0.02494 \ \Omega/\text{cell pair}$$

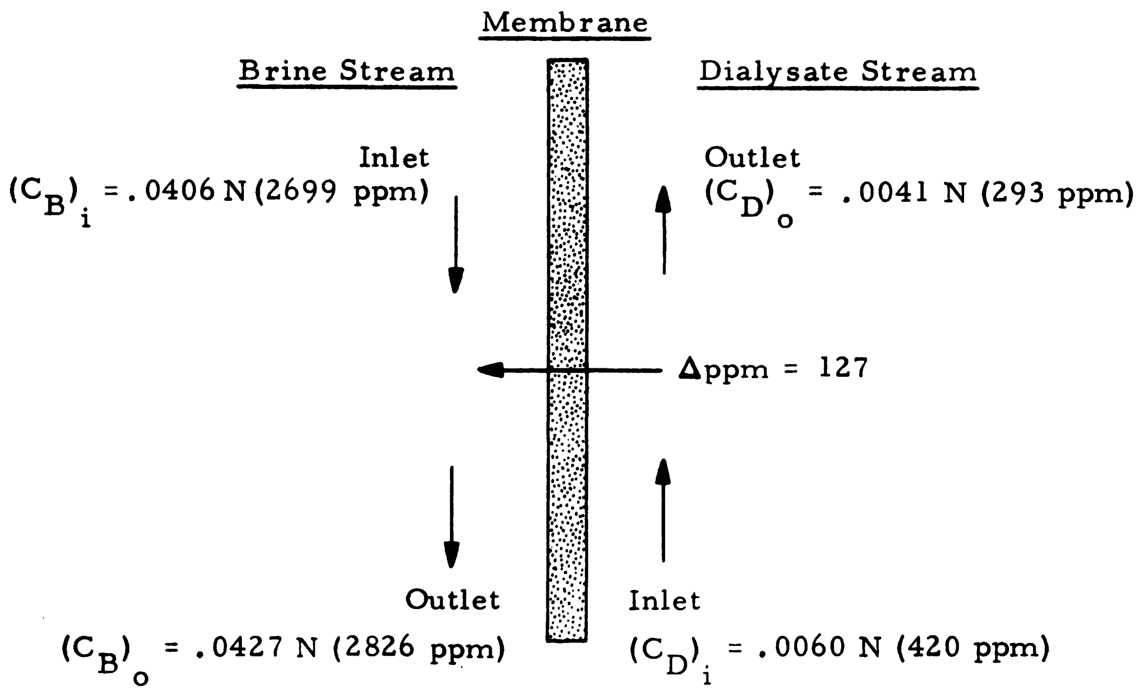

C1846

Figure 37. Mass Balance of the Dialysate and Brine Streams for Stage IV, Webster, South Dakota

From Equation (100) and (101) and Figure 29,

$$R_{cat} + R_{an} = (\rho_{cat} + \rho_{an}) \frac{1}{A_p}$$

$$R_{cat} + R_{an} = \left[(C_a^{\,i} + k) + (C_a^{\,j} + q)\right] \frac{1}{A_p}$$

From Figure 37, the average concentration C_a, defined by Equation (40), can be calculated at the inlet and outlet. Because C_a varies with path coordinate z, the equation above was integrated from z = 0 to z = 111.76 cm. For explanation purposes, in this example of the calculation for Stage IV Webster, the use of the inlet and outlet average concentration will suffice.

<u>Inlet</u> $$(C_a)_i = \frac{2(.006)(.0427)}{.0487} = 0.01052 \text{ gm eq}/\ell$$

<u>Outlet</u> $$(C_a)_o = \frac{2(.0041)(.0406)}{.0447} = 0.00744 \text{ gm eq}/\ell$$

Substituting the correct data in the above equation for Webster, S. D.,

$$R_{cat} + R_{an} = \left\{\left[(.01052)^{.3838} + 48.0\right] + \left[(.00744)^{.0817} + 160\right]\right\} \frac{.023}{9574}$$

$$= 0.0005018\ \Omega/\text{cell pair}$$

Substituting into Equation (58)

$$R = (R_{cat} + R_{an}) + (R_d + R_b)$$

$$= 0.000,5018 + 0.02494$$

$$= 0.0254418\ \Omega/\text{cell pair}$$

or in area units,

$$R = 0.0254418 \times 9574 = 243,579\ \Omega\text{-cm}^2/\text{cell pair}$$

This approximate method provides a fairly accurate result, i.e., 243.579 (approximate method), and 249,579 (exact method). (See Table I.)

(b) Channel Resistance, $\bar{R}_L$

$$\frac{1}{R_\ell} = \frac{1}{R_d} + \frac{1}{\bar{R}_b}$$

Refer to Figure 38 for channel dimensions

Dialysate

Substituting the following values into Equation (56) where (see Figure 38)

U_d = 4.246 cm

V_d = 3.770 cm

p_d = 2.828×10^3 Ω-cm

ℓ = 0.075 cm

y = 0.023 cm

N = 216 cell pairs

$$\overline{R}_d = \frac{2.828 \times 10^3 \times 2 \times (.075 + .023)\ 216}{4.246 \times 3.77} = 7.479 \times 10^3\ \Omega/\text{stack}$$

and substituting the following values in Equation (55)

ρ_b = 0.370×10^3 Ω-cm

y_b = 2.818 cms

$$\overline{R}_b = \frac{0.370 \times 10^3 \times 2 \times (.075 + .023)\ 216}{\pi/4(2.818)^2}$$

Substituting equations (55) and (56) into Equation (57)

$$\overline{R}_\ell = \frac{1}{\dfrac{1}{\overline{R}_d} + \dfrac{1}{\overline{R}_b}} = \frac{10^{+3}}{0.1337 + 0.3983} = 1.880 \times 10^3\ \Omega/\text{stack}$$

$$= \underline{83.329 \times 10^3}\ \Omega/\text{cell pair}$$

We can now evaluate, $\Psi = \dfrac{\overline{R}_\ell}{R} = \dfrac{83,329.0}{249.579} = 342.10$

From Figure 14, or Equation (54),

$$\left(\frac{i_\ell}{i_o}\right) = \text{fraction of current leakage}$$

$$= 0.0011, \text{ i.e., less than } 1\% \text{ current leakage}$$

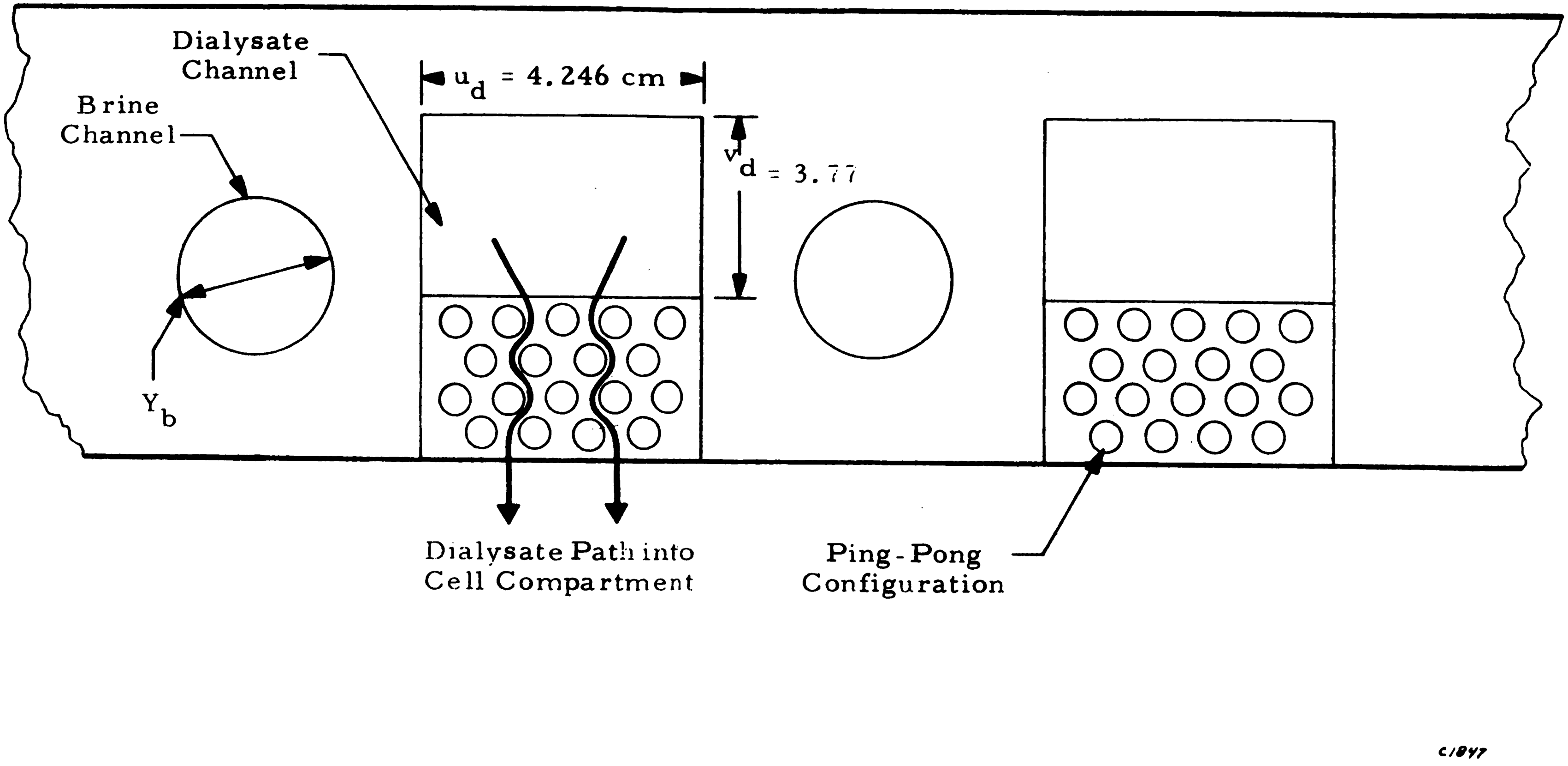

Figure 38. Channel Dimensions of Brine and Dialysate Streams as Shown by a Dialysate Gasket, from the Stack at Webster, South Dakota

Substituting into Equation (65), if we use data for

stack voltage $E = 240$ volts

and current $i_o = 35$ amps

$$R_{d.\ell} = \frac{E}{i_L} = \frac{E}{.0011\, i_o} = \frac{240}{.0011 \times 35} = 6418.0\ \Omega/\text{stack}$$

This result is for the fourth stack at Webster (Seko(23) p. 591). Obviously, the higher $R_{d.\ell}$ the better because it will be in parallel with the stack current. In area-resistance units,

$$R_{d.\ell} = \frac{6418 \times 9574}{216} = 284,470\ \Omega\text{-cm}^2/\text{cell pair}$$

3.3.6 Calculation of the Corrected Coulomb Efficiency Based Solely on the Water Transfer Processes

In Equation (68) is substituted the following data for Stage IV Webster, S. D.

$$\omega_t = \omega_a + \omega_b = 0.446 + 0.666 = 1.132\ 1/F$$

$$C_o = (C_d)_i = .006\ N$$

$$C_T = (C_d)_o = .0041\ N$$

$\eta_D = 0.914$ from manufacturer.

The result is: $\eta = 0.9078$.

3.3.7 Calculation of Resistance Due to Membrane Selectivity

The values from the first stack at Webster, South Dakota plant are substituted into Equation (80) below, if

$$E_s = 240 \text{ volts}$$

$$I = 35 \text{ amps}$$

$$t_+^a = (1 - t_-^a) = (1 - 0.9809) = 0.0191$$

$$t_-^c = (1 - t_+^c) = (1 - 0.9573) = 0.0427$$

$$R_s = \frac{E_s}{I(t_-^c + t_+^a)} = \frac{128.0}{10.(.0618)} = 207.12 \text{ ohms/stack} \qquad (80)$$

or

$$R_s = (R_3 \text{ in Figure 22}) = \frac{207.12 \times 9574}{216} = 9180.4 \ \Omega\text{-cm}^2/\text{cell pair}$$

3.3.8 Calculation of Resistance Due to Membrane Potential

Substituting Equations (73) and (74) into (75) and then into Equation (76) we get

$$R_{m.p} = \frac{2RT}{i_o F} \left\{ \ln \frac{(C_{b,m})_z}{(C_{d,m})_z} \right\} \times (t_+^c + t_-^a - 1) \ \Omega\text{-cm}^2/\text{cell pair} \qquad (76)$$

Since $(C_{b,m})_z$, the brine surface concentration and $(C_{d,m})_z$, the dialysate surface concentration both vary along the flow path, z, the above equation was integrated to obtain an average $(C_{b,m})/(C_{d,m})$ ratio. To do this, the concentration profile of both the dialysate and brine streams from inlet to exit would have to be known. As a starting point, the simplified expressions of Shaffer and Mintz$^{(31)}$ or Spiegler's ideas$^{(32)}$ led us to assume the following concentration profile along the flow path:

$$\text{Dialysate:} \quad (C_D)_z = (C_D)_i \ \exp\left(\frac{z}{m} \ln C_{Do}/C_{Di}\right) \qquad (102)$$

In the bulk solution,

$$\text{Brine:} \quad (C_b)_z = (C_B)_i \ \exp\left(\frac{z}{m} \ln C_{Bo}/C_{Bi}\right) \qquad (103)$$

Hence, Equation (76) becomes,

$$R_{m.p} = \frac{2RT\,(t_+^c + t_-^a - 1)}{i_o F} \ \frac{1}{m} \int_{z=0}^{m} \ln \frac{(C_{Bi})}{(C_{Di})} \exp\left[\frac{z}{m}(\ln C_{Bo}/C_{Bi} - \ln C_{Do}/C_{Di})\right] \qquad (104)$$

Replacing the integration by summation and using the data from Table VIII for Webster Stage IV,

$$R_{m.p} = 260.16 \text{ ohms-cm}^2/\text{cell pair}$$

3.3.9 Electrodialysis of Sea Water

3.3.9.1 Operating Characteristics

The power requirements for a hypothetical sea water conversion plant were calculated. In order to effect a direct comparison with the power requirements for desalinating brackish water, the same stack design as used in the Buckeye, Arizona plant was assumed. Since the salt concentration of sea water is roughly 18 times that of the brackish water at Buckeye, it was necessary to increase the number of stages in the hypothetical plant to 5, and to increase the total effective membrane area within each stage to 10 times that of a single Buckeye stage. This entailed a corresponding reduction in the ratio of $i_{operating}/i_{lim}$, as explained below. All other operating characteristics, such as flow velocity and current efficiency, were taken to be the same as those used at Buckeye. Refer to Table VIII, IX and X for operating data, and Figure 39 for material balance.

3.3.9.2 Mathematical Determination of $i_{operating}$

An exponential relationship between the amount of salt to be removed and the number of stages required was derived and applied to the Buckeye plant in order to determine the value of i_{op} at any given stage. Let C_n = dialysate concentration (e. p. m.) after passing through n stages; C_o = initial concentration of sea water (593.685 e. p. m.). Then

$$\frac{C_n}{C_o} = e^{-n\theta} \qquad (105)$$

where

$$\theta = \frac{K(A_p)\, M\nu^{0.6}\, (C.F.)\, \eta}{2\, F\, Q\, (31.544)} = \text{operating constant.}$$

(Obtained from Section 3.1.1, Equations (5), (8), (9) and (10).)

For the two-stage desalination of brackish water at the present Buckeye plant, we find that $\theta = 0.8238$ (using $K = 0.1903$ and $A_p = 3252\ cm^2$). If we now divide θ by $K\, A_p$, we obtain

$$\frac{C_n}{C_o} = e^{-n\theta'\, K\, A_p} \qquad (106)$$

TABLE XX

MAJOR CONSTITUENTS OF SEA WATER[(a)]

Ionic Composition	Parts per Million	Equivalents per Million
1/2 Ca^{++}	400	19.96
1/2 Mg^{++}	1,272	104.62
Na^{+}	10,561	459.41
K^{+}	380	9.72
Cl^{-}	18,980	535.40
HCO_3^{-}	142	2.33
$SO_4^{=}$	2,649	55.55
Br^{-}	65	0.81
Total dissolved solids	34,449	593.9[(b)]
Equivalent Weight of Solution	58.00	

(a) Reference (31)

(b) For charge neutrality, the total e.p.m. is equal to either the sum of the e.p.m. of the positive or negative ions in the solution.

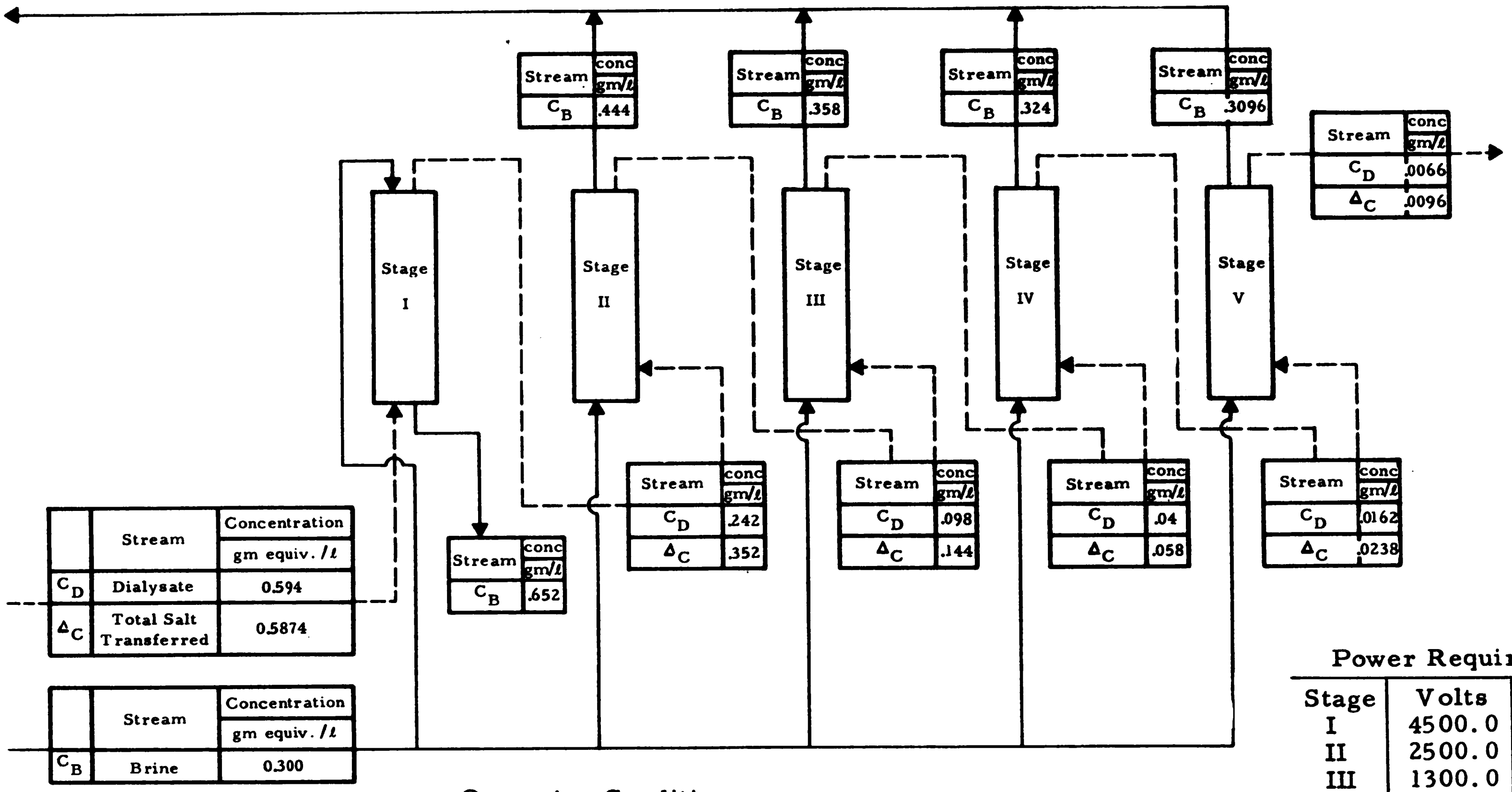

Power Requirements

Stage	Volts	Amp
I	4500.0	747.35
II	2500.0	303.66
III	1300.0	123.39
IV	700.0	50.200
V	300.0	20.382

Operating Conditions

Temperature = 26.7°C
"Substages" per Stage (series) = 10 (each stage above consists of 10 substages in series)
Stacks per Stage = 3
Membranes per Stack = 550
Usable area per Stage = 32522.0
Dialysate flow rate = 0.3252 gal/min channel
Type of ion exchange membranes:
Cation — Ionics #61AZL 183 (thickness 0.06 cms)
Anion — Ionics #111BZL 183 (thickness 0.06 cms)

c2226

Figure 39. Flow Sheet and Material Balance for Hypothetical Sea Water Plant With Buckeye, Arizona, Equipment and Conditions

where $\theta' = \theta/K A_p = .00133$. We require a product water salt conc. of 6.645 e.p.m. To achieve this desalination ratio we shall employ five stages wherein the total usable area per membrane $= 10 A_p = 32{,}520 \text{ cm}^2$. Hence (106) becomes

$$\frac{6.645}{593.685} = e^{-5(.00133)\,32{,}520\,K}$$

or

$$89.343 = e^{216\,K}$$

$$\ln 89.343 - 4.49 = 216\,K$$

$$K = \frac{4.49}{216} = .0208 = i_{op}/i_{lim}.$$

We may now use Equation (105)to predict i_{op} at each stage:

$$i_{op} = K\, i_{lim} = .0208\,(\text{C.F.})\, M\, \nu^{0.6} \log \text{mean } C_n \qquad (107)$$

M = constant = 590

ν = linear flow velocity = 12.495 cm/sec

$\log \text{mean } C_n = \dfrac{C_n - C_{n-1}}{\ln C_n/C_{n-1}}$ at the n'th stage (eq/cc).

i_{op} = operating current density (amps/cm^2).

Refer to Table IV for results of the Sea Water Plant.

3.3.10 Electrodialysis of Projected Plants

After calculating the resistance analogues and comparing the results for each stage at Webster and Buckeye, an attempt is now made to predict what the resistance analogue of a future or projected plant would be, providing several detrimental factors are favorably improved during the next few years. A short description of each projected assumption is described below. All unmentioned factors are held contant for both the plants discussed. Table III shows the results. To comprehend the effect of the following assumption, Table III should be compared to Tables I and II

3.3.10.1 Concentration Polarization

Equation (2) is changed to

$$\delta = 20 - 10.7\,Q \text{ microns}$$

Reasoning is based on the fact that future development in spacer design, hydrodynamic control and membrane surface phenomena would at least half the diffusion layer thickness.

3.3.10.2 Ohmic Polarization

It is thought that advances in membrane technology, operating and pretreatment procedures could possibly lower the ohmic resistance tenfold.

3.3.10.3 Composite Cell Pair

Membrane advances would result in at least the lowering of membrane resistances by fifty percent. Hence, the intercepts for the membranes in Figure 36 are halved.

3.3.10.4 Membrane Polarization

Provided considerable advances take place in minimizing the diffusion layer thickness, δ, the limiting case would occur when the concentration gradient across the layer is negligible (i.e., $\delta \rightarrow 0$). Hence, instead of using the membrane surface concentrations, we could, in the limit use the bulk concentrations in Equations (73) and (74). This would lower the final membrane resistances as shown in Table III.

3.3.10.5 Neglected Effects

Duct leakage at present is negligible (less than 1% — see Section 3.3.5). Membrane selectivity although not a hundred percent is at present very close (within the 98 to 100 percent range). Although electrode polarization does contribute some resistance to the stack, it is very small, and has less effect the more cell pairs used per stack. It is conceivable that many times more cell pairs per stack could in future be used, and so minimizing the electrode effects.

3.3.11 Discussion of Calculated Values

The area resistance for the factors listed in Tables I through IV were calculated as described in the above sections.

The composite cell pair resistance consists of membrane resistance and electrolyte resistance. The relative importance of these two factors is shown in Table XIX. The composite cell pair resistance in general increases with inlet feed concentration as can be noticed in the Tables I - IV in progressing from the first stage to the latter stages. Webster water contains the least electrolyte and gives the highest value for composite cell pair resistance. A comparison of membrane resistance to electrolyte resistance at various positions along the flow path are shown in Table XIX. The membrane resistance in the Webster plant is low and insignificant, as the feedwater changes in composition to that in the sea water plant, the membrane resistance becomes greater than the electrolyte resistance and is twenty percent of the total cell pair resistance In the Webster plant membrane resistance is only two percent of the total stack resistance. The calculation for the projected plants assumed that the membrane resistance was one-half that used in the present plants. As indicated in Table III, the composite cell pair resistances are not appreciably changed by this membrane improvement.

The concentration polarization values represent the resistance of the diffusion layers adjacent to the membrane surface. Compared to other factors, this resistance is minor and represents at most five percent of total cell pair resistance.

The resistance due to ohmic polarization is a major factor in total cell pair resistance. It represents over 40 percent of the total resistance in Stage I at Webster. It is estimated that in a sea water plant this factor could account for as high as sixty percent of the total. In calculating ohmic polarization values for the projected plants, assumptions were made that ohmic polarization could be reduced to ten percent of its present value.

Duct leakage and selectivity resistances are parallel to the desalting resistances in the network equations. The high resistance values found for these factors are desirable and make only minor contributions to total stack resistance. In the projected plants the assumption was made that the influence of these factors could be reduced to an even greater extent, makint their contributions completely insignificant.

Membrane polarization is a major factor contributing as much as 87 percent of the total resistance in the last stage of a sea water plant. The resistance values for the projected plants are based on the assumption that concentration polarization in the diffusion layer can be reduced to 50 percent of its present value. The lower value of the membrane polarization for the projected Webster plant is due partly to lower concentration gradients in the diffusion layer which in turn is brought about by a higher flow velocity.

Electrode polarization is a minor factor, making up about one-tenth of one percent of the total resistance.

The power index was calculated for each stage using Equation (85A). These values are reported in the last column of Tables I through IV. The index is proportional to the electrical power required to treat 1000 gallons of water. This index decreases from first to last stage for all plants, and increases from plant to plant as the salinity of the feed water increases as is expected. The index can be used to compare stack or plant design only when the same feed water is used and when the same change in salinity is obtained. For example, a direct comparison between the Webster plant and the improved Webster plant can be made with the power index figures which are lower for the latter. The power index can therefore be used to optimize stack and plant design.

STATEMENT OF INVENTION

The Douglas Astropower Laboratory of the Douglas Aircraft Company Missile and Space Systems Division does hereby certify that to the best of its knowledge and belief no inventions resulted from performance under this contract.

REFERENCES

1. Mason and Rust; An Engineering Evaluation of the Electrodialysis Process Adapted to Computer Methods for Waste Deslination, Office of Saline Water Report 134, February (1965)

2. Cooke, B. A.; "Some Phenomena Associated with Concentration Polarization in Electrodialysis," First International Symposium on Water Desalination, October 3-9, 1965, SWD/18.

3. Weiner, S. A.; Sea Water Conversion Laboratory, Report No. 65-6, University of California, Berkeley.

4. Rosenberg, N. W. and Tirrell, C. E.; "Limiting Currents in Membrane Cells," Industrial & Eng. Chemistry, April 57, 49, 4, 781.

5. Gregor, H. P.; Bruins, Paul F. and Rothenberg, M.; "Boundary Layer Dimensions in Dialysis," I & ER Process Design & Development 4, No. 1, January 1965, p. 3.

6. Spiegler, K. S.; "Saline Water Conversion Research in Israel," Saline Water Conversion II, Advances in Chemistry Series 38, p. 179 (1963).

7. Mason, E. A. and Kirkham, T. A.; C.E.P. Symposium Series No. 24, 55 (1959), p. 173.

8. Private Communication with Dr. John Nordin from the Demonstration Unit at Webster, South Dakota.

9. Weiner, S. A.; "The Effect of Temperature on Electrodialytic Demineralization," Bull. Chem. Soc., 38, Japan (1965), p. 2002.

10. Spiegler, K. S.; "Determination of Resistance Factors in Porous Diaphragms and Electrodes," Journal of the Electrochemical Soc., 113, 161 February 1966.

11. Forgacs, C.; Dechema, Monogr. 47, 601 (1962).

12. Levich, V.; Physiochemical Hydrodynamics, Chapter 6, Prentice-Hall, 1962.

13. Mantell; Electrochemical Engineering, McGraw-Hill, New York, 1966, pp. pp. 53 f.

14. Wilson, J. R.; Demineralization by Electrodialysis, p. 268, Butterworth, London (1960).

15. Mandersloot, W. G. B.; Journal of the Electrochemical Soc. 111, No. 7, 838 (1964).

16. Bergsma, Dr. F.; Dechema Monogr. 47, 449 (1962).

17. Solt, G. S.; First Internation Symposium on Water Deslination, October 3-9, 1965, Washington, D. C. SWD/3.

18. Teorell, T.; Proc. Soc. Expt, Biol. Med. 33, 282 (1935).

19. Meyer, K. H. and Sievers, J. F.; Helv. Chim. Acta 19, 649 (1936) and Helv. Chim. Acta 20, 634 (1937).

20. The Encyclopedia of Electrochemistry; Edited by C. A. Hampel, p. 802, Reinhold (1964).

21. Forgacs, C.; First International Symposium on Water Desalination, October 3-9, 1965, Washington D. C., SWD/83.

22. Spiegler, K. S.; Electrochemical Operations in Ion-Exchange Technology, ed. by F. C. Nachod - F. Schubert, Academic Press, Inc. 1956, p. 165.

23. Seko, M.; Dechema, Monogr. 47, 575 (1962).

24. Private Communication with E. J. Parsi, Ionics, Inc.

25. Private Communication with W. E. Katz, Ionics, Inc.

26. Kirkham, T. A.; Paper presented April 4, 1963, Division of Water and Waste Chemistry, A.C.C., Los Angeles, California.

27. Mandersloot, W. G. B.; First International Symposium on Water Desalination, Oct. 3-9, 1965, Washington, D. C., SWD/40.

28. An Investigation of the Transport Properties of Ion Exchange Membranes, Arthur D. Little, Inc., Report No. C-66143, Contract 14-01-0001-372.

29. Graydon, W. F.; Canadian J. Chem. 66, 1549 (1962).

30. Wilson, J. R.; Demineralization by Electrodialysis, p. 268, Butterworth, London (1960).

31. Shaffer and Mintz in Principles of Desalination, ed. by K. S. Spiegler, Academic Press, 1966, N. Y.

32. Private Communication with K. S. Spiegler.

APPENDIX A

COLLOIDAL COAGULATION

APPENDIX A

COLLOIDAL COAGULATION

Conceivably, scale formation can occur within the stack by the flocculation of colloidal particles.(A1) Consequently, it is of importance to consider the kinetics of colloidal coagulation. Using the authoritative monography by V. G. Levich,(A2) equations predicting the rate of coagulation of colloidal particles were derived for three types of fluid conditions

A. 1 Brownian Motion (Stagnant Fluid)

Using the diffusion equation,

$$\frac{\partial n}{\partial t} = D \frac{1}{r^2} \frac{\partial}{\partial r} \left(r^2 \frac{\partial n}{\partial r} \right) \tag{1A}$$

where

n = concentration of colloidal particles in the fluid (n_o = bulk concentration)

t = time

r = a = radius of the colloidal particle (10^{-4} - 10^{-7} cms)

D = diffusion coefficient of dispersed particles

Smoluchowski was able to derive the rate of coagulation per unit volume of dispersion as

$$N = 8\pi D \, a \, n_o^2 \tag{2A}$$

where

D, obtained from Stokes-Einstein formula $= \frac{kT}{3\pi\mu a}$

k = Boltzman's Constant

T = Temperature, degrees absolute

A. 2 Gradient Coagulation (Laminar Flow)

In the electrodialysis unit, rectanular flow channels exist and the laminar region will manifest itself near the membrane surface even though turbulent flow at the center of the channel is predominant. The following theory is developed without the presence of spacers or turbulent promoters in the channels. For overall laminar flow only, the rate of coagulation per unit volume is given by:

$$N_{Grad} = \frac{32}{3} n_o^2 \Gamma a^3 \qquad (3A)$$

where Γ = velocity gradient of the fluid, $\left(\frac{dv_z}{dx}\right)$, and is easy to obtain if we know the velocity profile (A3) in a narrow slit. (See Figure A-1.)

$$v_z = \frac{(\rho_o - \rho_\ell) B^2}{2} \left[1 - \left(\frac{x}{B}\right)^2\right] \qquad (4A)$$

and

$$\Gamma = \frac{dv_z}{dx} = \left(\frac{\Delta\rho}{\mu L}\right) B = \text{Maximum at } x = \pm B \qquad (5A)$$

where

$2B$ = distance between membranes

L = length of membrane

W = width of membrane

$\rho_o - \rho_L$ = includes both pressure and the gravity forces exerted onto the fluid

$$= (p_o - p_L) - \rho g(L) \qquad (6A)$$

$\Delta\rho$ = $\Delta p - \rho g L$

ρ = density of fluid

p_z = pressure at some point z

μ = viscosity of fluid

A.3 Coagulation of Colloids in Turbulent Flows

We assume that a diffusion of particles occurs toward a sphere of radius r, such that the distribution of the particles may be characterized by the diffusion equation below, (refer to Figure A-2)

$$\text{div}\,(D_* \,\text{grad}\, n) = 0 \qquad (7A)$$

where

D_* = effective diffusion coefficient

R = coagulation radius $\approx 10^{-5}$ cm

λ_o = microscale of turbulence $\approx 10^{-2}$ cm

a = diameter of particle, cm

$\epsilon_o = \frac{\epsilon}{\rho}$

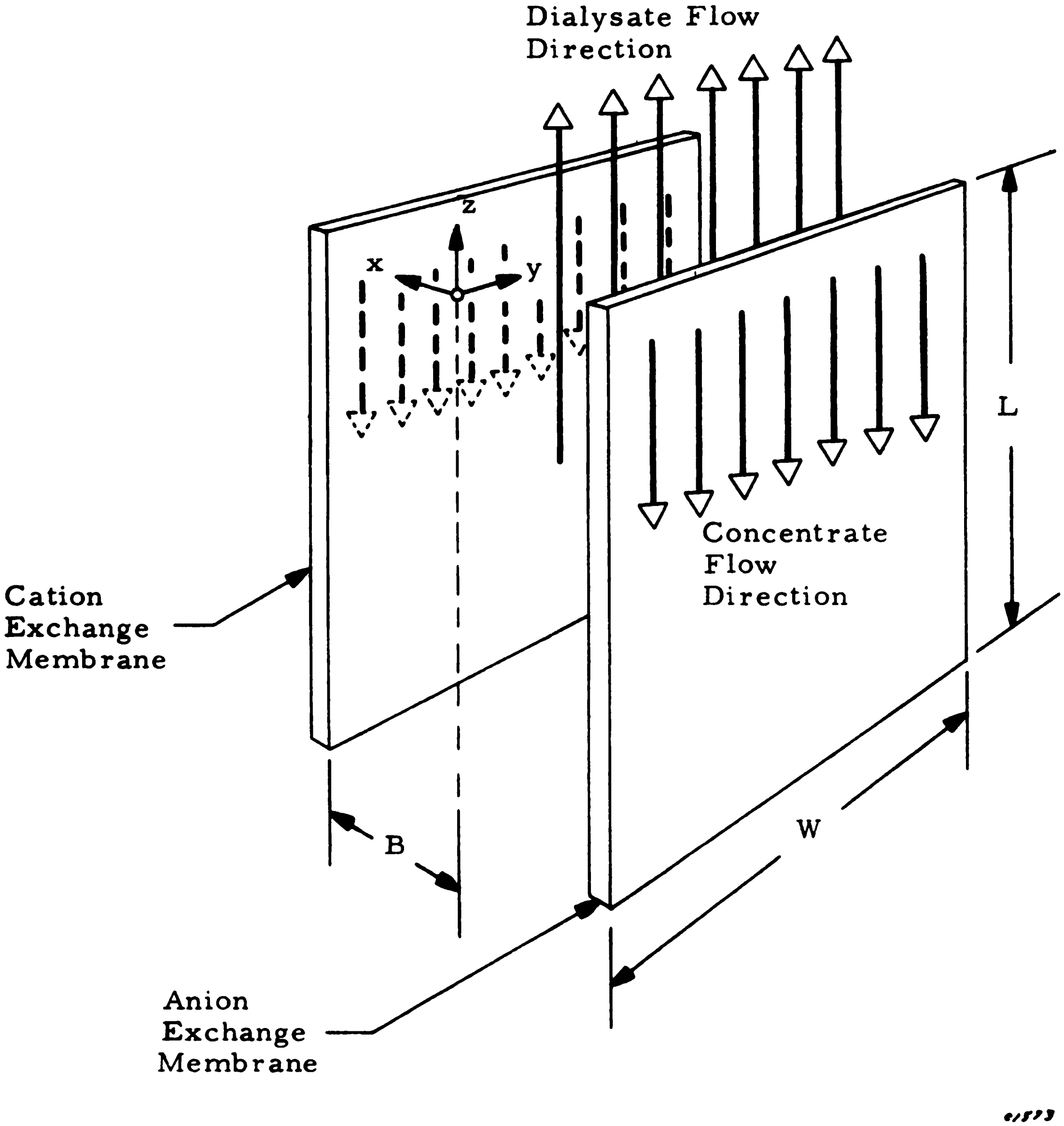

Figure A-1. Schematic Diagram of the Electrodialysis Flow Channel

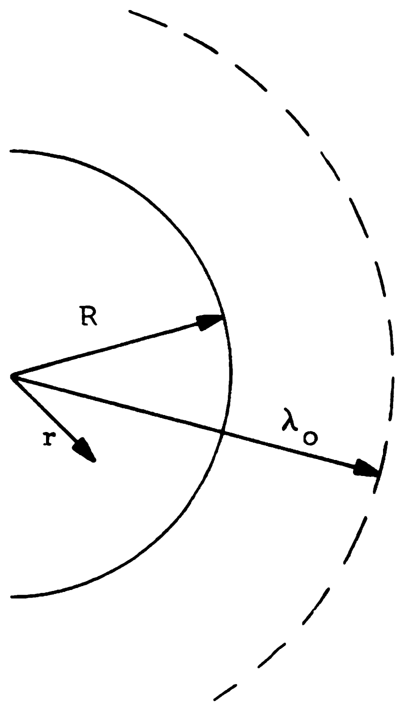

61574

Figure A-2. Coagulation in Spherical Coordinates

ϵ = energy dissipated/unit volume and is characteristic for a given flow, ergs/cm^3 sec

ρ = density of the fluid, gms/cm^3

ν = $\frac{\mu}{\rho}$ = kinematic viscosity

β = constant

r = radial distance in spherical coordinates

Intergrating equation (7A), substituting for D_{turb}, for the case where the eddies (λ) are smaller (in size) than the turbulent microscale (λ_o).

$$D_* = D_{turb} \sim \nu_\lambda \cdot \lambda \sim \beta \sqrt{\frac{\epsilon_o}{\nu}} \; \lambda^2 \text{ for } \lambda < \lambda_o \tag{8A}$$

We get

$$\beta \sqrt{\frac{\epsilon_o}{\nu}} \; \Gamma^4 \left(\frac{\partial n}{\partial r}\right) = C_1 \text{ where } r < \lambda_o \tag{9A}$$

Intergrating equation (9A) with boundary conditions

$n = 0$ at $r = R$

$n = n_o$ as $r \rightarrow \infty$

and allowing for continuity of n over the surface $r = \lambda_o$ we find,

$$n \approx \frac{n_o}{1 + \frac{2}{7}\frac{R^3}{\lambda_o^3}} \left(1 - \frac{R^3}{\lambda^3}\right), \; r < \lambda_o \tag{10A}$$

Flux of particles across one square centimeter (1 cm^2) of surface of the sphere of coagulation, R, is equal to:

$$j = D_* \left(\frac{\partial n}{\partial \Gamma}\right)_{r = R} = D_{turb} \left(\frac{\partial n}{\partial \Gamma}\right)_{r = R} \tag{11A}$$

Differentiating equation (10A) and let r = R, and substitute the result into equation (11A). Also substitute D_{turb} from equation (8A) into equation (11A).

$$j = \frac{3 n_o R \beta \sqrt{\frac{\epsilon_o}{\nu}}}{1 + \frac{2}{7}\frac{R^3}{\lambda_o^3}} \approx 3 n_o R \beta \sqrt{\frac{\epsilon_o}{\nu}} \tag{12A}$$

if

$\frac{2}{7}\frac{R^3}{\lambda_o^3}$ is very small then j is a constant.

The total number of encounters per unit time, brought about by turbulence agitation, or the rate of coagulation is

$$N_{turb} = (4\pi R^2)\, n_o j = 12\pi\beta \sqrt{\frac{\epsilon_o}{\nu}}\; R^3\, n_o^2 \tag{13A}$$

Expressing ϵ in terms of fluid flow velocity v, and large scale motions L where $\epsilon \sim \frac{v^3}{L^2}$, equation (13A) becomes

$$N_{turb} \sim \frac{R^3 n_o^2 v^{\frac{3}{2}}}{\sqrt{\nu L}} \sim \frac{R^3 v n_o^2 (N_{R_e})^{\frac{3}{2}}}{L^2} \tag{14A}$$

If one can separate the phenomena of saturation precipitation from colloidal coagulation and precipitation on the membrane surface, then the importance of the latter effect on the R_{ohmic} polarization can be evaluated. Note that in equation (14A), coagulation rate is proportional to the velocity to the one and a half power. Once we know the size of the colloidal particles in the stream and can determine the velocity and turbulence in the channel, an increase in the turbulence will cause a thinner diffusion layer (beneficial) and an increase in the rate of coagulation (detrimental) — or in terms of resistances, R_{cp} will decrease and $R_{ohmic\ pol}$ will increase. A trade-off point exists.

A.4 References

A1 Cooke, B. A. and Mandersloot, W. G. B., Trans. Inst. Chem. Engrs., 37, 14 (1959).

A2 Levich, V. G., Physiochemical Hydrodynamics, p. 207, Prentice-Hall (1962).

A3 Bird, R. B.; Stewart, W. E. and Lightfoot, E. N.; Transport Phenomena, p. 62, John Wiley (1962).

APPENDIX B

THEORETICAL PREDICTION OF MEMBRANE RESISTANCE COMBINING THE STATISTICAL THEORY OF MEARES, ET AL., AND SPIEGLER'S FORMATION FACTOR

APPENDIX B

THEORETICAL PREDICTION OF MEMBRANE RESISTANCE COMBINING THE STATISTICAL THEORY OF MEARES, ET AL., AND SPIEGLER'S FORMATION FACTOR

B.1 Discussion

The purely theoretical prediction of a membrane's resistance in some known salt solution is the result of the following discussion. It is significant to note, that the work presented below combines the statistical theory of J. S. Makie and P. Meares,(B1) and the recent work on porous diaphragms by K. S. Spiegler.(B2) An added section on nonrigid membranes is also presented.

In order to determine the resistance that a membrane will exhibit when placed between two electrodes, which are passing current, it is necessary to predict its resistivity. Recognizing that the streams, flowing countercurrently, are of different and varying composition, the membrane resistivity will also vary from top to bottom of the channel.

Although it is somewhat naive to choose an average composition between the streams and then evaluate the membrane's resistivity when saturated with this solution, at present no better approach is available. Mason and Kirkham(B3) have used this approach defining an average normality, C_a, at any point along the flow path, as

$$\frac{1}{C_a} = \frac{1}{2}\left(\frac{1}{C_d} + \frac{k}{C_b}\right) \tag{1B}$$

where

C_d = dialysate concentration

C_b = brine concentration

$k = \dfrac{\text{brine compartment thickness}}{\text{dialysate compartment thickness}} = \dfrac{t_b}{t_d}$

Assume that the average concentration, C_a is linear with path length, z, from channel bottom to top of stack. Define a mean C_a between inlet and outlet average C_a as follows

$$(C_a)_{\text{mean}} = \frac{1}{2}\left\{\left[\frac{2\,C_d\,C_b}{C_d + C_b}\right]_{\text{bottom}} + \left[\frac{2\,C_d\,C_b}{C_d + C_b}\right]_{\text{top}}\right\} \qquad (2B)$$

It has recently been shown by K. S. Spiegler,(B2) that the porous path through a diaphragm (rigid) by ions and gas molecules are similar, although certain corrections for ion-exchange membranes must be made. Both membrane swelling and the lowering of the resistivity due to adsorbed water would necessitate such corrections.

B.1.1 Rigid Membranes

A glass diaphragm is an example of this classification. One of the distinguishing factors between rigid and nonrigid (organic ion exchange) membranes, is that the porosity, e, is constant for the former but variable for the latter. A discussion of this phenomenon is given in the following section.

K. S. Spiegler(B2) defines a formation (resistance) factor:

$$F_E = \rho^1/\rho = \theta^2/e \qquad (3B)$$

where

ρ^1 = resistivity of the material when the pores are filled with a conductive liquid, ohms-cms.

ρ = resistivity of liquid without the diaphragm, ohms-cms

θ = tortuosity of the pore model = $\dfrac{\text{real path length}}{\text{geometric path length}}$

e = dry porosity (≡ non-solid volume fraction of the diaphragm)

Starting from the lattice model for polymer solutions, J. S. Makie and P. Meares(B1) derived,

$$\theta = \frac{1 + V_p}{1 - V_p} \qquad (4B)$$

where

V_p = volume fraction of the polymer

V_p = (1 - e), by definition.

substituting into equation (4B)

$$\theta = \frac{[1 + (1 - e)]}{[1 - (1 - e)]} = \frac{(2 - e)}{e} \qquad (5B)$$

Substituting equation (5B) into equation (3B) and solving for ρ^1,

$$\rho^1 = \rho\left(\frac{\theta^2}{e}\right) = \rho\frac{(2 - e)^2}{e^3} \qquad (6B)$$

therefore

$$F_E = \frac{(2 - e)^2}{e^3} = \text{formation factor.} \qquad (7B)$$

Refer to Figure B-1 for plot of F_E versus e.

B.1.2 Nonrigid Membranes

The porosity, e, as described in the above equations, is constant for rigid membranes or diaphragms, but when swelling occurs, e, will increase, as is the case with organic ion exchange membranes. To compensate for this phenomena, e will be increased by the wet to dry volume ratio, R_W or by adding a swelling porosity component e_s. The lowering of the membrane resistivity due to the presence of adsorbed water within the pores would in essence also result in a higher value of e. An empirical adjustment factor (A_D) will be used in the latter effect.

The modified membrane porosity, e^1 is given by

$$\begin{aligned} e^1 &= e + e_s \\ &= e\left(1 + \frac{e_s}{e}\right) \\ &= e \,.\, R_W \qquad (8B) \end{aligned}$$

where

$$R_W = \frac{e + e_s}{e} = \frac{\text{wet volume}}{\text{dry volume}}$$

For the adsorbed water effect, instead of using F_E as defined by equation (3B), a modified $F_E^!$ will be defined, where

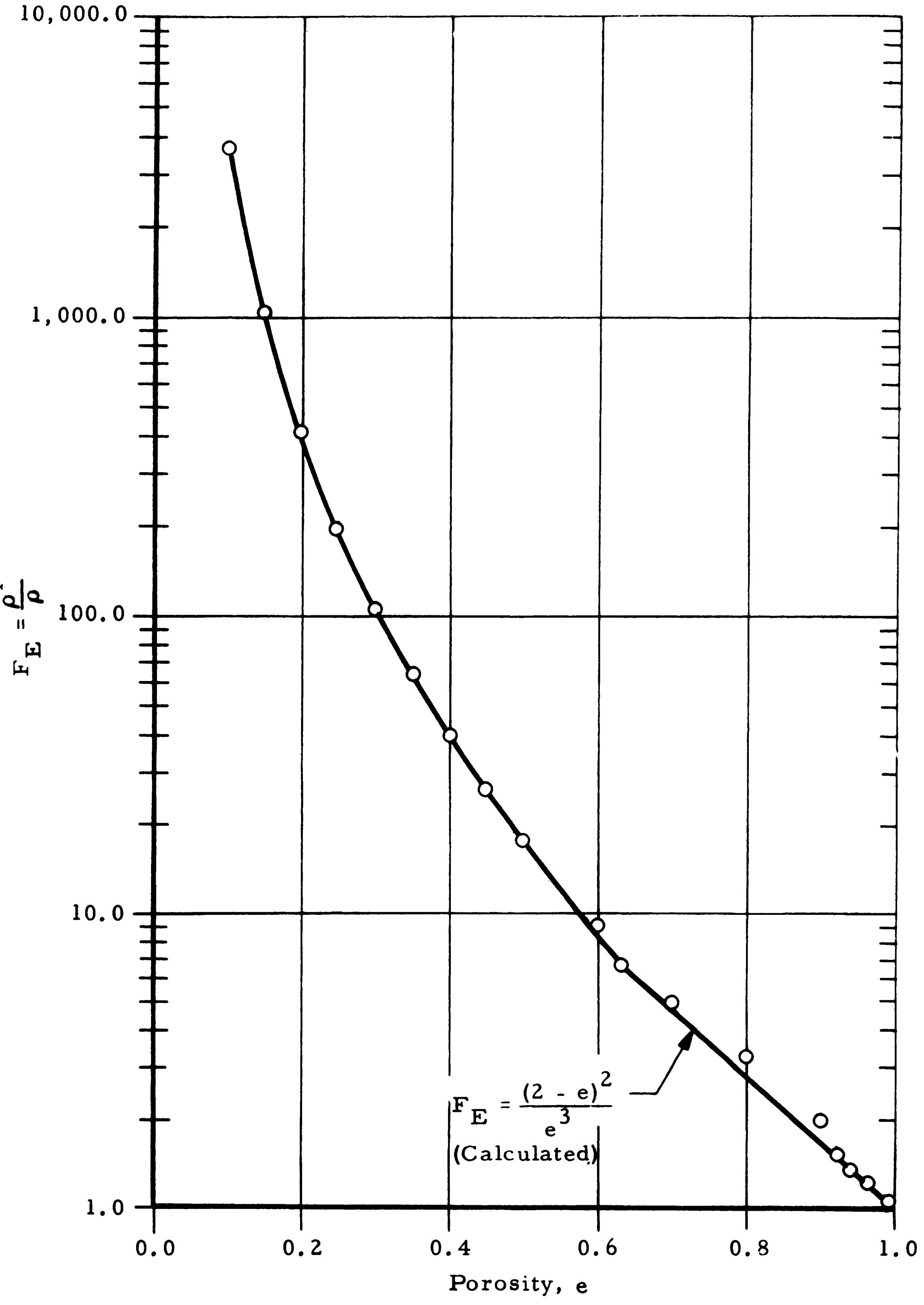

Figure B-1. Plot of the Ratio of the Membrane Resistivity (ρ^1) to the Solution Resistivity (ρ) Versus Porosity (e)

$$F'_E = \frac{(2 - e)^2}{e^3} \quad A_D \qquad (9B)$$

where empirically

$$A_D = e^{(3 + R_W)} \qquad (10B)$$

Hence, if e, dry porosity and R_W, wet to dry volume ratio are obtained from the manufacturer, using e^1, modified porosity, we can determine F_E, formation factor from Figure B-1 and finally ρ^1 at various points along the flow path.

B.2 Resistance Analogue of Membrane Resistance

After evaluating ρ^1, membrane resistivity at a given concentration, the cationic or, anionic membrane resistance analogue can easily be evaluated from the definition

$$\overline{R}_{\text{cat or anionic}} = \rho^1 \ell, \text{ ohms-cm}^2. \qquad (11B)$$

where

ℓ = thickness of the membrane, cms

B.3 References

B1 Makie, J. S. and Meares, P., Proc. Roy. Soc. (London) A 232 (1955), p. 498.

B2 Spiegler, K. S., "Determination of Resistance Factors in Porous Diaphragms and Electrodes," Journal of the Electrochemical Soc., 113, 161 February 1966.

B3 Mason, E. A. and Kirkham, T. A., C.E.P. Symposium Series No. 24, 55 (1959), p. 173.

APPENDIX C

HYDRODYNAMIC FLOW

APPENDIX C
HYDRODYNAMIC FLOW

The equations of continuity and motion apply to turbulent flow, but it is nigh impossible to solve them because the turbulent eddies fluctuate widely about their mean velocity and pressure. By averaging the equations of change, "time smoothed" equations result, which in turn need empirical expressions for the "turbulent momentum flux." The spacer network is inserted between the ion exchange membranes so as to increase turbulence and lower polarization near the membrane surface. The complex spacer pattern such as the expanded spacer design (see Figures C-1, C-2, C-3), will be used to determine local Reynold's numbers so as to predict which areas within the network are more susceptible to scale deposit as a result of stagnant or slow liquid spots. Since the statistical theory of turbulence is in its embryonic stage and the complexity of the problem is enormous, no attempt here will be made to set up flux equations across the network and membrane. A semi-qualitative description will be attempted, using Reynold's number to describe the kind of flow at various local points. The following assumptions are made.

1. The fluid flow direction will be perpendicular to section A-A in Figures C-1 and C-2.
2. The flow is equally distributed across the spacer network.
3. The velocity, calculated fromthe volumetric flow rate across some chosen cross-sectional area, is representative of the fully developed average velocity of the profile in the prechosen cross-section.
4. Equivalent diameter, D_e, is equal to four times the hydraulic radius, R_H, which is the ratio of the stream cross-sectional area to the wetted perimeter.
5. Dimensions of the expanded spacer as shown in Figures C-4, C-5 and C-6 are obtained from Figure 8 of "Electrodialysis Equipment and Membranes," by H. J. Cohan, 53rd Annual Meeting of AIChE, Symposium on Saline Water Conversion, Dec. 4-7, 1960.(C1)

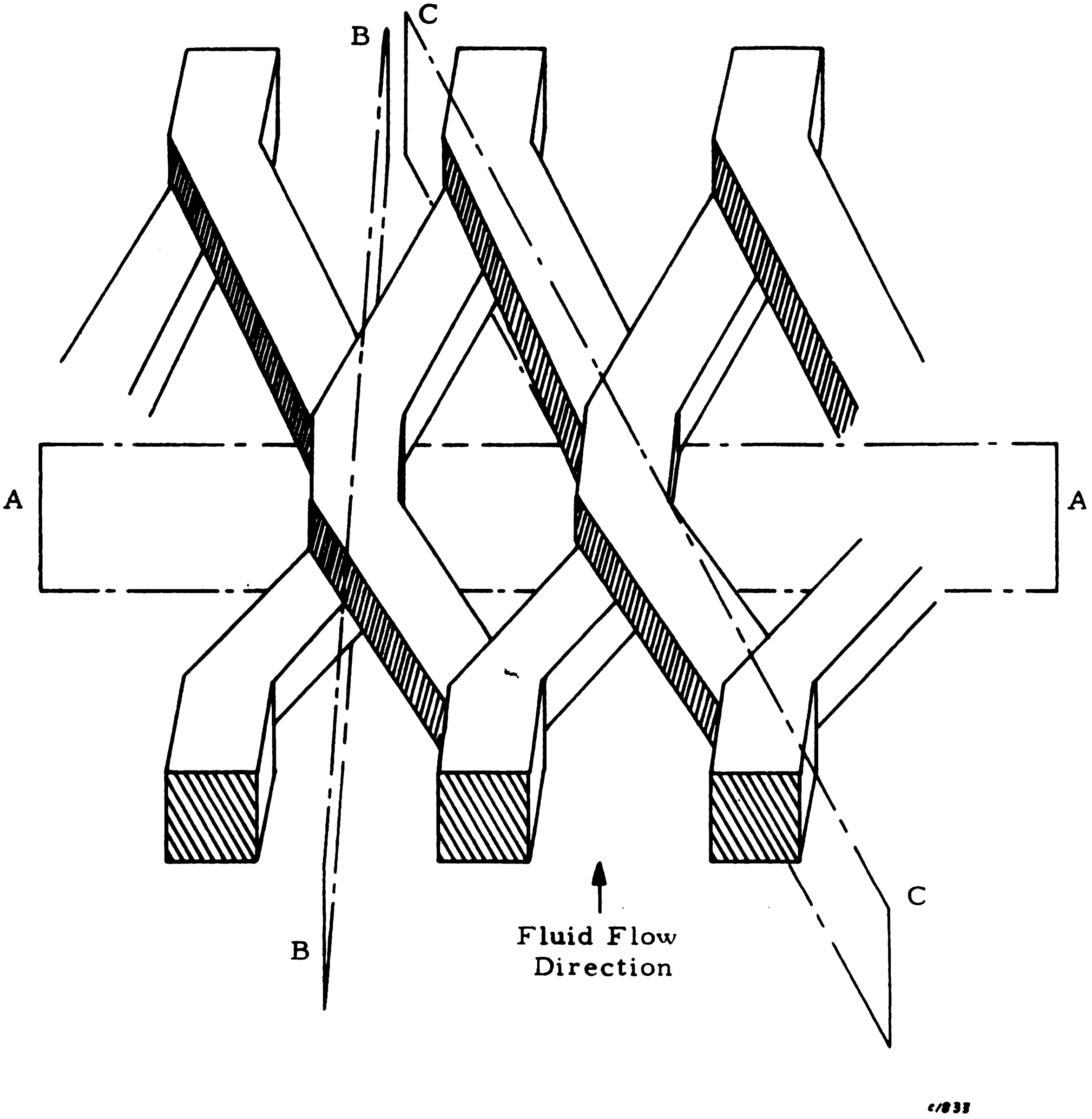

Figure C-1. Isometric View of Expanded Spacer Design

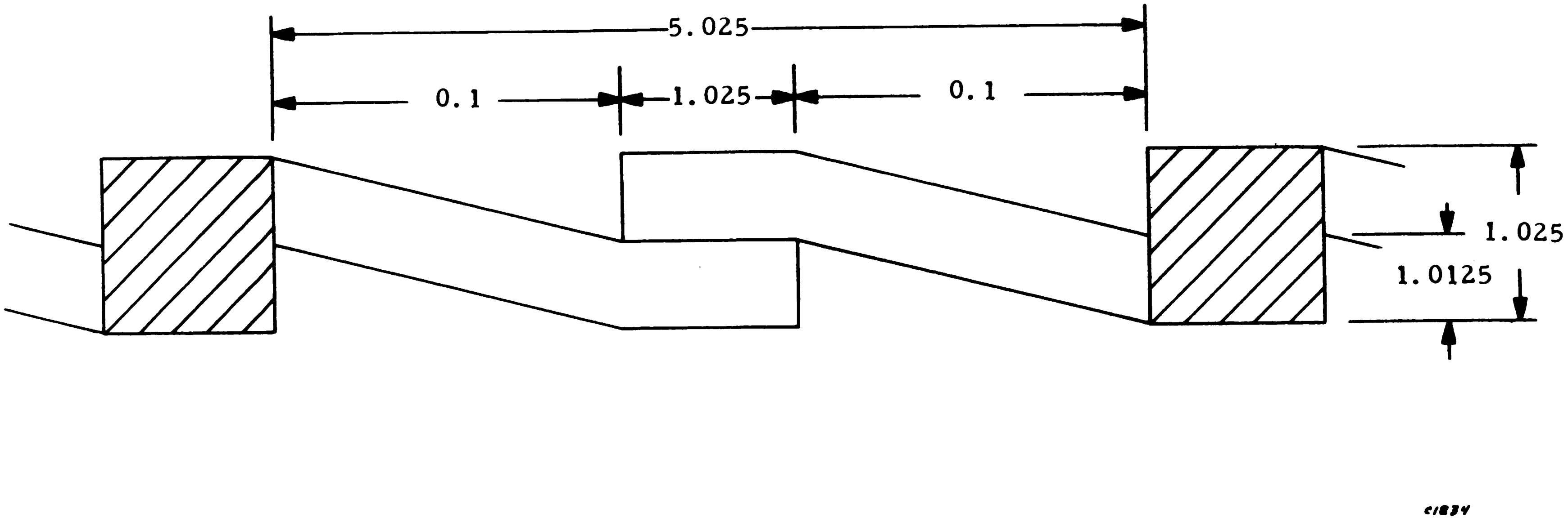

Figure C-2. Section A-A (from Figure C-1) of Expanded Spacer Design

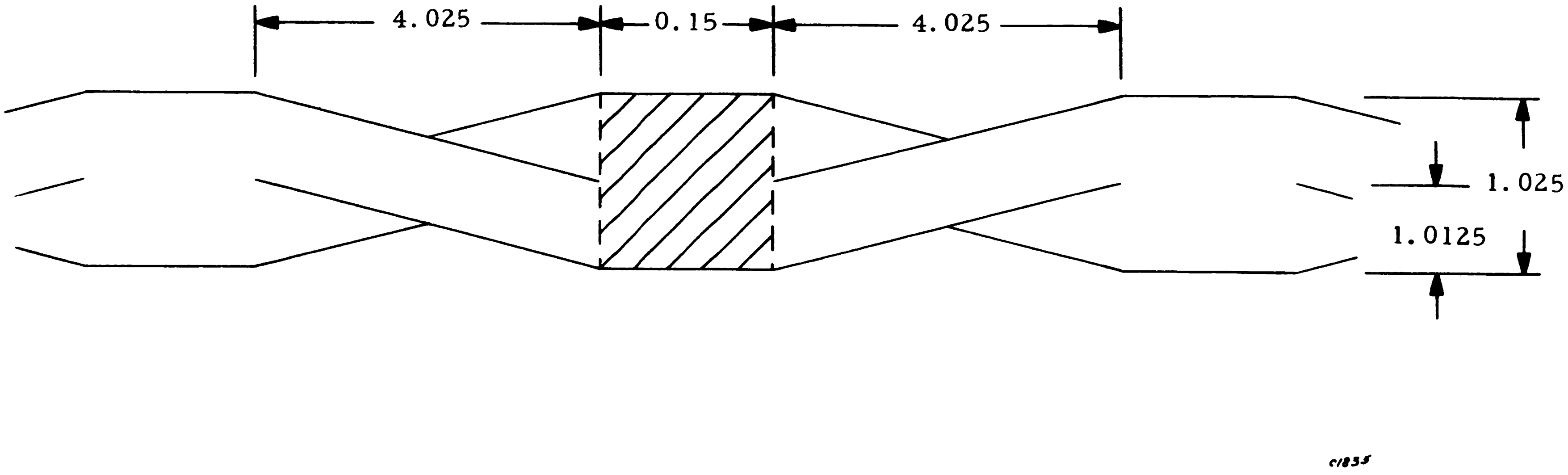

Figure C-3. Section B-B (from Figure C-1) of Expanded Spacer Design

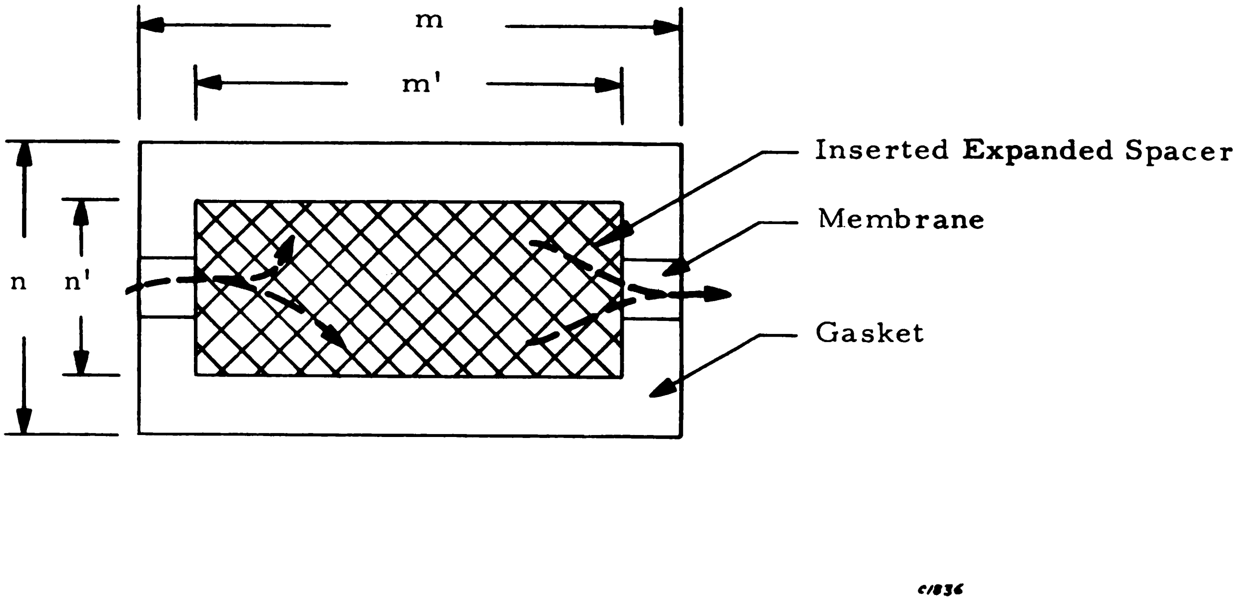

Figure C-4. Plan View of Gasket, Membrane and Spacer
(Define $m' = \sqrt{p}\ m$ and $n' = \sqrt{p}\ n$)

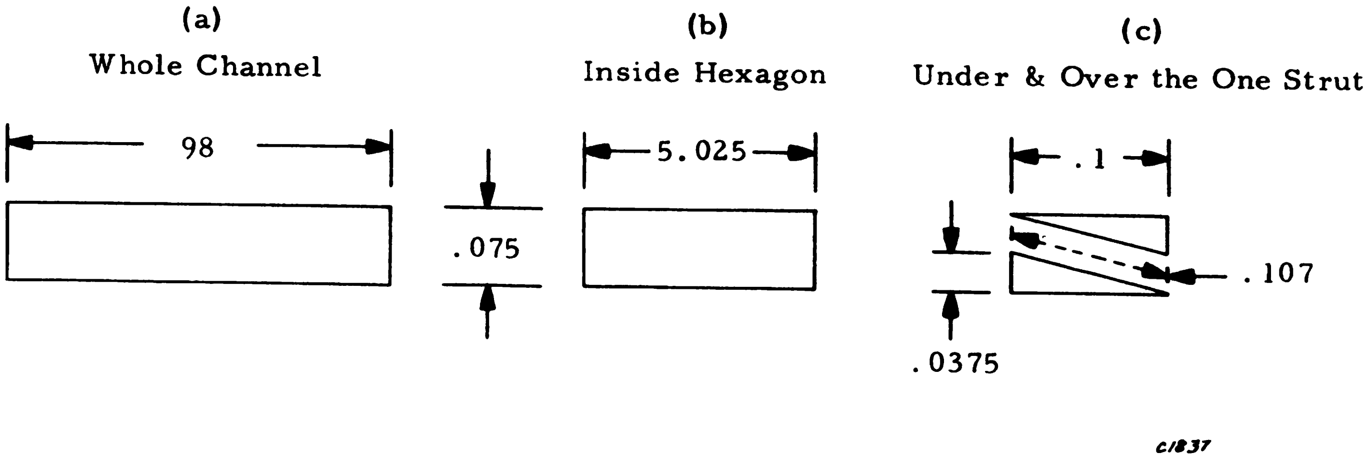

Figure C-5. Cross-Sectional Area Facing Flow for Each Case (Dimensions in cms)

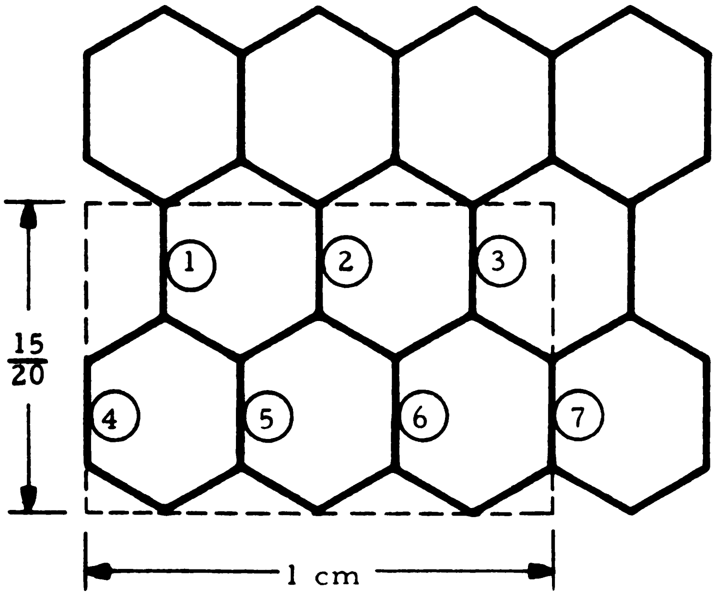

c/838

Figure C-6. Number of Expanded Spacer Contact Points Per Unit Area, $n = \left(\dfrac{7}{\frac{15}{20} \times 1}\right) \qquad \left(\dfrac{28}{3}\right) \longrightarrow$

The following ratio $(N_{Re} \cdot \frac{\mu}{\rho})$ will be evaluated for three different cases: the first case for the empty channel without a spacer (Figure C-5a); the second case with the fluid flowing inside the hexagon design of the spacer, perpendicular to plane A-A (Figures C-1, C-2 and C-5b); thirdly when the fluid passes under and over the strut at plane C-C (Figures C-1, C-3 and C-5c).

The equations below are now applied to the data obtained from Webster, South Dakota.(C2)

$$\text{Volumetric flow rate} = Q \text{ gal/min channel}$$

$$= \left(\frac{3,785}{60}\right) \cdot Q \text{ cm}^3\text{/sec, channel}$$

$$\text{Reynolds number is defined: } N_{Re} = \rho \frac{D_e V}{\mu}$$

$$\text{Comparison ratio used: } \left(N_{Re} \cdot \frac{\mu}{\rho}\right) = D_e V \tag{1C}$$

where

V = local velocity cm/sec

D_e = equivalent diameter, cms

$= rR_H = 4 \dfrac{\text{area of stream cross-section}}{\text{wetted perimeter}}$

Refer to Table C-I.

From column (7) Table C-I we conclude that, the flux equations and their vector directions must be evaluated (not possible with present technological tools) to determine the turbulence inducing effects of the spacer design. This conclusion is based on the unreasonable prediction from column (7) that the N_{Re} is higher without the spacer than with. A statistical approach would be necessary so as to account for the random turbulent eddies, but with the present extremely complex configuration this is not possible. This is an area where considerably more experimental and theoretical study is needed.

TABLE C-I

COMPARING TURBULENCE FOR THREE DIFFERENT CONFIGURATIONS

Position (Case)	R_H cms	D_e cms	Local Volumetric(a) Flow Rate cc/sec	Cross Sectional(b) Area cm^2	Velocity cm/sec	$\left(N_{Re} \cdot \frac{\mu}{\rho}\right) = D_e V$(c) cm^2/sec
No Spacer (1)	2(.075+98)	.15	$\left(\frac{3785}{60}\right) Q$	.075x98	6.68	1.003
Within Hexagon (2)	$\frac{.075x.275}{2(.075x.275}$	.12	$\left(\frac{3785}{60x294}\right) Q$	.075x.275	8.1	0.975
Across Strut (3)	$\frac{.0375x.1}{2(.1+.0375+.107)}$	.031	$\left(\frac{3785}{2x60x294}\right) Q$	.00375	22.0	0.691

(a) Q for Webster = 0.779 gal/min channel

Number of hexagon (in n' width) = $3 \frac{\text{Hex}}{\text{cm}}$ x 98 cm = 294

(b) Area available for flow across the strut = $2(.0375\text{x}.1\text{x}\frac{1}{2}) = \frac{.00375}{\text{cm}^2}$ (from Figure C-5c)

(c) At 40°F $\left(\frac{\rho}{\mu}\right)_{water} = \frac{62.43}{1.54\text{x}6.72\text{x}10^{-4}\,(12\text{x}2.54)^2} = 64.6\ \text{sec/cm}^2$

i.e. N_{Re} for each case (i) $(N_{Re}) = 64.8$

(ii) $(N_{Re}) = 63.0$

(iii) $(N_{Re}) = 44.6$

REFERENCES

C1 Cohan, H. J., "Electrodialysis Equipment and Membranes," 53rd Annual Meeting of AIChE, Symposium on Saline Water Conversion, December 4-7, 1960.

C2 Seko, M., Dechema, Monogr. 47, 575 (1962).

APPENDIX D

NOMENCLATURE

APPENDIX D

NOMENCLATURE

Symbol **Definition**

A = temperature dependent constant in the Onsager equation

a = actual membrane cross-sectional area, cm^2 (=mxn)

A_D = empirical adjustment factor for F'_E

B = temperature dependent constant in the Onsager equation

C_a = average concentration of a cell pair, gm equiv/liter

$(C_a)_{mean}$ = mean of C_a at the bottom and top of the stack channel, gm equiv/liter

$_{d \text{ or } b}(C_b)_x$ = bulk dialysate or brine concentration at some point x along the fluid path length from the bottom of the channel upwards

$_{d \text{ or } b}(C_b)_{o \text{ or } i}$ = dialysate or brine bulk concentration (outlet or inlet), gm equiv/liter

C_d, C_b = shortened notation of dialysate and brine bulk solution concentration, gm equiv/liter

$_{d \text{ or } b}(C_m)_{o \text{ or } i}$ = dialysate or brine membrane surface concentration (outlet or inlet) gm equiv/liter

D_L = Diffusion coefficient

e = porosity (non-solid volume fraction of the membrane)

e^1 = η_D, coulombic efficiency (not including the water transfer losses)

E_S = stack voltage, volts

EPM = total equivalents of cation per million in feed water

F = Faraday's No., coulombs/gm equiv

F_B = concentration stream exit flow rate, ml/sec

F_D = dilute stream exit flow rate, ml/sec

F_E = formation factor for a rigid membrane

F'_E = formation (resistance)factor for a flexible membrane

GPD_{pw} = gal/day of product water

I = stack current, amps

i = stack current density, amps/cm^2

i_ℓ = current leakage due to duct losses, $\frac{amp}{cm^2}$

k = ratio of brine to dialysate compartment thickness

K_1, K_2, K_3 = constants in the generalized R_p versus C_a equation

$\ell_a \ell_c$ = anionic or cationic exchange membrane thickness, cms

m = overall membrane length, cms

M_S = membranes/stack

N = number of cell pairs/stack

n = overall membrane width, cms

p = fraction of membrane area available for desalination

ppm = parts per million of dissolved salt

Q = volumetric flow rate, gal/min, channel

$\bar{R}_b$ = brine channel resistance, Ω/stack

R_{cat}, R_{an} = cationic or anionic exchange membrane resistances respectively, Ω- cm^2

R_{cp} = concentration polarization resistance, Ω- cm^2

$\bar{R}_d$ = dialysate channel resistance, Ω/stack

$R_{d.\ell.}$ = parasitic duct loss resistance, Ω/stack

$\bar{R}_\ell$ = equivalent channel resistance, Ω/stack

R_{ohmic} = rate of change in ohmic polarization resistance of stack, ohms hr^{-1}

R_p = equivalent cell pair resistance, Ω/cell pair

$(R_p)_x$ = cell pair resistance at some specific distance x, up from the bottom (x = O) of the stack, Ω - cm^2

R_w = wet to dry volume ratio of the membrane

S = $\frac{1000}{\Lambda}$ at given temperature for NaCl solution

T = temperature, °C

t = time of operation, hours

t^a_-, t^c_+ = transport number of counter ion in anion and cation exchange membranes respectively

t^c_-, t^a_+ = transport numbers of the co-ions in the cation and anion exchange membrane respectively, where $t^c = 1 - t^c_+$ and $t^a_+ = 1 - t^a_-$

$t_{d \text{ or } b}$ = transport number of counter ion in anion and cation exchange solution (dialysate or brine)

u_d = dialysate channel width (rectangular cross-section) cms

v_d = dialysate channel height, cm

V_p = volume fraction of the polymer (solid)

w = ave equivalent wt of dissolved salts, gm equiv/liter

w_c , w_a = primary hydration number for sodium and chloride ions respectively

w_t = primary hydration number for both sodium and chloride ions

x' = fraction open area of spacer

Y_b = brine channel diameter (circular cross-section), cms

y_d, y_b = dialysate or brine compartment thickness, cms

<u>Greek</u>

δ = diffusion layer thickness, cm

ρ = tortuosity of the pore model

Λ = equivalent conductance at concentration $_{d \text{ or } b}(C_b)_{o \text{ or } i}$

Λ_{α} = equivalent conductance at infinite dilution

d or b$(p_{ave})^{o \text{ or } i}_{m \text{ or } b}$ = average resistivity (dialysate or brine at the inlet or outlet) of solution at membrane surface (m) and the bulk solution (b), Ω - cm

$\rho^{c} \rho^{a}$ = resistivity of the cationic or anionic membranes respectively, Ω - cm

ρ(Ca)mean = resistivity of the solution at $(Ca)_{mean}$, Ω - cm

ρ^{d}, ρ^{b} = resistivity of the dialysate and brine bulk solution respectively, Ω- cm

d or b$^{\rho}$ mean = mean resistivity of ρ_{ave} at the inlet and outlet of dialysate or brine streams, Ω - cm

ρ_{ohmic} = rate of change in ohmic resistivity, ohms cm^2 per cell pair per hour

ψ = dimensionless channel resistance, $= \frac{\overline{R}_{\ell}}{R_p N}$

☆U. S. GOVERNMENT PRINTING OFFICE : 1967 O - 256-935